TROPANE ALKALOID BIOSYNTHESIS IN *ATROPA BELLADONNA*

By

Matthew Bedewitz

A DISSERTATION

Submitted to
Michigan State University
in partial fulfillment of the requirements
for the degree of

Plant Breeding, Genetics, and Biotechnology - Horticulture - Doctor of Philosophy

2021

ABSTRACT

TROPANE ALKALOID BIOSYNTHESIS IN *ATROPA BELLADONNA*

By

Matthew Bedewitz

A chemically diverse set of specialized flavorings, fragrances, and medicinal metabolites are produced by plants to modulate their interactions with pollinators, herbivores, and other biotic and abiotic stresses. Tropane alkaloids are one group of these specialized metabolites which are produced in phylogenetically distinct plant families and include the narcotic cocaine and the pharmaceutical compounds hyoscyamine and scopolamine. Scopolamine is produced in the roots of plants in the Solanaceae family and serves as the precursor to semi-synthetic tropane pharmaceuticals. A set of eleven tissue-specific transcriptomes was generated from the tender perennial Solanaceous plant *Atropa belladonna*, deadly nightshade, to fill gaps in the biosynthetic pathway from putrescine to scopolamine. This dissertation describes the identification of enzymes which complete three missing portions of the scopolamine biosynthetic pathway. These are the biosynthesis of tropinone, the diversion of phenylalanine into production of phenyllactic acid, and the activation and conjugation of phenyllactic acid with tropine to form littorine, a late pathway precursor to scopolamine.

Tropinone is the first metabolite in this pathway with the characteristic 8-azabicyclo[3.2.1]octane tropane core. This pharmacore was synthesized in a classic biomimetic chemical synthesis, but the mechanism for tropinone biosynthesis has remained an open question in all species which produce these compounds. The *A. belladonna* lateral root transcriptome revealed that tropinone biosynthesis proceeds

through an atypical polyketide synthase which uses an imine as its starter, and that the polyketide is cyclized to tropinone by a cytochrome P450.

Tropic acid, the specialized acyl group for both hyoscyamine and scopolamine, is produced from the primary metabolite phenylalanine through the intermediate phenyllactic acid. Aromatic aminotransferases are one route by which amino acids can be dedicated to specialized metabolism. Six aromatic aminotransferases are present in the *A. belladonna* transcriptome, and one of these, ArAT4, is a root-specific phenylalanine aminotransferase required for biosynthesis of phenyllactic acid and ultimately, scopolamine. In contrast to other aminotransferases which equilibrate multiple amino acids, this enzyme is highly directional for the consumption of phenylalanine and production of tyrosine.

Littorine, a precursor of hyoscyamine and scopolamine, is the ester of tropine and phenyllactic acid. The mechanism for phenyllactic acid activation and esterification have remained as an open question of tropane alkaloid biosynthesis since the discovery of littorine. Two routes exist for activation and conjugation in plants, through either coenzyme A thioesters or glucose esters. In *A. belladonna*, littorine biosynthesis proceeds through a glucose ester of phenyllactic acid produced by a glucosyltransferase, UGT84A27, and an acyltransferase, LITTORINE SYNTHASE. This contrasts with cocaine acylation in the Erythroxylaceae, which uses a different route highlighting the repeated, independent origin of tropane alkaloid biosynthesis in plants.

The enzymes identified in this dissertation have completed three missing sections of the tropane alkaloid biosynthetic pathway in *A. belladonna*, resulting in a nearly complete pathway, suitable for engineering.

ACKNOWLEDGEMENTS

In addition to the many teachers I have had in the course of my education, I would like to thank Dr. Cornelius Barry, who has been my mentor for very nearly a decade. From my first months of undergraduate study to the completion of my dissertation he has prioritized his students and his lab, and this has helped me to persevere through times when I doubted my interests and the field I had chosen. Corny has always been there for advice and discussion and he has been instrumental in my development as a researcher.

The members of Barry have also been important to my development as a scientist. I would like to thank the many undergraduate researchers I have had the privilege to work with and mentor in turn, David, Julia, Charles, Ivan, and Josh, and especially Joe, who helped me immensely in building the foundation for exploration of the broader tropane alkaloid pathway and Bill, who was my first mentor when I joined Corny's lab. I have also had constant friends in Dr. Satya Swathi Nadakuduti and Dr. Radin Sadre, who I have been able to turn to for advice and commiseration.

I also want to thank the members of my guidance committee, Dr. Rob Last, Dr. Dean DellaPenna, and Dr. Dan Jones for agreeing to be on my committee. In particular, I want to thank Dan for his tireless service to, and support of, the research community at Michigan State University both as the director of the Mass Spectrometry and Metabolomics Core facility and as a collaborator in my research. I want to thank Dr. Kevin Walker and fellow graduate students Tyler and Prakash for their advice and support during my forays into synthetic chemistry

TABLE OF CONTENTS

LIST OF TABLES

LIST OF FIGURES

CHAPTER ONE

Specialized metabolism and tropane alkaloids in the Solanaceae

Metabolism and metabolomics in non-model plant systems

Metabolites are small molecules which are produced in living systems during metabolism, through both enzymatic and non-enzymatic means (Harris, 2008; Ralser, 2018). These molecules can be divided into two broad categories, primary and specialized (formerly called secondary) metabolites. Primary metabolites are compounds required during an organism's life cycle, and can include sugars, lipids, organic acids, and the proteinogenic amino acids. Specialized metabolites are those compounds that are not primary metabolites, and in plants can include compounds used for defense, attraction of pollinators, or interaction with biotic and abiotic factors encountered within the environment (Shonle and Bergelson, 2000; Carmona and Fornoni, 2013; Miranda-Pérez et al., 2016; Pichersky and Raguso, 2016). The typical specialized metabolic pathway is often subject to rapid evolution in response to shifting selection pressures, resulting in phylogenetic restriction, where a compound or group of related compounds may be present in a single family, genus, or species. Further attributes of specialized metabolic pathways include restrictions in tissue type and cell type localization, gene clustering, and gene co-regulation (Pichersky and Lewinsohn, 2011; Milo and Last, 2012; Chae et al., 2014; Nützmann and Osbourne, 2014).

The concept of the metabolome, the set of an organism's metabolites, was first coined in 1998, analogous to the genome and the transcriptome (Oliver et al., 1998). Metabolomics was revolutionized by the development and adoption of ultra-high performance liquid chromatography (UPLC) and high-resolution mass spectrometry (MS), which enabled better resolution of structurally similar metabolites and better assignment of potential

formulas, respectively (Balogh, 2004; Swartz, 2005). These advances allowed the development of improved metabolite libraries and cataloging of known metabolites, and in turn, better assessment of unknown metabolites (Halket et al., 2005; Kind and Fiehn, 2007; Horai et al., 2010). Around the same time, the first full genomes were published for humans and *Arabidopsis thaliana*, marking the start of the "-omics" era (Kaul et al., 2000; Lander et al., 2001). For specialized metabolism, the omics era expanded the range of study through generation of expressed sequence tag (EST) libraries rather than metabolomics, which could be produced from specific tissue types, enriched for sequences relevant to a known target pathway, such as tropane alkaloids in *Hyoscyamus niger*, where an EST library from the roots was used to identify a cytochrome P_{450} in tropane biosynthesis, or the monoterpene indole alkaloid (MIA) pathway in *Catharanthus roseus*, where an EST library from the leaf epidermis revealed several candidate MIA biosynthetic transcripts, one of which was confirmed to act in that pathway (Li et al., 2006; Murata et al., 2008). The advent of next-generation sequencing (NGS) in the late 2000's further lowered the barrier to exploration of specialized metabolism by reducing the cost of sequencing, and as such, enabling the generation of more sequencing data (Kim and Buell, 2015). An example of the utility of lower-cost NGS in probing a pathway only found in non-model species comes from mayapple, *Podophyllum hexandrum*, where an existing Medicinal Plants Consortium RNA-seq dataset was augmented by an additional RNA-seq dataset based on wounded leaf to identify 29 candidates for the biosynthesis of an etoposide aglycone (Figure 1.1) (Lau and Sattely, 2015). In this example, additional resources were needed to go from candidates to a confirmed pathway, including a system for high-throughput transient gene expression for pathway reconstruction in a

heterologous system, and metabolomics to identify desirable outputs from the reconstruction, step by step (Lau and Sattely, 2015). The above examples illustrated the use of NGS data and high-throughput screening in a reverse genetic context, but these technologies are also used in the study of specialized metabolism in forward genetics, as was done for a variant of opium poppy (*Papaver somniferum*) producing noscapine (Figure 1.1) (Winzer et al., 2012). In that example, *P. somniferum,* opium poppy, plants producing noscapine were identified using metabolomic screening, and found through NGS to possess a gene cluster unique to noscapine biosynthesis, and the candidates in the cluster were screened using loss-of-function by virus induced gene silencing (VIGS) (Winzer et al., 2012). In the cases with poppy and mayapple, the combination of NGS, metabolomics, and high-throughput functional analysis with transient expression or VIGS was used to reconstruct entire multistep pathways, in contrast to earlier studies where poorer throughput or a lack of NGS resources led to identification of single pathway steps at a time (Li et al., 2006; Murata et al., 2008).

Alkaloids and their importance to humans

Specialized metabolism in plants occupies a vast chemical space, comprising a mix and match between sugars, amino acids, fatty acids, isoprenoids, phenylpropenoids and metabolites derived from these components, but this diversity can be summarized broadly into terpenoids, phenolics, and alkaloids (Alseekh and Fernire, 2018). Alkaloids are defined as all compounds possessing a basic nitrogen atom in a heterocyclic ring and are named for the alkaline aqueous solutions such compounds produce. The term was coined in 1819 but did not come into wider usage until a review in 1882 (Meißner, 1819;

Jacobsen, 1882; Aniszewski, 2007; Nic et al., 2014). Alkaloids do not share common structures with one another across their classes, nor do they have common biochemical origins, a trait that sets them apart from the other major groups of specialized metabolites (Hesse, 2002). Some major types of alkaloids relevant to humans include purine alkaloids like the legal recreational drug caffeine, benzylisoquinoline alkaloids (BIAs) which include diverse structures and uses, such as the painkiller opioid morphine, the potential chemotherapeutic noscapine, and colchicine, used variously as a treatment for gout, a chemotherapeutic, and in plant cell culture to induce polyploidy, MIAs, which include the chemotherapeutic drugs camptothecin, vincristine and vinblastine, the antimalarial quinine, and the pesticide strychnine, and tropane alkaloids, which include both narcotics and pharmacueticals, such as cocaine and scopolamine (Figure 1.1) (Dermen, 1940; Ye et al., 1998; O'Connor and Maresh, 2006; Aniszewski, 2007; Kuo et al., 2015).

The broad uses and popularity of alkaloids have led to substantial efforts in cultivation of species which produce them, as well as to recapitulate their production in tractable microbial systems when agricultural production is unable to match demand. The former case can be observed in cultivation of coffee, cocoa, and tea which are all producers of caffeine, theobromine, and related purine alkaloids (Figure 1.1), with global agricultural yields in the millions of tons, and in cultivation of *P. somniferum* in Tasmania for legal opioids and Afghanistan for illicit opioids (Legislative Council Select Committee Inquiry: Tasmanian Poppy Industry, 2012; Diby et al., 2017; Afghanistan Opium Poppy Survey, 2017). Despite the successful and profitable cultivation of poppy for its alkaloids in Tasmania, the risk associated with the highly concentrated supply has led to considerable

efforts and advances made in the production of these compounds in microbes, including production of thebaine and noscapine (Figure 1.1) in brewer's yeast, *Saccharomyces cerevisiae*, though these first complete reconstructed pathways were not economical at yields of less than 1 µg L^{-1} and 1.64 µM, respectively (Galanie et al., 2015; Li and Smolke, 2016). Further noscapine engineering in yeast with an improved yield of 2.2 mg L^{-1} has been reported through expression tuning and optimization of culture medium and conditions (Li et al., 2018). An alternative route to thebaine has been pursued in *Escherichia coli* with co-cultivation of multiple strains, each possessing only a portion of the whole opioid pathway, where yields of 2.1 mg L^{-1} are reported, still short of economic viability compared to agriculture, but indicative of the potential for microbial production of alkaloids with long biosynthetic pathways (Nakagawa et al., 2016). Similarly, the low agricultural yield of vincristine and vinblastine from *C. roseus* has driven efforts into yeast production, resulting in engineering of a pathway to strictosidine (Figure 1.1), the key branch point and intermediate in MIA biosynthesis leading to those compounds, but at an uneconomical yield as in opioid engineering (Brown et al., 2015). The current incomplete state of the tropane alkaloid biosynthetic pathway has prevented efforts to engineer *de novo* tropane production in microbial systems.

Tropane alkaloids are characterized by a fused *N*-methyl-8-azabicyclo[3.2.1]octane ring system, with the most pharmaceutically used compounds being various esters, including the narcotic, cocaine, and atropine (DL-hyoscyamine) and scopolamine, which are pharmaceuticals (Figure 1.1). Atropine and scopolamine are synthesized by select members of from the Solanaceae family are currently used medicinally as anticholinergic

agents for their antagonism of one or more muscarinic acetylcholine receptors (Grynkiewicz and Gadzikowska, 2008). Atropine is a general inhibitor with pharmacologically relevant affinity and access to all five acetylcholine receptors and is used as part of a cocktail with an oxime and a diazepam to alleviate symptoms from organophosphorus pesticide poisoning (Eddleston et al., 2008; RamaRao et al., 2014). Scopolamine is used to treat post-operative nausea, though both it and atropine are effective inhibitors of the 5-HT_3 receptor which is targeted for this purpose (Lochner and Thompson, 2016). Some semisynthetic drugs derived from atropine or scopolamine include tiotropium and ipratropium, which are prescribed for treatment of chronic obstructive pulmonary disorder (COPD), tiotropium being the first long-acting muscarinic antagonist approved for this purpose (Figure 1.1) (Mastrodicasa et al., 2017).

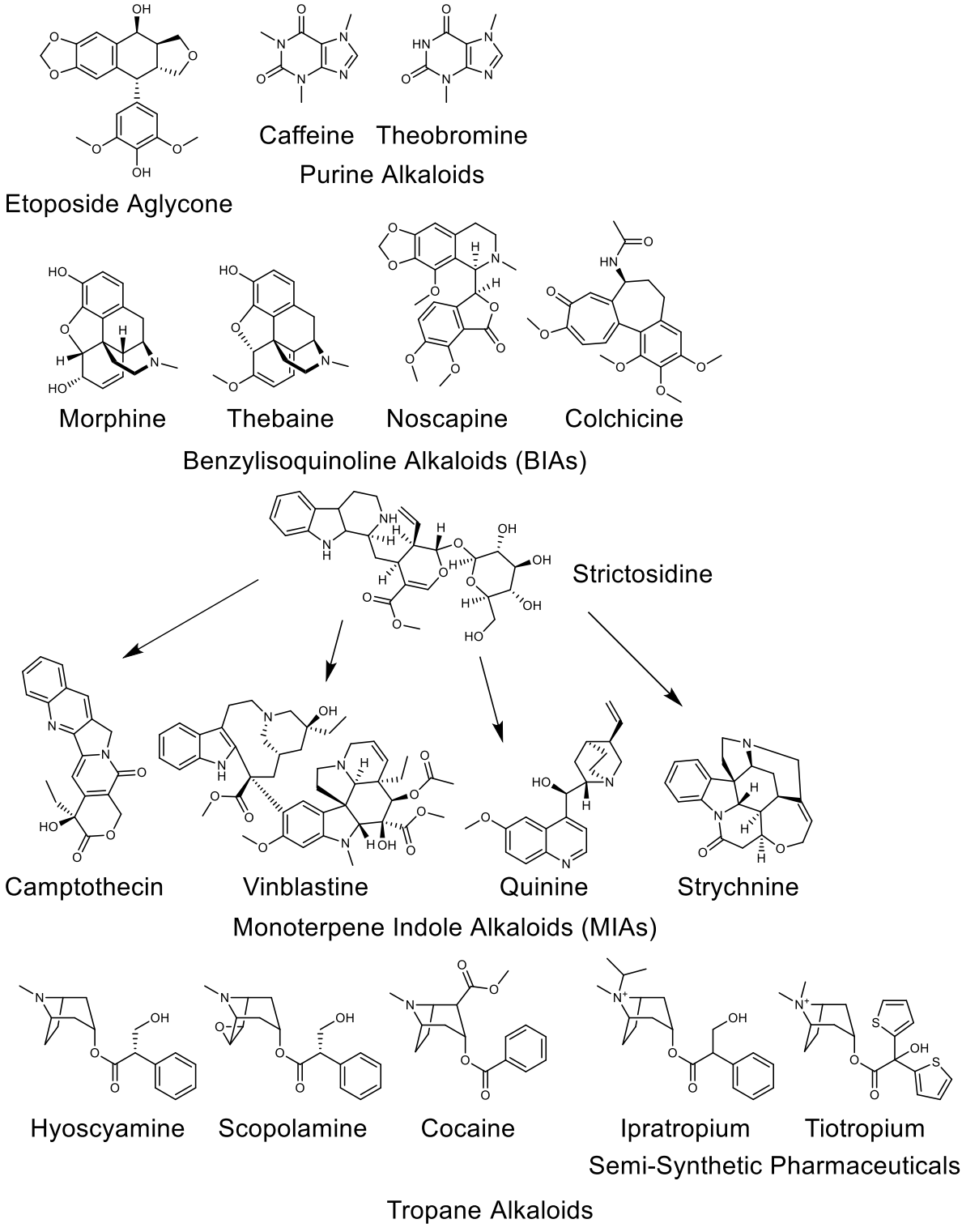

Figure 1.1 Select plant specialized metabolites and pharmaceuticals

Structures of alkaloid examples from the purine, benzylisoquinoline, monoterpene indole, and tropane classes are provided.

Identification and early investigations of tropane alkaloids

The first tropane alkaloid purified was atropine from *A. belladonna* in 1831 and independently in 1833 (Mein, 1831; Geiger and Hesse, 1833). The first synthesis of the tropane core as tropinone was accomplished through a lengthy synthesis starting from cycloheptanone, though this was surpassed by Robinson in the first classic biomimetic chemical synthesis (Willstätter, 1901; Robinson, 1917). The biomimetic Robinson route used methylamine, succinic dialdehyde, and acetone dicarboxylic acid, with the biomimetic steps involving amine-aldehyde imine formation, followed by decarboxylative condensation between the imine and acetone dicarboxylic acid through its β-keto acid chemistry. The rings are closed by a second reaction cycle using the second aldehyde of succinic dialdehyde and the second β-keto acid group of the dicarboxylate (Figure 1.2) (Robinson, 1917). The biomimetic synthesis led to a proposal by Robinson that a similar mechanism might produce the compound *in planta* (Robinson, 1955). Following these synthetic efforts, the biosynthesis of the tropane alkaloids hyoscyamine and cocaine was studied in the Solanaceae and Erythroxylaceae, respectively, using radiolabeled precursor and intermediate candidate compounds. This has resulted in the near-complete identification of the tropane biosynthetic pathway for hyoscyamine and scopolamine in the Solanaceae.

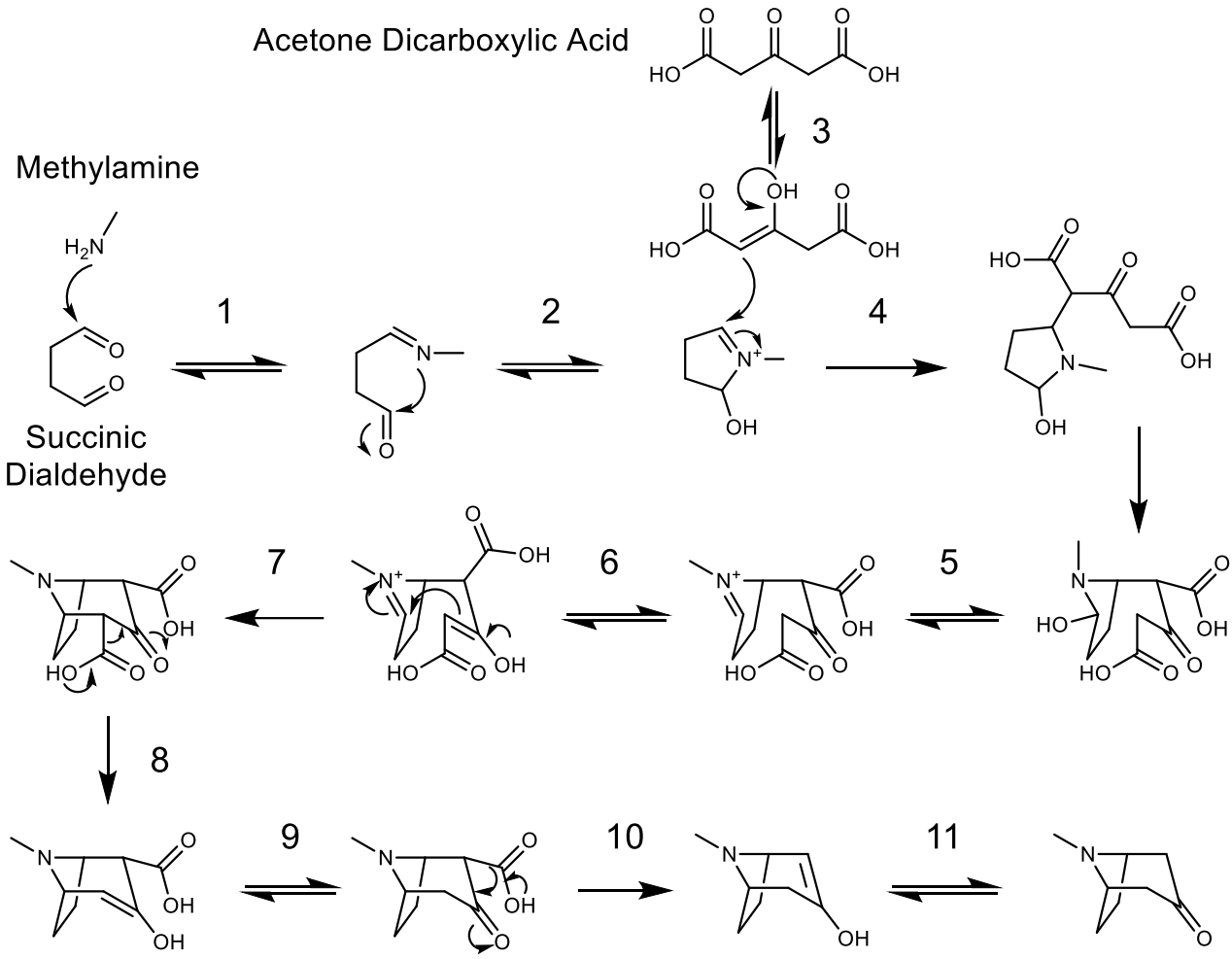

Figure 1.2 The biomimetic Robinson tropinone synthesis mechanism

In the Robinson tropinone synthesis, methylamine attacks one aldehyde group on succinic dialdehyde (1) to form an imine, where the nitrogen performs a second attack on the second aldehyde (2) to create the pyrrolidine ring. Acetone dicarboxylic acid undergoes a keto-enol tautomerization (3), driving the first carbon-carbon bond formation (4). The first condensation product is redrawn for clarity and will undergo a dehydration (5) to produce a second imine, while also undergoing further keto-enol tautomerization (6), driving the second carbon-carbon bond formed in the reaction (7), which produces the tropane core. The first loss of carbon dioxide (8) leaves an enol, which undergoes keto-enol tautomerization (9), allowing the second loss of carbon dioxide (10), where a final keto-enol tautomerization (11) produces tropinone.

Origin of the first ring of tropane alkaloids

The first ring in tropane alkaloid biosynthesis is shared with nicotinoid alkaloids and is comprised of a 5-member nitrogen containing ring (Leete et al., 1958; Tiburcio and Galston 1985). Putrescine is the primary metabolite which provides the carbon and nitrogen for this ring, but in plants, putrescine itself is derived the proteinogenic amino acids arginine and ornithine. These amino acids can furnish putrescine via several routes. The route from ornithine is the most direct, requiring a single enzyme, ORNITHINE DECARBOXYLASE, (ODC). ODC activity was first identified in plants from *Nicotiana tabacum* plants and cell cultures, and *Solanum lycopersicum* ovaries, and the gene was cloned from *Datura stramonium* (Yoshida, 1969; Heimer and Mizrahi, 1982; Michael et al., 1996). A second route to putrescine biosynthesis, unique to plants and beginning with arginine, utilizes ARGININE DECARBOXYLASE (ADC) activity, which was also identified in *N. tabacum*, but first cloned from *Avena strigosa* (Yoshida 1969; Bell and Malmberg, 1990). ADC activity produces agmatine, which is converted to *N*-carbamoylputrescine by AGMATINE IMINOHYDROLASE (AIH), and then to putrescine by *N*-CARBAMOYLPUTRESCINE AMIDOHYDROLASE (NCPAH). Both relevant genes for the remainder of this pathway were identified from *Arabidopsis thaliana* which lacks the redundant ODC pathway (Hanfrey et al., 2001; Piotrowski et al., 2003; Janowitz et al., 2003; Illingworth et al., 2003). Arginine can be converted to ornithine through ARGINASE, which also possesses AGMATINASE activity producing putrescine, constituting a third route for biosynthesis (Muszyńska and Reifer, 1968; Cheema et al., 1969; Chen et al., 2004; Patel et al., 2017). (Figure 1.3). Incorporation of carbon from ornithine into tropanes was first determined using labeled ornithine fed to *Datura inoxia* plants and producing

asymmetrically labeled hyoscyamine (Leete et al., 1954). Arginine was assumed to contribute to the tropane pathway through its metabolic linkage to ornithine. Initial asymmetric labelling of tropanes in *D. inoxia* and *D. stramonium* was followed by labeling studies which produced symmetrically labeled products in *H. niger*, which would be more indicative of putrescine as the direct precursor (Leete 1962; Leete 1964; Hashimoto et al., 1989a).

The role and position of putrescine in tropane biosynthesis was solidified through examination of putative enzyme activities in both *D. stramonium* and *A. belladonna*. No activity was found for methylation of ornithine or for arginine, but activity was found for methylation of putrescine. Further activities were assessed in these tropane producing species for ADC, ODC, and arginase, together indicating that both arginine and ornithine can furnish putrescine, and that putrescine is the dominant route to the *N*-methylputrescine used for tropane alkaloid biosynthesis. The labeling studies conducted indicated incorporation from labeled ornithine, arginine, agmatine, and putrescine, which are consistent with the positive enzyme activities assayed in each species (Walton et al., 1990). These data are consistent with previous studies in *H. niger*, where ornithine and arginine decarboxylase activities were found, alongside PUTRESCINE *N*-METHYLTRANSFERASE (PMT) activity, and where labeled ornithine, arginine, and putrescine were strongly incorporated into hyoscyamine (Hashimoto et al., 1989b; Hashimoto et al., 1989c). The relative contributions of the two decarboxylative pathways was probed in *D. stramonium* using specific inhibitors, with the finding that both pathways are involved in this species (Robins et al., 1990).

The gene encoding the enzyme for (PMT) activity was first cloned from *N. tabacum*, and subsequently cloned from tropane producing species such as *A. acutangulus* and *S. tuberosum* (Hibi et al., 1994; Liu et al., 2005; Stenzel et al., 2006,). *N*-methylputrescine is subsequently oxidized to *N*-methylaminobutyraldehyde. This activity was identified in *N. tabacum*, and was confirmed in *H. niger*, *D. stramonium*, and *Brugmansia candida x aurea* (Mizuzaki et al., 1972; Hashimoto et al., 1990). The activity identified was preferential to *N*-methylputrescine, with little activity using symmetrical polyamines such as putrescine or cadaverine (Boswell et al., 1999). The gene encoding METHYLPUTRESCINE OXIDASE activity (MPO) was identified by two groups simultaneously from *N. tabacum,* a species which lacks tropanes, but still produces nicotine (Heim et al., 2007; Katoh et al., 2007). Once oxidized, this intermediate can undergo a spontaneous cyclization to an *N*-methyl-Δ^1-pyrrolinium cation through an intramolecular Mannich reaction, forming the first tropane ring (Figure 1.3).

Creating the second ring of the tropane core

For many years, the three carbon bridge across the pyrrolidine ring was hypothesized to derive from acetoacetate, based upon labeling studies where feeding of labeled hygrine resulted in label incorporation into tropanes in *Datura metel*, *D. stramonium*, and *Scopolia lurida* (Kaczkwski et al., 1961; Liebisch et al., 1972). These experiments were later refined, with the finding that hygrine is an unlikely precursor of tropanes (Abraham and Leete, 1995). Instead the most complex compound which is efficiently incorporated into tropanes is an ethyl ester of 4-(1-methyl-pyrrolidine)-3-oxo-butanoic acid. In each case, the ester was fed as a racemic mixture with two labeled carbons, and the recovered

tropanes indicated incorporation of both enantiomers (Abraham and Leete 1995; Robins et al., 1997). The enzymes responsible for the conversion of *N*-methyl-Δ^1-pyrrolinium to tropinone through a 4-(1-methyl-pyrrolidine)-3-oxo-butanoic acid intermediate in *A. belladonna* were recently identified as a PYRROLIDINE POLYKETIDE SYNTHASE (PyKS) and a cytochrome P_{450}, CYP82M3, (TROPINONE SYNTHASE, TS) (Bedewitz et al., 2018). Tropinone is subsequently reduced to one of a pair of epimeric alcohols, tropine (α) and pseudotropine (β), via TROPINONE REDUCTASE I or II, respectively, to produce a suitable acylation acceptor (Figure 1.3) (Hashimoto et al., 1992; Nakajima et al., 1993).

Biosynthetic origins of the tropate acyl group

Hyoscyamine is the ester of tropine with (*S*)-tropic acid. *In vivo* labelling studies indicated that the tropic acid moiety of hyoscyamine is derived from rearrangement of L-phenylalanine (Leete, 1960; Leete et al., 1975; Nyman 1994). Further labeling studies using phenylpyruvic acid, the α-keto acid congener of L-phenylalanine, indicated that this metabolite can also provide the acyl group for hyoscyamine (Liebisch et al., 1970). Around the same time as these labeling studies, a novel tropane alkaloid was identified, comprised of tropine and D-phenyllactic acid, forming (*R*)-littorine (Evans and Major, 1968; Cannon et al., 1969). The potential for this compound to serve as an intermediate in hyoscyamine biosynthesis was tested through additional labeling work. First, labeled L-phenylalanine was shown to furnish the phenyllactic acid moiety of littorine (Evans and Woolley, 1969). Subsequent feeding of littorine, labeled on both the tropine and phenyllactate moieties, was found to label hyoscyamine in its tropine and tropate moieties, but the ratio of the two labels was substantially altered in the recovered

hyoscyamine from the provided tracer. This anomaly was approached with two hypotheses, both supposing that the provided littorine was hydrolysed *in planta* and that the labeled tropine was re-esterified. The first hypothesis stated that the hydrolysed phenyllactic acid was rearranged to tropic acid, then re-esterified, the second stated that hydrolyzed phenyllactic acid was diluted with a pool of cold phenyllactic acid and that phenyllactic acid could be easily esterified to tropine, reforming littorine with an altered label ratio (Leete and Kirven, 1974). Feeding of labeled DL-phenyllactic acid was also shown to label the tropic acid moiety of hyoscyamine, though this did not resolve the question of when the rearrangement occurs (Evans and Woolley 1976). Additional labeling studies solidified the placement of phenyllactic acid as the phenylalanine derivative closest to the rearrangement into tropic acid, as opposed to a rearrangement of phenylpyruvic acid (Ansarin and Woolley, 1992). To test the hypothesis that phenyllactic acid undergoes rearrangement to tropic acid and is subsequently esterified to form hyoscyamine, another set of labeling experiments was performed, using phenyllactic acid or tropic acid, with the result that phenyllactic acid label incorporation is superior to tropic acid label incorporation. This result implied that phenyllactic acid might be esterified to form littorine, and only then undergo rearrangement to hyoscyamine, in contrast to Leete's earlier results (Robin et al., 1994).

The dedication of phenylalanine to hyoscyamine biosynthesis was confirmed enzymatically by the identification of a root specific, directional, and preferential PHENYLALANINE AMINOTRANSFERASE (ArAT4) from *A. belladonna* (Bedewitz et al., 2014). This aminotransferase produces the previously implicated phenylpyruvic acid,

which can be reduced to phenyllactic acid by a root specific PHENYLPYRUVIC ACID REDUCTASE (PPAR) (Qiu et al., 2018). The identity of the enzymes responsible for the incorporation of D-phenyllactic acid into littorine are not yet known, nor is the route, though a phenyllactoyl-CoA intermediate has been proposed, analogous to the final step in cocaine biosynthesis, using a BAHD acyltransferase for the transfer of the acyl group to tropine (Robins et al., 1994; Schmidt et al., 2015; Kim et al., 2016). Alternatively, there exists a second type of acyltransferases in plants referred to as serine carboxypeptidase-like acyltransferases (SCPLs) which could potentially catalyze this reaction using a glucose ester of D-phenyllactic acid (Bontpart et al., 2015). Once formed, (*R*)-littorine is rearranged into hyoscyamine aldehyde by a cytochrome P_{450}, CYP80F1, trivially known as LITTORINE MUTASE (Li et al., 2006). The reaction of littorine mutase confirms that rearrangement of phenyllactate to tropate occurs as an ester of tropine, and not as the free acid, as indicated by Robins in 1994. At present, the enzyme responsible for reduction of this aldehyde to the natural product hyoscyamine remains an unanswered question in tropane alkaloid biosynthesis. Hyoscyamine is at this point hydroxylated to first form 6β-hydroxyhyoscyamine (anisodamine), and then oxidized a second time to form the epoxide scopolamine by HYOSCYAMINE-6β-HYDROXYLASE/EPOXYGENASE, (H6H) (Figure 1.3) (Hashimoto and Yamada, 1987; Hashimoto et al., 1987; Matsuda et al., 1991).

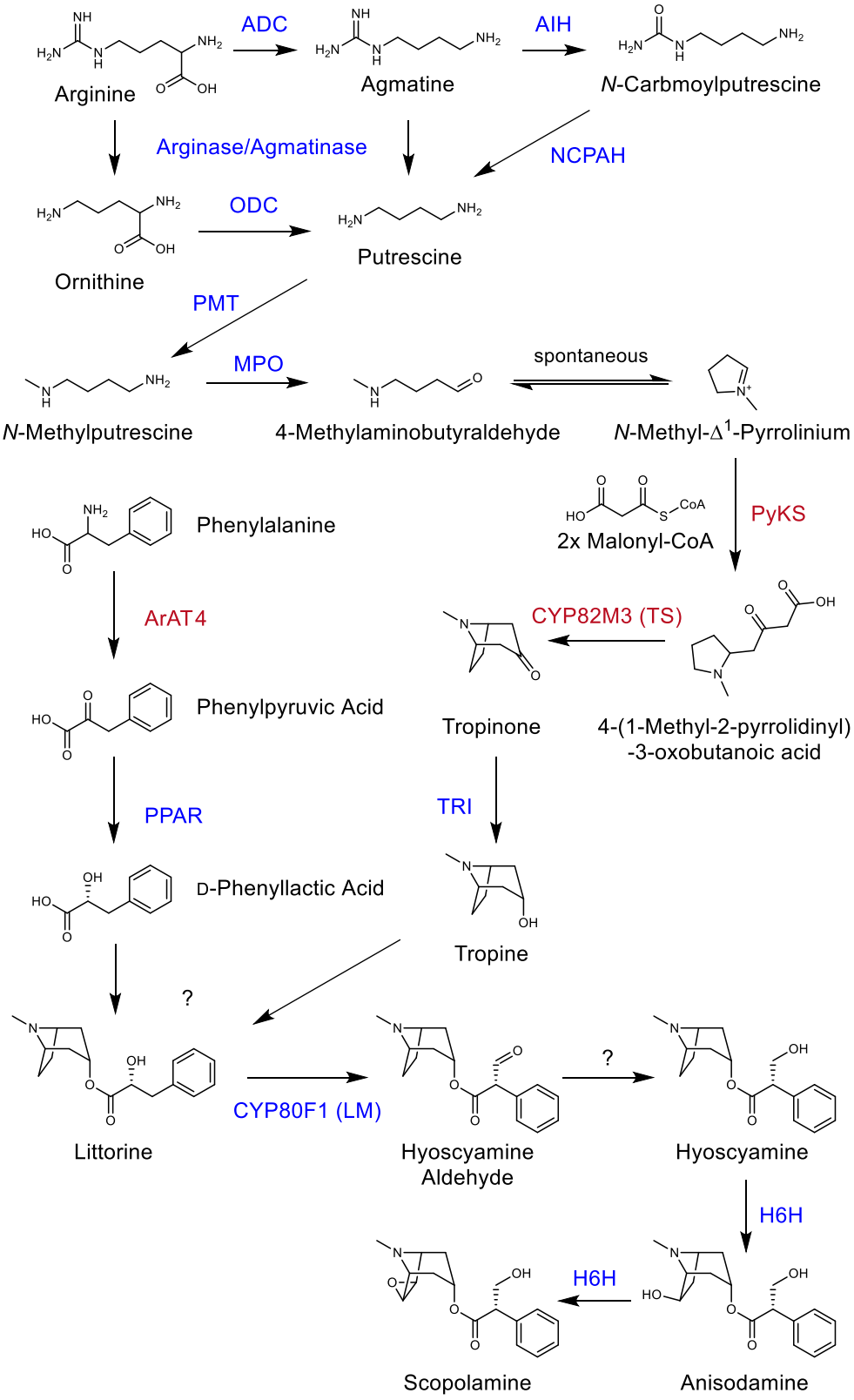

Figure 1.3 The tropane alkaloid biosynthesis pathway from arginine and ornithine to scopolamine

Figure 1.3 (cont'd)

Experimentally validated enzymes are shown in blue, enzymes published in the course of this thesis are shown in red, and unknown reactions are noted with question marks. Enzyme abbreviations are as follows: ADC; arginine decarboxylase, ODC; ornithine decarboxylase, AIH; agmatine iminohydrolase, NCPAH; *N*-carbamoylputrescine amidohydrolase, PMT; putrescine methyltransferase, MPO; methylputrescine oxidase, PyKS; pyrrolidine polyketide synthase, CYP80M3 (TS); tropinone synthase, TRI; tropinone reductase I, ArAT4; phenylalanine aminotransferase, PPAR; phenylpyruvic acid reductase, CYP80F1 (LM); littorine mutase, H6H; hyoscyamine-6β-hydroxylase/epoxygenase.

Localization of tropane alkaloid biosynthesis

Tropane alkaloids in the Solanaceae are, in general, produced in the roots, with more production in the lateral roots than the taproot in species where taproots are formed. Regarding the enzymatic steps required to produce putrescine, a putative ODC transcript with root preferential expression was identified in *A. belladonna*, as well as putative ADC and arginase transcripts with root preferential expression from *A. acutangulus* (Bedewitz et al., 2014; Cui et al., 2015). The first committed step in tropane alkaloid biosynthesis, PMT is similarly expressed only in roots, and has been found to be expressed very specifically in the root pericycle in *A. belladonna* (Figure 1.4) (Suzuki et al., 1999a). Both of the tropinone reductases, TRI and TRII have been found to have root preferential expression (*Brugmansia arborea* and *Withania somnifera*) or accumulation, particularly to the endodermis and cortex (*H. niger* and *S. tuberosum*), though the TR transcripts from *B. arborea* and *W. somnifera* and the protein from *S. tuberosum* were also found in other tissue types, predominantly stems or tissues derived from stems such as stolons for *S. tuberosum* (Nakajima et al., 1999; Nakajima and Hashimoto, 1999; Kaiser et al., 2006; Kushwaha et al., 2013; Qiang et al., 2016). The ArAT4 and PPAR transcripts responsible for producing phenyllactic acid in *A. belladonna* were identified and confirmed in part by their root preferential expression, and PPAR was localized to the pericycle and endodermis of the roots (Bedewitz et al., 2014; Qiu et al., 2018). The littorine mutase transcript from *H. niger* has been shown to have highly specific root expression, but it has not been localized to the cellular level (Li et al., 2006). The H6H protein, however, has been localized to the roots in the pericycle for several species, including *A. belladonna*, *Duboisia myoporoides*, *H. gyorffi*, *H. muticus*, and *H. niger* (Hashimoto et al., 1991;

Kanegae et al., 1994; Suzuki et al., 1999b). Exceptions to this pattern of root localization for H6H are found in *Hyoscyamus senecionis*, which expresses H6H in the aerial parts of the plant, with the significant result that those parts contain scopolamine, rather than atropine, as their major alkaloid, and in *A. belladonna* where there is H6H protein in anthers as well as roots (Suzuki et al., 1999b; Dehghan et al., 2013). Tissue and cell-specific expression are common features in plant specialized metabolic pathways and have been used to identify candidate specialized metabolism genes in multiple pathways and systems, including acylsugars in tomato, triterpenes in oat, MIAs in *C. roseus*, and BIAs in *P. somniferum* (Mylona et al., 2008; Schilmiller et al., 2012; Onoyovwe et al., 2013; Schilmiller et al., 2015; Dugé de Bernonville et al., 2015; Fan et al., 2016). The root preferential expression profile of tropane alkaloid biosynthetic genes in the Solanaceae provides a useful filter for identifying new candidate genes in this pathway.

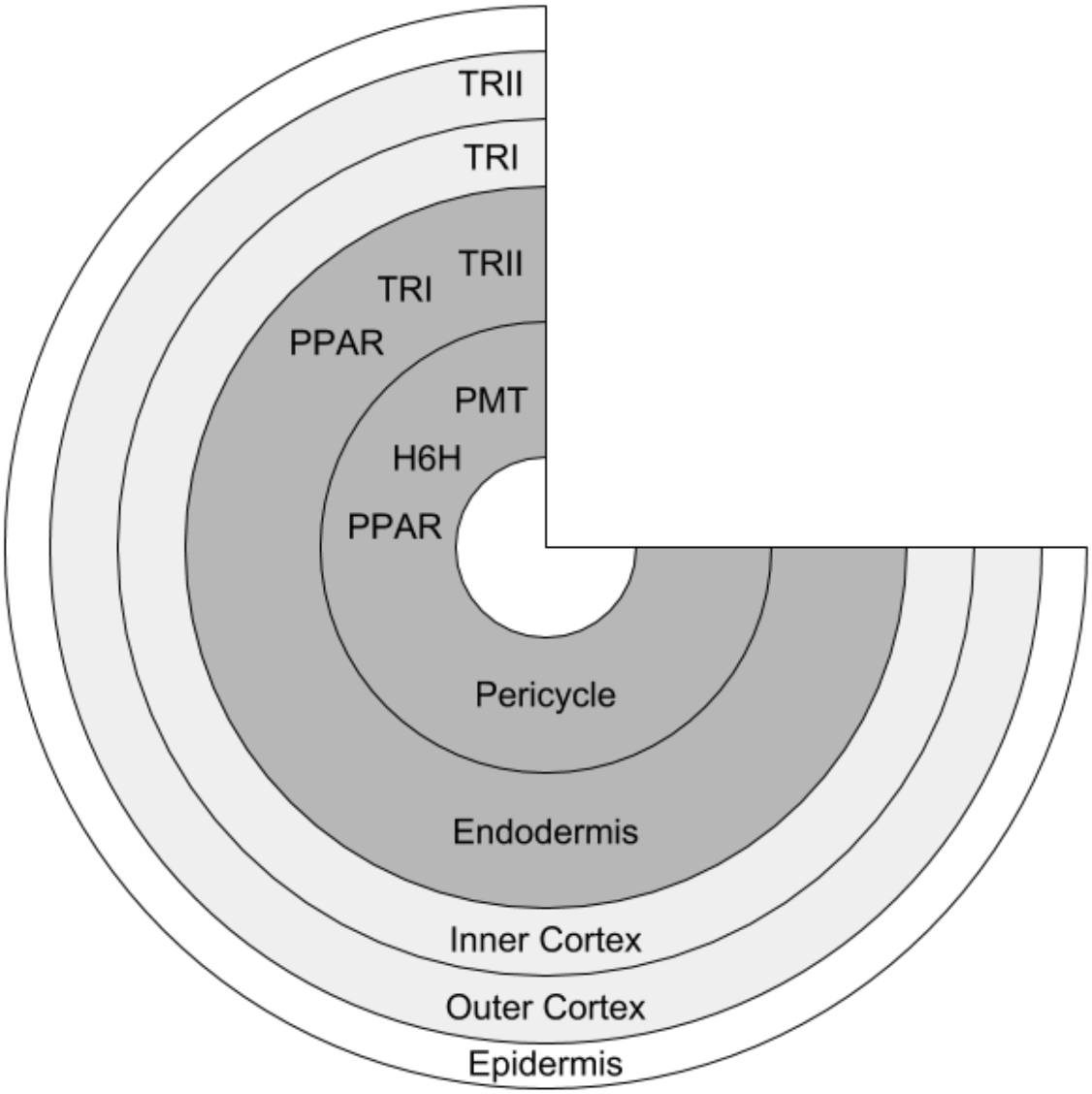

Figure 1.4 Localization of tropane alkaloid biosynthesis in Solanaceae roots

The cell layers in Solanaceous lateral roots are shaded according to the number of tropane alkaloid biosynthetic genes which are expressed or enzymes which accumulate in that cell layer. Enzyme abbreviations are as follows: PMT; putrescine methyltransferase, TRI; tropinone reductase I, TRII; tropinone reductase II, PPAR; phenylpyruvic acid reductaseH6H; hyoscyamine-6β-hydroxylase/epoxygenase.

Tropane alkaloid diversity in plants

The main legitimate commercial source for tropane alkaloids for pharmaceutical purposes are plantations of *Duboisia leichhardtii x myoporoides* hybrids which have been bred for alkaloid content as well as agronomic traits such as drought resistance and pest resistance as well as reduced environmental effect on alkaloid content and composition (Ohlendorf, 1996). *Duboisia* is a more basal Solanaceous genus, as compared to *Atropa*, *Hyoscyamus*, or *Datura*, though all these genera produce hyoscyamine and scopolamine (Eich, 2008; Särkinen et al., 2013). Although hyoscyamine and scopolamine are the most well studied tropane alkaloids, they represent only one class of this diverse group of alkaloids.

In the Solanaceae, tropinone is the first metabolite bearing the fused-ring system, and the first branch point for chemical diversity through generation of the epimers tropine (α) and pseudotropine (β). Both tropine and pseudotropine can be esterified in the tribe Datureae which contains the genera *Datura* and *Brugmansia*, with a variety of aliphatic acyl groups, most commonly acetic acid and tiglic acid (Eich, 2008). In these genera, there also exist tropanes with additional hydroxylations and aliphatic esters on those groups (Eich, 2008). In the broader Solanaceae, pseudotropine is the source of calystegine alkaloids, which are demethylated and polyhydroxylated sugar mimics (Dräger, 2004).

The morning glory family, Convolvulaceae, is phylogenetically related to the Solanaceae as both are within the Solanales. This family also contains tropanes, most consistently calystegines, but also esters of benzoic and cinnamic acid derivatives (Dräger, 2004, Eich, 2008). There are also unusual tropanes present in some species, such as

prenylated tropane esters, monoterpene esters, and tropanes with a rearranged core where the 3-hydroxyl group is transferred to the 2-position (Jenett-Siems, et al., 2005; Ott et al., 2006; Ott et al., 2013). A single tropane related activity has been isolated from this family, PMT, in two enzymes, PMT1 and PMT2 in *Calystegia sepium*, which is the namesake for the calystegine alkaloids, indicating the potential relatedness and common origin for tropane alkaloid biosynthesis in these two closely related families and the potential for the existence of orthologous activities to the identified steps in Solanaceous tropane biosynthesis (Teuber et al., 2007).

In contrast, the tropane biosynthetic pathway in Erythroxylaceae appears to be independently derived, with the major natural tropane esters possessing a carbomethoxy moiety not found in the Solanaceae. The analogous step to the Solanaceous tropinone reductases I and II is methylecgonone reductase (MecR) in *Erythroxylum coca* (Jirschitzka et al., 2012). This enzyme was recruited from the aldo-keto reductases, whereas the tropinone reductases were derived from short-chain dehydrogenase reductases, emphasizing the independent evolution of tropanes in these lineages (Jirschitzka et al., 2012). The only additional dedicated tropane biosynthetic enzyme identified to date in the Erythroxylaceae is cocaine synthase, a BAHD acyltransferase whose analogous Solanaceae activity is yet unknown (Schmidt et al., 2015). The overwhelming bias in favor of root biosynthesis for Solanaceous tropanes is contrasted in *Erythroxylum coca*, where both the TR analogous enzyme MecR and COCAINE SYNTHASE are localized to leaves, rather than roots, further highlighting the independent origin of tropane alkaloid biosynthesis (Jirschitzka et al., 2012; Schmidt et al., 2015). The

Erythroxylaceae also contains calystegine alkaloids, a point of structural commonality with the Solanales, as well as with Moraceae and Brassicaceae, two further tropane containing families where calystegines are found (Asano et al., 1994; Brock et al., 2005; Brock et al., 2006; Reinhardt et al., 2014).

In the Brassicaceae, there is a single enzyme identified in tropane alkaloid biosynthesis, a bifunctional tropinone reductase (CoTR) from the short-chain dehydrogenase reductase family which produces both tropine and pseudotropine in *Cochlearia officinalis* (Brock et al., 2008). *Cochlearia*, in addition to calystegines, also contains an ester of tropine with 3-hydroxybenzoic acid, cochlearine (Platonova and Kuzovkov, 1963; Liebisch et al., 1973). No tropane pathway enzymes are currently known from Moraceae, so that pathway's relatedness to other tropane pathways cannot yet be speculated upon. Regardless, Erythroxylaceae, Brassicaceae, and Moraceae are all members of the Rosid lineage, which is ~100 million years removed from the Solanales, which are in the Asterid lineage (Zeng et al., 2017). That CoTR and MecR have been recruited from different groups of oxidoreductases implies that tropanes have evolved at least twice in the Rosid lineage in addition to the TRs of Solanaceae, which would represent a third origin event (Brock et al., 2008; Jirschitzka et al., 2012). More basally divergent still than these groups are the Proteales, including Proteaceae, which contains alkaloids which are structurally similar to tropanes, but are not reported to contain any specific compounds in common with other tropane producers, potentially representing a fourth independent origin of tropane alkaloid biosynthesis in plants. These compounds often include a third fused ring in the core, or a phenyl ring connected by carbon-carbon bonds, termed pyranotropanes

and benzyltropanes, respectively, as well as hydroxylated and esterified derivatives (Bick et al., 1971; Lounasmaa et al., 1980; Butler et al., 2000; Griffin and Lin, 2000; Yang et al., 2017; Zeng et al., 2017).

A. belladonna as a model species for exploring tropane alkaloid biosynthesis

Societies since antiquity have noted both the potential medicinal uses and the dangers of tropane bearing plants, including henbane (*Hyoscyamus* spp.), mandrake (*Mandragora* spp.), and deadly nightshade (*Atropa* spp.) The earliest such mention is found in the Egyptian *Ebers Papyrus* from 1530 BCE for mandrake and henbane, with tomb artwork following for mandrake (Daunay et al., 2007). It was not until the work *De Materia Medica* by the Greek physician Dioscorides that *Atropa* was recognized as a separate plant from mandrake (Lee, 2007). Aside from mythological interpretations and religious uses, including mandrake as the drug given by Circe during the Odyssey, the association with the Greek Fate Atropos – whose job is to cut the thread of life, and as addition to wine consumed during the mystery rituals of Dionysus, these plants also found employment in producing twilight sleep, an early form of anesthesia (Holzman, 1998; Lee, 2007). During the medieval and early modern periods, these herbs became associated with the practice of witchcraft, particularly as ingredients of ‘flying ointments’ comprised of “hemlock, nightshade, henbane, and mandrake” as reported by Andrés Laguna in his commentary on *De Materia Medica*. This ointment was further reported to produce a deep stupor (the twilight sleep) and vivid hallucinations when applied by Laguna, and took 36 hours to wear off (Rothman, 1972). In the time since the pure compound hyoscyamine was isolated, these plants and their alkaloids have been implicated in accidental and

purposeful poisonings, with a 1911 report detailing 682 cases of poisoning, with 60 fatalities, further underlining the narrow therapeutic window noted by Dioscorides (Rothman, 1972; Lee, 2007).

Atropa is a basal genus within the tribe Hyoscyameae, derived from an ancient hybridization event between a tetraploid ancestor and an unknown, extinct diploid ancestor as determined using a retrotransposon marker (Yuan et al., 2006). The Hyoscyameae tribe originated in South America, then spread to Eurasia where the tribe diversified within the Mediterranean region with all its genera established by the end of the Miocene epoch (Tu et al., 2010). As noted, many of the alkaloid producing members of the tribe Hyoscyameae are polyploid, thus, use of next generation sequencing to assemble an *Atropa* genome would face difficulty from the allohexaploid genome of *A. belladonna* (Tu et al., 2005; Volkov et al., 2017). However, this task, while difficult, is not insurmountable, as evidenced by the recently completed genome of allohexaploid wheat (Appels et al., 2018). As such, it was determined that a transcriptome-based approach would be the most useful in approaching alkaloid biosynthesis in *A. belladonna*.

Research aims: Transcriptome-guided elucidation of tropane alkaloid biosynthesis in *A. belladonna*

At the onset of this research, the study of tropane alkaloid biosynthesis had not entered the genomics era and many gaps in our understanding of how these pharmaceutically important metabolites are synthesized remained, even in the Solanaceae family where hyoscyamine and scopolamine biosynthesis had been studied for decades. For example:

- Which enzymes are responsible for the conversion of *N*-methyl-Δ^1-pyrrolinium to tropinone and what is the role of the 4-(1-methyl-pyrrolidine)-3-oxo-butanoic acid intermediate identified by Leete and coworkers in the early 1990's?
- Second, what enzymes are required for committing phenylalanine into the tropane pathway?
- Third, what is the underlying mechanism for producing littorine from tropine and phenyllactic acid? Does this reaction require a BAHD acyltransferase or an SCPL acyltransferase, and their respective coenzyme A thioester or glucose-ester linked activated intermediates?

The research presented in this thesis addresses these questions using *Atropa belladonna* as a model species, a tender perennial in the Solanaceae family that has been used for centuries in traditional medicine and synthesizes hyoscyamine and scopolamine. This research was facilitated by the generation of a multi-tissue transcriptome assembly of *A. belladonna* that facilitated the identification of candidate genes in tropane alkaloid biosynthesis based on their preferential expression in root tissues, the site of tropane production in the Solanaceae. A virus-induced gene silencing (VIGS) system was also established in *A. belladonna* that enabled the potential role of candidate genes in tropane alkaloid biosynthesis to be investigated and this approach was paired with new methods to simultaneously and rapidly detect and quantify tropane alkaloids and their precursors by liquid-chromatography mass spectrometry based metabolite profiling. These combined resources were utilized together with more traditional biochemical methods to identify and characterize five new enzymes that catalyze steps in tropane alkaloid biosynthesis.

REFERENCES

REFERENCES

Afghanistan Opium Survey 2017 (2017). (Vienna).

Legislative Council Select Committee Inquiry: Tasmanian Poppy Industry (2012). (Hobart).

Abraham, T.W. and Leete, E. (1995). New Intermediate in the Biosynthesis of the Tropane Alkaloids in *Datura innoxia*. J. Am. Chem. Soc. **117**: 8100–8105.

Alseekh, S. and Fernie, A.R. (2018). Metabolomics 20 Years On: What Have We Learned and What Hurdles Remain? Plant J. **94**: 933–942.

Aniszewski, T. (2007). Definition, Typology and Occurrence of Alkaloids. In Alkaloids - Secrets of Life: Alkaloid Chemistry, Biological Significance, Applications and Ecological Role. (Elsevier: Amsterdam).

Ansarin, M. and Woolley, J.G. (1993). The Obligatory Role of Phenyllactate in the Biosynthesis of Tropic Acid. Phytochemistry **32**: 1183–1187.

Appels, R. et al. (2018). Shifting the limits in wheat research and breeding using a fully annotated reference genome. Science. **361: eaar7191**.

Asano, N., Oseki, K., Tomioka, E., Kizu, H., and Matsui, K. (1994). *N*-Containing Sugars from *Morus alba* and their Glycosidase Inhibitory Activities. Carbohydr. Res. **259**: 243–255.

Balogh, M.P. (2004). Debating Resolution and Mass Accuracy. LCGC North Am. **7**: 152–159.

Bedewitz, M.A. et al. (2014). A Root-Expressed L-Phenylalanine:4-Hydroxyphenylpyruvate Aminotransferase Is Required for Tropane Alkaloid Biosynthesis in *Atropa belladonna*. Plant Cell **26**: 3745–3762.

Bedewitz, M.A., Jones, A.D., D'Auria, J.C., and Barry, C.S. (2018). Tropinone Synthesis via an Atypical Polyketide Synthase and P450-Mediated Cyclization. Nat. Commun. **9**: 5281.

Bell, E. and Malmberg, R.L. (1990). Analysis of a cDNA Encoding Arginine Decarboxylase from oat reveals Similarity to the *Escherichia coli* Arginine Decarboxylase and Evidence of Protein Processing. Mol. Gen. Genet. **224**: 431–436.

Bick, I.R.C., Bremner, J.B., and Gillard, J.W. (1971). Methyl (*p*-Hydroxybenzoyl) Acetate and an Alkaloid, Bellendine, from *Bellendena montana*. Phytochemistry **10**: 475–477.

Bontpart, T., Cheynier, V., Ageorges, A., and Terrier, N. (2015). BAHD or SCPL Acyltransferase? What a Dilemma for Acylation in the World of Plant Phenolic Compounds. New Phytol. **208**: 695–707.

Boswell, H.D., Dräger, B., McLauchlan, W.R., Portsteffen, A., Robins, D.J., Robins, R.J., and Walton, N.J. (1999). Specificities of the Enzymes of *N*-Alkyltropane Biosynthesis in *Brugmansia* and *Datura*. Phytochemistry **52**: 871–878.

Brock, A., Bieri, S., Christen, P., and Dräger, B. (2005). Calystegines in Wild and Cultivated *Erythroxylum* Species. Phytochemistry **66**: 1231–1240.

Brock, A., Brandt, W., and Dräger, B. (2008). The Functional Divergence of Short-Chain Dehydrogenases Involved in Tropinone Reduction. Plant J. **54**: 388–401.

Brock, A., Herzfeld, T., Paschke, R., Koch, M., and Dräger, B. (2006). Brassicaceae Contain Nortropane Alkaloids. Phytochemistry **67**: 2050–2057.

Brown, S., Clastre, M., Courdavault, V., and O'Connor, S.E. (2015). De novo Production of the Plant-Derived Alkaloid Strictosidine in Yeast. Proc. Natl. Acad. Sci. **112**: 3205–3210.

Butler, M.S., Katavic, P.L., Davis, R.A., Forster, P.I., Guymer, G.P., and Quinn, R.J. (2000). 10-Hydroxydarlingine, a New Tropane Alkaloid from the Australian Proteaceous Plant *Triunia erythrocarpa*. J. Nat. Prod. **63**: 688–689.

Cannon, J.R., Joshi, K.R., Meehan, G. V., and Williams, J.R. (1969). The Tropane Alkaloids from Three Western Australian *Anthocercis* Species. Aust. J. Chem. **22**: 221–227.

Carmona, D. and Fornoni, J. (2013). Herbivores Can Select for Mixed Defensive Strategies in Plants. New Phytol. **197**: 576–585.

Chae, L., Kim, T., Nilo-Poyanco, R., and Rhee, S.Y. (2014). Genomic Signatures of Specialized Metabolism in Plants. Science. **344**: 510–513.

Cheema, P.S., Padmanaban, G., and Sarma, P.S. (1969). Arginase from *Lathyrus sativus*. Phytochemistry **8**: 409–411.

Chen, H., McCaig, B.C., Melotto, M., He, S.Y., and Howe, G.A. (2004). Regulation of Plant Arginase by Wounding, Jasmonate, and the Phytotoxin Coronatine. J. Biol. Chem. **279**: 45998–46007.

Cui, L., Huang, F., Zhang, D., Lin, Y., Liao, P., Zong, J., and Kai, G. (2015). Transcriptome Exploration for Further Understanding of the Tropane Alkaloids Biosynthesis in *Anisodus acutangulus*. Mol. Genet. Genomics **290**: 1367–1377.

Daunay, M.C., Laterrot, H., and Janick, J. (2008). Iconography and History of Solanaceae: Antiquity to the 17th Century. Horticulture Reviews **34**: 1-111.

Dehghan, E., Shahriari Ahmadi, F., Ghotbi Ravandi, E., Reed, D.W., Covello, P.S., and Bahrami, A.R. (2013). An Atypical Pattern of Accumulation of Scopolamine and other Tropane Alkaloids and Expression of Alkaloid Pathway Genes in *Hyoscyamus senecionis*. Plant Physiol. Biochem. **70**: 188–194.

Dermen, H. (1940). Colchicine Polyploidy and Technique. Bot. Rev. **6**: 599–635.

Diby, L., Kahia, J., Kouamé, C., and Aynekulu, E. (2017). Tea, Coffee, and Cocoa. Encycl. Appl. Plant Sci.: 420–425.

Dong, Y., Burch-Smith, T.M., Liu, Y., Mamillapalli, P., and Dinesh-Kumar, S.P. (2007). A Ligation-Independent Cloning Tobacco Rattle Virus Vector for High-Throughput Virus-Induced Gene Silencing Identifies Roles for NbMADS4-1 and -2 in Floral Development. Plant Physiol. **145**: 1161–1170.

Dräger, B. (2004). Chemistry and Biology of Calystegines. Nat. Prod. Rep. **21**: 211–223.

Dugé De Bernonville, T., Clastre, M., Besseau, S., Oudin, A., Burlat, V., Glévarec, G., Lanoue, A., Papon, N., Giglioli-Guivarc'H, N., St-Pierre, B., and Courdavault, V. (2015). Phytochemical Genomics of the Madagascar Periwinkle: Unravelling the Last Twists of the Alkaloid Engine. Phytochemistry **113**: 9–23.

Eckart Eich (2008). Solanaceae and Convolvulaceae: Secondary Metabolites - Biosynthesis, Chemotaxonomy, Biological and Economic Significance (Springer: Berlin).

Eddleston, M., Buckley, N.A., Eyer, P., and Dawson, A.H. (2008). Management of Acute Organophosphorus Pesticide Poisoning. Lancet **371**: 597–607.

Evans, W.C. and Major, V.A. (1968). The Alkaloids of the Genus *Datura*, section Brugmansia. Part V. Alkaloids of *D. sanguinea* R. and P. and Related Esters of Tropane-3α,6β,7β-triol. J. Chem. Soc. C **0**: 2775–2778.

Evans, W.C. and Woolley, V.A. (1969). Biosynthesis of the (+)-2-Hydroxy-3-Phenylpropionic Acid Moiety of Littorine in *Datura sanguinea* and *Anthocercis littorea*. Phytochemistry **8**: 2183–2187.

Evans, W.C. and Woolley, J.G. (1976). Biosynthesis of C6-C3 Acids in *Datura innoxia*. Phytochemistry **15**: 287–289.

Fan, P., Miller, A.M., Schilmiller, A.L., Liu, X., Ofner, I., Jones, A.D., Zamir, D., and Last, R.L. (2016). In vitro Reconstruction and Analysis of Evolutionary Variation of the Tomato Acylsucrose Metabolic Network. Proc. Natl. Acad. Sci. **113**: E239–E248.

Galanie, S., Thodey, K., Trenchard, I.J., Interrante, M.F., and Smolke, C.D. (2015). Complete Biosynthesis of Opioids in Yeast. Science. **349**: 1095–1100.

Geiger and Hesse (1833). Darstellung des Atropins. Ann. der Pharm. **5**: 43–81.

Griffin, W.J. and Lin, G.D. (2000). Chemotaxonomy and Geographical Distribution of Tropane Alkaloids. Phytochemistry **53**: 623–637.

Grynkiewicz, G. and Gadzikowska, M. (2008). Tropane Alkaloids as Medicinally Useful Natural Products and their Synthetic Derivatives as New Drugs. Pharmacol. Reports **60**: 439–463.

Halket, J.M., Waterman, D., Przyborowska, A.M., Patel, R.K.P., Fraser, P.D., and Bramley, P.M. (2005). Chemical Derivatization and Mass Spectral Libraries in Metabolic Profiling by GC/MS and LC/MS/MS. J. Exp. Bot. **56**: 219–243.

Hanfrey, C., Sommer, S., Mayer, M.J., Burtin, D., and Michael, A.J. (2001). *Arabidopsis* Polyamine Biosynthesis: Absence of Ornithine Decarboxylase and the Mechanism of Arginine Decarboxylase Activity. Plant J. **27**: 551–560.

Harris, E. (2008). Biochemical Facts behind the Definition and Properties of Metabolites. FDA. https://www.fda.gov/ohrms/dockets/ac/03/briefing/3942b1_08_Harris Paper.pdf. Accessed 23 December 2018

Hashimoto, T., Hayashi, A., Amano, Y., Kohno, J., Iwanari, H., Usuda, S., and Yamada, Y. (1991). Hyoscyamine 6β-Hydroxylase, an Enzyme Involved in Tropane Alkaloid Biosynthesis, is Localized at the Pericycle of the Root. J. Biol. Chem. **266**: 4648–4653.

Hashimoto, T., Mitani, A., and Yamada, Y. (1990). Diamine Oxidase from Cultured Roots of *Hyoscyamus niger*: Its Function in Tropane Alkaloid Biosynthesis. Plant Physiol. **93**: 216–221.

Hashimoto, T., Kohno, J., and Yamada, Y. (1987). Epoxidation *in vivo* of Hyoscyamine to Scopolamine does not Involve a Dehydration Step. Plant Physiol. **84**: 144–147.

Hashimoto, T., Nakajima, K., Ongena, G., and Yasuyuki, Y. (1992). Two Tropinone Reductases with Distinct Stereospecificities from Cultured Roots of *Hyoscyamus niger.* Plant Physiol. **100**: 836–845.

Hashimoto, T. and Yamada, Y. (1987). Purification and Characterization of Hyoscyamine 6β-Hydroxylase from Root Cultures of *Hyoscyamus niger* L. Hydroxylase and Epoxidase Activities in the Enzyme Preparation. Eur. J. Biochem. **164**: 277–285.

Hashimoto, T., Yamada, Y., and Leete, E. (1989). Species-Dependent Biosynthesis of Hyoscyamine. J. Am. Chem. Soc. **111**: 1141–1142.

Hashimoto, T., Yukimune, Y., and Yamada, Y. (1989). Putrescine and Putrescine *N*-Methyltransferase in the Biosynthesis of Tropane Alkaloids in Cultured Roots of *Hyoscyamus albus* - II. Incorporation of Labeled Precursors. Planta **178**: 131–137.

Hashimoto, T., Yukimune, Y., and Yamada, Y. (1989). Putrescine and Putrescine *N*-Methyltransferase in the Biosynthesis of Tropane Alkaloids in Cultured Roots of *Hyoscyamus albus* - I. Biochemical Studies. Planta **178**: 123–130.

Heim, W.G., Sykes, K.A., Hildreth, S.B., Sun, J., Lu, R.H., and Jelesko, J.G. (2007). Cloning and Characterization of a *Nicotiana tabacum* Methylputrescine Oxidase Transcript. Phytochemistry **68**: 454–463.

Heimer, Y.M. and Mizrahi, Y. (1982). Characterization of Ornithine Decarboxylase of Tobacco Cells and Tomato Ovaries. Biochem J. **201**: 373–376.

Heinrich Friedrich Georg Mein (1831). Ueber die Darstellung des Atropins in weissen Kristallen. Ann. der Pharm. **6**: 67–72.

Hesse, M. (2002). Alkaloids: Nature's Curse or Blessing? (Wiley-VCH: Weinheim, Germany).

Hibi, N., Higashiguchi, S., Hashimoto, T., and Yamada, Y. (1994). Gene Expression in Tobacco Low-Nicotine Mutants. Plant Cell **6**: 723–735.

Holzman, R.S. (1998). The Legacy of Atropos, the Fate Who Cut the Thread of Life. Anesthesiology **89**: 241–249.

Horai, H. et al. (2010). MassBank: A Public Repository for Sharing Mass Spectral Data for Life Sciences. J. Mass Spectrom. **45**: 703–714.

Illingworth, C., Mayer, M.J., Elliott, K., Hanfrey, C., Walton, N.J., and Michael, A.J. (2003). The Diverse Bacterial Origins of the *Arabidopsis* Polyamine Biosynthetic Pathway. FEBS Lett. **549**: 26–30.

Jacobsen, O. (1882). Alkaloide. Handwörterb der Chemie: 213–422.

Janowitz, T., Kneifel, H., and Piotrowski, M. (2003). Identification and Characterization of Plant Agmatine Iminohydrolase, the Last Missing Link in Polyamine Biosynthesis of Plants. FEBS Lett. **544**: 258–261.

Jenett-Siems, K. et al. (2005). Chemotaxonomy of the Pantropical Genus *Merremia* (Convolvulaceae) Based on the Distribution of Tropane Alkaloids. Phytochemistry **66**: 1448–1464.

Jirschitzka, J., Schmidt, G.W., Reichelt, M., Schneider, B., Gershenzon, J., and D'Auria, J.C. (2012). Plant tropane Alkaloid Biosynthesis Evolved Independently in the Solanaceae and Erythroxylaceae. Proc. Natl. Acad. Sci. **109**: 10304–10309.

Kaczkowski, J., Schütte, H.R., and Mothes, K. (1961). Die Rolle des Acetats in der Biosynthese der Tropanalkaloide. Biochim. Biophys. Acta **46**: 588–594.

Kaiser, H., Richter, U., Keiner, R., Brabant, A., Hause, B., and Dräger, B. (2006). Immunolocalisation of Two Tropinone Reductases in Potato (*Solanum tuberosum* L.) Root, Stolon, and Tuber Sprouts. Planta **225**: 127–137.

Kanegae, T., Kajiya, H., Amano, Y., Hashimoto, T., and Yamada, Y. (1994). Species-Dependent Expression of the Hyoscyamine 6β-Hydroxylase Gene in the Pericycle. Plant Physiol. **105**: 483–490.

Katoh, A., Shoji, T., and Hashimoto, T. (2007). Molecular Cloning of *N*-Methylputrescine Oxidase from Tobacco. Plant Cell Physiol. **48**: 550–554.

Kaul, S. et al. (2000). Analysis of the Genome Sequence of the Flowering Plant *Arabidopsis thaliana*. Nature **408**: 796–815.

Kim, N., Estrada, O., Chavez, B., Stewart, C., and D'Auria, J.C. (2016). Tropane and Granatane Alkaloid Biosynthesis: A Systematic Analysis. Molecules **21**: 11.

Kind, T. and Fiehn, O. (2007). Seven Golden Rules for Heuristic Filtering of Molecular Formulas Obtained by Accurate Mass Spectrometry. BMC Bioinformatics **8**: 105.

Kuo, M.C., Chang, S.J., and Hsieh, M.C. (2015). Colchicine Significantly Reduces Incident Cancer in Gout Male Patients: A 12-year Cohort Study. Med. **94**: E1570.

Kushwaha, A.K., Sangwan, N.S., Trivedi, P.K., Negi, A.S., Misra, L., and Sangwan, R.S. (2013). Tropine Forming Tropinone Reductase Gene from *Withania somnifera* (Ashwagandha): Biochemical Characteristics of the Recombinant Enzyme and Novel Physiological Overtones of Tissue-Wide Gene Expression Patterns. PLoS One **8**: 9.

Lander, E.S. et al. (2001). Initial Sequencing and Analysis of the Human Genome. Nature **409**: 860–921.

Lau, W. and Sattely, E.S. (2015). Six Enzymes from Mayapple that Complete the Biosynthetic Pathway to the Etoposide Aglycone. Science. **349**: 1224–1228.

Lee, M.R. (2007). Solanaceae IV: *Atropa belladonna*, Deadly Nightshade. J. R. Coll. Physicians Edinb. **37**: 77–84.

Leete, E., Marion, L., and Spenser, I.D. (1954). Biogenesis of Hyoscyamine. Nature **174**: 650–651.

Leete, E. (1960). The Biogenesis of Tropic Acid and Related Studies on the Alkaloids of *Datura stramonium*. J. Am. Chem. Soc. **82**: 612–614.

Leete, E. (1958). The Biogenesis of Nicotine. V. New Precursors of the Pyrrolidine Ring. J. Am. Chem. Soc. **80**: 2162–2164.

Leete, E. (1964). Biosynthesis of Hyoscyamine: Proof that Ornithine-2-C14 Yields Tropine Labelled at C-1. Tetrahedron Lett. **5**: 1619–1624.

Leete, E. (1962). The Stereospecific Incorporation of Ornithine into the Tropine Moiety of Hyoscyamine. J. Am. Chem. Soc. **84**: 55–57.

Leete, E. (1979). Biosynthesis and Metabolism of the Tropane Alkaloids. Planta Med. **36**: 97–112.

Leete, E. and Kirven, E.P. (1974). Biosynthesis of Tropic Acid: Feeding Experiments with Cinnamoyltropine and Littorine. Phytochemistry **13**: 1501–1504.

Leete, E., Kowanko, N., and Richard, A. (1975). Use of Carbon-13 Nuclear Magnetic Resonance to Establish That the Biosynthesis of Tropic Acid Involves an Intramolecular Rearrangement of Phenylalanine. J. Am. Chem. Soc. **97**: 6826–6830.

Li, R., Reed, D.W., Liu, E., Nowak, J., Pelcher, L.E., Page, J.E., and Covello, P.S. (2006). Functional Genomic Analysis of Alkaloid Biosynthesis in *Hyoscyamus niger* Reveals a Cytochrome P450 I

Li, X., Qiang, W., Qiu, F., Chen, M., Lan, X.Z., Liao, Z.H., and Liu, X.Q. (2017). Cloning and Characterization of an Aromatic Amino Acid Aminotransferase (ArAT) Gene Involved in Tropane Alkaloid Biosynthesis from *Hyoscyamus niger*. Yaoxue Xuebao **52**: 172–179.

Li, Y., Li, S., Thodey, K., Trenchard, I., Cravens, A., and Smolke, C.D. (2018). Complete Biosynthesis of Noscapine and Halogenated Alkaloids in Yeast. Proc. Natl. Acad. Sci. **115**: E3922–E3931.

Li, Y. and Smolke, C.D. (2016). Engineering Biosynthesis of the Anticancer Alkaloid Noscapine in Yeast. Nat. Commun. **7**: 12137.

Liebisch, H., Bernasch, H., and Schütte, H.R. (1973). Zur Biosynthese der Tropanalkaloide: Die Biosynthese des Cochlearins. Z. Chem. **13**: 372–373.

Liebisch, H.-W., Peisker, K., Radwan, A.S., and Schütte, H.R. (1972). Zur biosynthese der tropanalkaloide. XI Die bildung der C3-brücke des tropins. Zeitschrift für Pflanzenphysiologie **67**: 1–9.

Liu, T., Zhu, P., Cheng, K. Di, Meng, C., and Zhu, H.X. (2005). Molecular Cloning and Expression of Putrescine *N*-Methyltransferase from the Hairy Roots of *Anisodus tanguticus*. Planta Med

Liu, Y., Schiff, M., Dinesh-Kumar, S.P., and Dinesh-Kumar, S.P. (2002). Virus-Induced Gene Silencing in Tomato. Plant J. **31**: 777–786.

Lochner, M. and Thompson, A.J. (2016). The Muscarinic Antagonists Scopolamine and Atropine are Competitive Antagonists at 5-HT3 Receptors. Neuropharmacology **108**: 220–228.

Lounasmaa, M., Pusset, J., and Sévenet, T. (1980). Benzyl-2 Tropanes et γ-Pyranotropanes, Alcaloïdes de *Knightia strobilina*. Phytochemistry **19**: 949–952.

Mastrodicasa, M.A., Droege, C.A., Mulhall, A.M., Ernst, N.E., Panos, R.J., and Zafar, M.A. (2017). Long Acting Muscarinic Antagonists for the Treatment of Chronic Obstructive Pulmonary Disease: A Review of Current and Developing Drugs. Expert Opin. Investig. Drugs **26**: 161–174.

Matsuda, J., Okabe, S., Hashimoto, T., and Yamada, Y. (1991). Molecular Cloning of Hyoscyamine 6β-Hydroxylase, a 2-Oxoglutarate-Dependent Dioxygenase, from Cultured Roots of *Hyoscyamus niger*. J

Meißner, W. (1819). Ueber ein neues Pflanzenalkaloide. J. für Chemie und Phys. **25**: 377–381.

Michael, A.J., Furze, J.M., Rhodes, M.J.C., and Burtin, D. (1996). Molecular Cloning and Functional Identification of a Plant Ornithine Decarboxylase cDNA. Biochem. J. **314**: 241–248.

Milo, R. and Last, R.L. (2012). Achieving Diversity in the Face of Constraints: Lessons from Metabolism. Science. **336**: 1663–1667.

Miranda-Pérez, A., Castillo, G., Hernández-Cumplido, J., Valverde, P.L., Borbolla, M., Cruz, L.L., Tapia-López, R., Fornoni, J., Flores-Ortiz, C.M., and Núñez-Farfán, J. (2016). Natural Selection Drives Chemical Resistance of *Datura stramonium*. PeerJ **4:e1898**.

Mizusaki, S., Tanabe, Y., Noguchi, M., and Tamaki, E. (1972). *N*-Methylputrescine Oxidase from Tobacco Roots. Phytochemistry **11**: 2757–2762.

Murata, J., Roepke, J., Gordon, H., and De Luca, V. (2008). The Leaf Epidermome of *Catharanthus roseus* Reveals Its Biochemical Specialization. Plant Cell **20**: 524–542.

Muszyńska, G. and Reifer, I. (1968). Purification, Properties and Inhibition of Plant Arginase. Acta Biochim. Pol. **15**: 55–66.

Mylona, P., Owatworakit, A., Papadopoulou, K., Jenner, H., Qin, B., Findlay, K., Hill, L., Qi, X., Bakht, S., Melton, R., and Osbourn, A. (2008). *Sad3* and *Sad4* Are Required for Saponin Biosynthesis and Root Development in Oat. Plant Cell **20**: 201–212.

Nakagawa, A., Matsumura, E., Koyanagi, T., Katayama, T., Kawano, N., Yoshimatsu, K., Yamamoto, K., Kumagai, H., Sato, F., and Minami, H. (2016). Total Biosynthesis of Opiates by Stepwise Fermentation Using Engineered *Escherichia coli*. Nat. Commun. **7**: 10390.

Nakajima, K., Hashimoto, T., and Yamada, Y. (1993). Two Tropinone Reductases with Different Stereospecificities are Short-Chain Dehydrogenases Evolved from a Common Ancestor. Proc. Natl. Acad. Sci. **90**: 9591–9595.

Nakajima, K. and Hashimoto, T. (1999). Two Tropinone Reductases, that Catalyze Opposite Stereospecific Reductions in Tropane Alkaloid Biosynthesis, are Localized in Plant Root with Different Cell-Specific Patterns. Plant Cell Physiol. **40**: 1099–1107.

Nakajima, K., Oshita, Y., Kaya, M., Yamada, Y., and Hashimoto, T. (1999). Structures and Expression Patterns of Two Tropinone Reductase Genes from *Hyoscyamus niger*. Biosci. Biotechnol. Biochem. **63**: 1756–1764.

Nic, M., Jirat, J., and Kosata, B. (2014). Compendium of Chemical Terminology Gold Book.

Nützmann, H.W. and Osbourn, A. (2014). Gene Clustering in Plant Specialized Metabolism. Curr. Opin. Biotechnol. **26**: 91–99.

Nyman, S. (1994). Incorporation of Arginine, Ornithine and Phenylalanine into Tropane Alkaloids in Suspension-Cultured Cells and Aseptic Roots of Intact Plants of *Atropa belladonna*. J. Exp. Bot. **45**: 979–986.

O'Connor, S.E. and Maresh, J.J. (2006). Chemistry and Biology of Monoterpene Indole Alkaloid Biosynthesis. Nat. Prod. Rep. **23**: 532–547.

Ohlendorf, W. (1996). Domestication and Crop Development of *Duboisia* spp. (Solanaceae). In Domestication and Commercialization of Non-Timber Forest Products in Agroforestry Systems, R.R.B. Leakey, A.B. Temu, M. Melnyk, and P. Vantomme, eds (Food and Agriculture Organization of the United Nations: Rome), pp. 183–187.

Oliver, S.G., Winson, M.K., Kell, D.B., and Baganz, F. (1998). Systematic Functional Analysis of the Yeast Genome. Trends Biotechnol. **16**: 373–378.

Onoyovwe, A., Hagel, J.M., Chen, X., Khan, M.F., Schriemer, D.C., and Facchini, P.J. (2013). Morphine Biosynthesis in Opium Poppy Involves Two Cell Types: Sieve Elements and Laticifers. Plant Cell **25**: 4110–4122.

Ott, S.C., Jenett-Siems, K., Pertz, H.H., Siems, K., Witte, L., and Eich, E. (2006). Bonabiline A, a Monoterpenoid 3α-Acyloxytropane from the Roots of *Bonamia spectabilis* Showing M3 Receptor Antagonist Activity. Planta Med. **72**: 1403–1406.

Ott, S.C., Jenett-Siems, K., Siems, K., Müller, F., Hilker, M., and Eich, E. (2013). Ipvelutine, 7β-Acetoxy-2α-(Tigloyloxy)tropane, an Unusual Tropane Alkaloid from *Ipomoea velutina* R. BR. (Convolvulaceae). Sci. Pharm. **81**: 543–548.

Patel, J., Ariyaratne, M., Ahmed, S., Ge, L., Phuntumart, V., Kalinoski, A., and Morris, P.F. (2017). Dual Functioning of Plant Arginases Provides a Third Route for Putrescine Synthesis. Plant Sci. **262**: 62–73.

Pichersky, E. and Lewinsohn, E. (2011). Convergent Evolution in Plant Specialized Metabolism. Annu. Rev. Plant Biol. **62**: 549–566.

Pichersky, E. and Raguso, R.A. (2016). Why Do Plants Produce So Many Terpenoid Compounds? New Phytol. **220**: 692–702.

Piotrowski, M., Janowitz, T., and Kneifel, H. (2003). Plant C-N Hydrolases and the Identification of a Plant *N*-Carbamoylputrescine Amidohydrolase Involved in Polyamine Biosynthesis. J. Biol. Chem. **278**: 1708–1712.

Platonova, T.F. and Kuzovkov, A.D. (1963). On The Alkaloids of the Arctic Spoonwort, *Cochlearia arctica* Schlecht. Med. Prom. SSSR **17**: 19–20.

Qiang, W., Xia, K., Zhang, Q., Zeng, J., Huang, Y., Yang, C., Chen, M., Liu, X., Lan, X., and Liao, Z. (2016). Functional Characterisation of a Tropine-Forming Reductase Gene from *Brugmansia arborea*, a Woody Plant Species Producing Tropane Alkaloids. Phytochemistry **127**: 12–22.

Qiu, F., Yang, C., Yuan, L., Xiang, D., Lan, X., Chen, M., and Liao, Z. (2018). A Phenylpyruvic Acid Reductase Is Required for Biosynthesis of Tropane Alkaloids. ACS Org. Lett. **20**: 7807–7810.

Ralser, M. (2018). An Appeal to Magic? The Discovery of a Non-Enzymatic Metabolism and its Role in the Origins of Life. Biochem. J. **475**: 2577–2592.

RamaRao, G., Afley, P., Acharya, J., and Bhattacharya, B.K. (2014). Efficacy of Antidotes (Midazolam, Atropine and HI-6) on Nerve Agent Induced Molecular and Neuropathological Changes. BMC Neurosci. <

Ratcliff, F., Martin-Hernandez, A.M., and Baulcombe, D.C. (2001). Tobacco Rattle Virus as a Vector for Analysis of Gene Function by Silencing. Plant J. **25**: 237–245.

Reinhardt, N., Fischer, J., Coppi, R., Blum, E., Brandt, W., and Dräger, B. (2014). Substrate Flexibility and Reaction Specificity of Tropinone Reductase-Like Short-Chain Dehydrogenases. Bioorg. Chem. **53**: 37–49.

Robins, R.J., Abraham, T.W., Parr, A.J., Eagles, J., and Walton, N.J. (1997). The Biosynthesis of Tropane Alkaloids in *Datura stramonium*: The Identity of the Intermediates Between *N*-Methylpyrrolinium Salt and Tropinone. J. Am. Chem. Soc. **119**: 10929–10934.

Robins, R.J., Parr, A.J., Bent, E.G., and Rhodes, M.J.C. (1991). Studies on the Biosynthesis of Tropane Alkaloids in *Datura stramonium* L. Transformed Root Cultures. Planta **185**: 385–390.

Robins, R.J., Woolley, J.G., Ansarin, M., Eagles, J., and Goodfellow, B.J. (1994). Phenyllactic Acid but not Tropic Acid is an Intermediate in the Biosynthesis of Tropane Alkaloids in *Datura* and *Brugmansia* Transformed Root Cultures. Planta **194**: 86–94.

Robinson, R. (1917). A Synthesis of Tropinone. J. Chem. Soc. Trans. **111**: 762–768.

Robinson, R (1955). The Structural Relations of Natural Products (Claredon Press: Oxford).

Rothman, T. (1972). De Laguna's Commentaries on Hallucinogenic Drugs and Witchcraft in Dioscorides' *Materia Medica*. Bull. Hist. Med. **46**: 562–567.

Särkinen, T., Bohs, L., Olmstead, R.G., and Knapp, S. (2013). A Phylogenetic Framework for Evolutionary Study of the Nightshades (Solanaceae): A Dated 1000-Tip Tree. BMC Evol. Biol. **13**: 214.

Schilmiller, A.L., Charbonneau, A.L., and Last, R.L. (2012). Identification of a BAHD Acetyltransferase that Produces Protective Acyl Sugars in Tomato Trichomes. Proc. Natl. Acad. Sci. **109**: 16377–16382.

Schilmiller, A.L., Moghe, G.D., Fan, P., Ghosh, B., Ning, J., Jones, A.D., and Last, R.L. (2015). Functionally Divergent Alleles and Duplicated Loci Encoding an Acyltransferase Contribute to Acylsugar Metabolite Diversity in *Solanum* Trichomes. Plant Cell **27**: 1002–1017.

Schmidt, G.W., Jirschitzka, J., Porta, T., Reichelt, M., Luck, K., Torre, J.C.P., Dolke, F., Varesio, E., Hopfgartner, G., Gershenzon, J., and D'Auria, J.C. (2015). The Last Step in Cocaine Biosynthesis Is Catalyzed by a BAHD Acyltransferase. Plant Physiol. **167**: 89–101.

Shonle, I. and Bergelson, J. (2000). Evolutionary Ecology of the Tropane Alkaloids of *Datura stramonium* L. (Solanaceae). Evolution (N. Y).

Stenzel, O., Teuber, M., and Dräger, B. (2006). Putrescine N-Methyltransferase in *Solanum tuberosum* L., a Calystegine-Forming Plant. Planta **223**: 200–212.

Suzuki, K.I., Yamada, Y., and Hashimoto, T. (1999). Expression of *Atropa belladonna* Putrescine *N*-Methyltransferase Gene in Root Pericycle. Plant Cell Physiol. **40**: 289–297.

Suzuki, K.I., Yun, D.J., Chen, X.Y., Yamada, Y., and Hashimoto, T. (1999). An *Atropa belladonna* Hyoscyamine 6β-Hydroxylase Gene is Differentially Expressed in the Root Pericycle and Anthers. Plant Mol. Biol. **40**: 141–152.

Swartz, M.E. (2005). UPLC™: An Introduction and Review. J. Liq. Chromatogr. Relat. Technol. **28**: 1253–1263.

Teuber, M., Azemi, M.E., Namjoyan, F., Meier, A.C., Wodak, A., Brandt, W., and Dräger, B. (2007). Putrescine *N*-Methyltransferases - A Structure-Function Analysis. Plant Mol. Biol. **63**: 787–801.

Tiburcio, A.F. and Galston, A.W. (1985). Arginine Decarboxylase as the Source of Putrescine for Tobacco Alkaloids. Phytochemistry **25**: 107–110.

Tu, T.-Y., Sun, H., Gu, Z.-J., and Yu, J.-P. (2005). Cytological studies on the Sino-Himalayan endemic *Anisodus* and four related genera from the tribe Hyoscyameae (Solanaceae) and their systematic and evolutionary implications. Bot. J. Linn. Soc. **147**: 457–468.

Tu, T., Volis, S., Dillon, M.O., Sun, H., and Wen, J. (2010). Dispersals of Hyoscyameae and Mandragoreae (Solanaceae) from the New World to Eurasia in the early Miocene and their biogeographic diversification within Eurasia. Mol. Phylogenet. Evol. **57**: 1226–1237.

Volkov, R.A., Panchuk, I.I., Borisjuk, N. V., Hosiawa-Baranska, M., Maluszynska, J., and Hemleben, V. (2017). Evolutional dynamics of 45S and 5S ribosomal DNA in ancient allohexaploid *Atropa belladonna*. BMC Plant Biol. **17**: 1–15.

Walton, N.J., Robins, R.J., and Peerless, A.C.J. (1990). Enzymes of *N*-Methylputrescine Biosynthesis in Relation to Hyoscyamine Formation in Transformed Root Cultures of *Datura stramonium* and *Atropa belladonna*. Planta **182**: 136–141.

Willstätter, R. (1901). Synthesen in der Tropingruppe. I. Synthese des Tropilidens. Justus Liebigs Ann. Chem. **317**: 204–265.

Winzer, T. et al. (2012). A *Papaver somniferum* 10-Gene Cluster for Synthesis of the Anticancer Alkaloid Noscapine. Science. **336**: 1704–1708.

Yang, F., Zhao, H., and Carroll, A.R. (2017). Tropane Alkaloids from the Australian Plant *Triunia montana* (Proteaceae). Tetrahedron Lett. **58**: 736–739.

Ye, K., Ke, Y., Keshava, N., Shanks, J., Kapp, J.A., Tekmal, R.R., Petros, J., and Joshi, H.C. (1998). Opium Alkaloid Noscapine is an Antitumor Agent that Arrests Metaphase and Induces Apoptosis in Dividing Cells. Proc. Natl. Acad. Sci. **95**: 1601–1606.

Yoshida, D. (1969). Formation of Putrescine from Ornithine and Arginine in Tobacco Plants. Plant Cell Physiol. **10**: 393–397.

Yuan, Y.W., Zhang, Z.Y., Chen, Z.D., and Olmstead, R.G. (2006). Tracking ancient polyploids: A retroposon insertion reveals an extinct diploid ancestor in the polyploid origin of *Belladonna*. Mol. Biol. Evol. **23**: 2263–2267.

Zeng, L., Zhang, N., Zhang, Q., Endress, P.K., Huang, J., and Ma, H. (2017). Resolution of Deep Eudicot Phylogeny and Their Temporal Diversification Using Nuclear Genes from Transcriptomic and Genomic Datasets. New Phytol. **214**: 1338–1354.

CHAPTER TWO

Tropinone Synthesis via an Atypical Polyketide Synthase and P450-Mediated Cyclization

Matthew A. Bedewitz[1], A. Daniel Jones[2,3], John C. D'Auria[4], and Cornelius S. Barry[1]

Summary

This study describes the identification and characterization of two enzymes involved in the biosynthesis of tropinone from the Solanaceous plant *Atropa belladonna*. Tropinone is the first alkaloid with the tropane core structure in the biosynthetic pathway from the amino acids arginine and ornithine to the medicinal alkaloids hyoscyamine and scopolamine. Techniques used to perform this work Virus Induced Gene Silencing (VIGS) to quickly characterize candidate genes in *A. belladonna*, transient heterologous protein expression in *Nicotiana benthamiana* to confirm the candidates in a tropane non-producing plant, heterologous protein production and purification to perform biochemical assays, and mass spectrometry to confirm the enzyme products from both plant extracts and biochemical assays.

Two enzymes were identified as being essential for biosynthesis of tropinone, and together were able to reconstitute this compound in *N. benthamiana* and in biochemical assays. These were AbPYKS, a polyketide synthase which utilizes an atypical, desaturated *N*-methylpyrrolidine during its reaction; and AbTS, which is a cytochrome

P450 that cyclizes the AbPYKS product to form tropinone. Identification of these enzymes is significant because the missing enzymes and unclear biochemical pathway was a hurdle to reconstitution of tropane alkaloid biosynthesis in an alternative system. Some possible directions enabled by this study include engineering the enzymes to accept alternative substrates to produce novel alkaloids of medicinal interest or to improve the enzymes' physiological behavior to improve production.

For the full text, please use the following link:

https://www.nature.com/articles/s41467-018-07671-3

CHAPTER THREE

A Root-Expressed L-Phenylalanine:4-Hydroxyphenylpyruvate Aminotransferase Is Required for Tropane Alkaloid Biosynthesis in *Atropa belladonna*

Matthew A. Bedewitz, Elsa Góngora-Castillo, Joseph B. Uebler, Eliana Gonzales-Vigil, Krystle E. Wiegert-Rininger, Kevin L. Childs, John P. Hamilton, Brieanne Vaillancourt, Yun-Soo Yeo, Joseph Chappell, Dean DellaPenna, A. Daniel Jones, C. Robin Buell, Cornelius S. Barry

The work summarized in the following chapter was performed as part of a collaboration. I was responsible for all research relating to *in planta* analysis, cloning, quantitative reverse transcription PCR, enzymology, and mass spectrometry

Summary

This study describes the identification and characterization of an enzyme involved in the biosynthesis of phenyllactic acid from the amino acid phenylalanine from the Solanaceous plant *Atropa belladonna*. Phenyllactic acid provides the acyl group needed to decorate the tropane core of the medicinal alkaloids hyoscyamine and scopolamine. Techniques used to perform this work Virus Induced Gene Silencing (VIGS) to quickly characterize candidate genes in *A. belladonna*, heterologous protein production and purification to perform biochemical assays, and mass spectrometry to confirm the relevant products from plant extracts and biochemical assays.

From the *A. belladonna* transcriptome developed by Elsa Góngora-Castillo and the Buell lab, a single candidate tyrosine aminotransferase gene was identified (*AbArAT4*) and knocked down using VIGS. Transient silencing of this gene caused a reduction in alkaloid content for all tropane alkaloids with a phenyllactic acid derived moiety and biochemical assays showed that the enzyme preferentially removes the amino group from phenylalanine, transferring the amino group to another compound to form a different amino acid, preferentially tyrosine. The study was significant because the substrate preference of this member of the tyrosine aminotransferase family is substantially altered compared to other characterized members, and because AbArAT4 is highly preferential for removal of the amino group from phenylalanine, not adding one (which would produce phenylalanine). This is highly unusual for enzymes of the family and other members have a far lower preference for directionality of the reaction.

For the full text, please use the following link:

https://academic.oup.com/plcell/article/26/9/3745/6100364

CHAPTER FOUR

Aromatic Tropane Esters Are Formed Via Glucose-ester Mediated Acylation in *Atropa belladonna*

Matthew A. Bedewitz[a], Joseph B. Uebler[a], Steven M. Hurney[b], Kevin D. Walker[b,c], A. Daniel Jones[b,c], and Cornelius S. Barry[a,1]

Abstract

Tropane alkaloids are plant specialized metabolites that include the narcotic cocaine and the pharmaceuticals hyoscyamine and scopolamine. Hyoscyamine and scopolamine are synthesized in the Solanaceae through a partially characterized pathway. Littorine, the precursor of hyoscyamine and scopolamine, is the ester of tropine and D-phenyllactic acid. The enzymes catalyzing littorine formation are unknown; although, a hypothesis developed a quarter century ago proposed the involvement of an acyl-CoA intermediate, a reaction catalyzed by BAHD acyltransferases. However, in this study, no evidence was obtained to support the involvement of BAHDs in tropane ester biosynthesis in *Atropa belladonna*. In contrast, we demonstrate that littorine is formed through glucose-ester mediated acylation. The UDP-glucosyltransferase, UGT84A27, generates a glucosyl-D-phenyllactate ester, and littorine synthase, a serine carboxypeptidase-like acyltransferase, transfers the phenyllactoyl moiety from the glucose ester to tropine, forming littorine. These data contrast with BAHD-mediated synthesis of the tropane ester cocaine in the Erythroxylaceae, highlighting the independent evolution of tropanes in plants. Additional *in planta* and *in vitro* characterization of UGT84A27 reveals catalytic promiscuity of this enzyme, indicative of a broader role in phenylpropanoid metabolism that extends beyond tropane alkaloid biosynthesis. In contrast, littorine synthase is catalytically more restricted, with a preference for tropine and glucosyl-1-*O*-D-phenyllactate as substrates.

Introduction

Collectively, plants synthesize hundreds of thousands of chemically distinct specialized metabolites. These specialized metabolites perform protective or signaling functions within the host plant, but their bioactive properties are also used by humans as medicines, narcotics, flavorings, and pesticides (Pichersky and Lewinsohn, 2011; Weng et al., 2012). The importance of plant specialized metabolites to human health and agriculture has resulted in considerable efforts to elucidate and manipulate their biosynthetic pathways to improve flux (Graham et al., 2010; Winzer et al., 2012; Galanie et al., 2015; Lau and Sattely, 2015; Fan et al., 2016). However, the complete biosynthetic pathways of many plant specialized metabolites remain undefined.

Combining precursor molecules from primary and secondary metabolism to form increasingly elaborate metabolites is a key driver of chemical diversity, and ester formation through acylation contributes greatly to the complexity of plant specialized metabolites (Anarat-Cappillino and Sattely, 2014). Acylation can change the physical and chemical properties of plant metabolites by altering the color, stability, transport, UV absorption properties, and storage location (Landry et al., 1995; Gomez et al., 2009; Cheynier et al., 2013; Bontpart et al., 2015). Acylation of an alcohol or amino acceptor molecule requires an activated acyl donor. In plants, acyl-CoA thioesters and 1-*O*-β-glucose esters typically serve this role. Acylation reactions that utilize acyl-CoA thioesters as the donor are catalyzed by BAHD [**B**EAT, **A**HCT, **H**CBT, **D**AT (D'Auria, 2006)] acyl transferases. BAHDs are encoded by gene families of 50-100 members that often occur as rapidly-evolving tandem duplicates (Tuominen et al., 2011). By contrast, acylations

using 1-*O*-β-glucose esters are catalyzed by serine carboxypeptidase-like acyltransferases (SCPLs) (Bontpart et al., 2015). Relative to BAHDs, fewer SCPLs are characterized but several participate in the synthesis of specialized metabolites, including the biosynthesis of the triterpenoid avenacins in *Avena strigosa* (Mugford et al., 2009), delphinidins in *Delphinium grandifolium* (Nishizaki et al., 2013), sinapoylated compounds in *Arabidopsis thaliana* (Lehfeldt et al., 2000; Shirley and Chapple, 2003), and a glucose polyester in *Solanum pennellii* (Li and Steffens, 2000).

Alkaloids are a structurally diverse group of specialized metabolites defined by the presence of nitrogen incorporated into one or more rings (Ziegler and Facchini, 2008). Tropane alkaloids consist of a cycloheptane ring with a nitrogen bridge, creating a bicyclic structure (Figure 4.1). The class includes the narcotic cocaine, synthesized by members of the Erythroxylaceae and the pharmaceuticals, hyoscyamine and scopolamine, which are synthesized by select members of the Solanaceae (Kim et al., 2016). Despite the vast pharmaceutical application of tropane alkaloids, their biosynthesis is not fully defined. Recently, identification of enzymes involved in cocaine biosynthesis reveals the independent evolution of tropane alkaloid biosynthesis in the Solanaceae and the Erythroxylaceae (Jirschitzka et al., 2012; Schmidt et al., 2015).

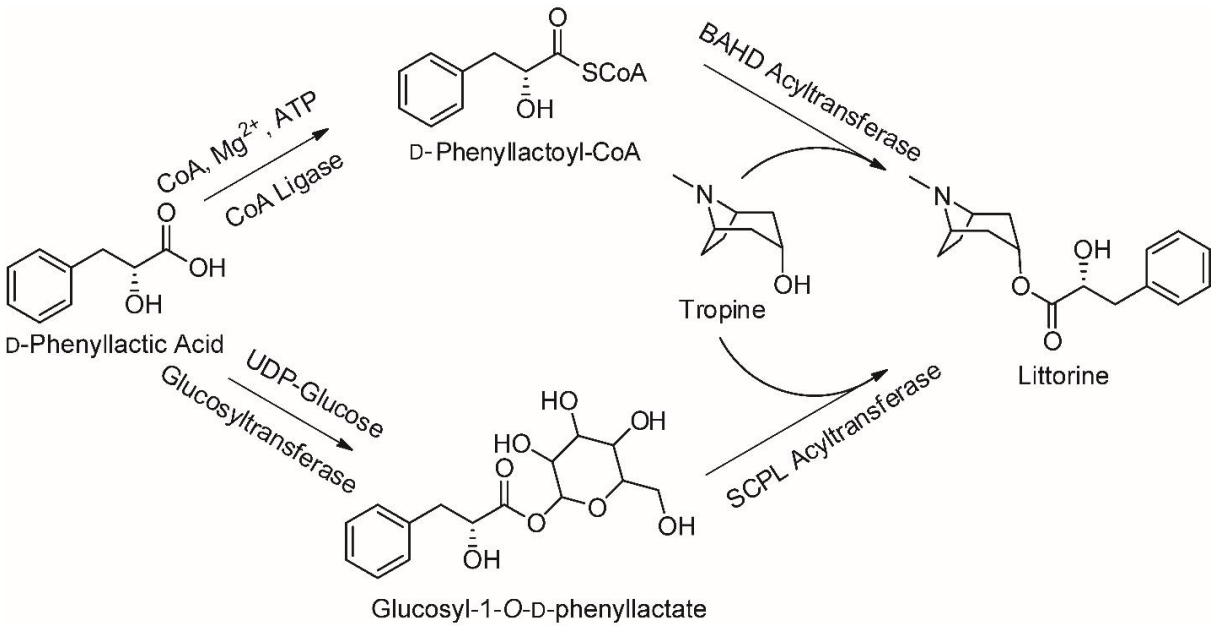

Figure 4.1 Proposed Pathways for Littorine Biosynthesis in the Solanaceae.

Littorine biosynthesis through an acyl-CoA intermediate: A possible route is an ATP-dependent ligase that couples coenzyme A and D-phenyllactic acid, followed by an acyl CoA-dependent acylation of tropine to form littorine. Alternatively, littorine biosynthesis could proceed through a glucose-ester intermediate using a UDP-glucosyltransferase catalyzed glucosylation of D-phenyllactic acid, followed by acyl glucosyl ester-dependent acylation of tropine to form littorine.

In the Solanaceae, tropinone is the first metabolite in the pathway with the characteristic [3.2.1] bicyclic ring structure and is formed from putrescine through a sequence of methylation by PUTRESCINE METHYLTRANSFERASE (PMT) (Hibi et al., 1994) oxidation to an aldehyde by METHYLPUTRESCINE OXIDASE (MPO) (Heim et al., 2007, Katoh et al., 2007), extension through PYRROLIDINE KETIDE SYNTHASE (PyKS) and cyclization mediated by CYP82M3, TROPINONE SYNTHASE (TS) (Bedewitz et al., 2018) (Figure 4.2). Tropinone is reduced to the epimers tropine (α-tropanol) and pseudotropine (β-tropanol) through the action of TROPINONE REDUCTASE I and II (TRI and TRII), respectively (Nakajima et al., 1993). Tropine is predominantly channeled toward scopolamine through littorine, an ester formed by condensation of tropine and D-phenyllactic acid (Robins et al., 1994). In contrast, pseudotropine typically undergoes *N*-demethylation and differential polyhydroxylations to produce calystegines (Drager, 2004). The phenyllactate moiety of littorine is derived through L-phenylalanine via an aromatic aminotransferase (ArAT4), and subsequently reduced by PHENYLPYRUVIC ACID REDUCTASE (PPAR) to yield phenyllactic acid (Kitamura et al., 1992; Bedewitz et al., 2014; Qiu et al., 2018) (Figure 4.2).

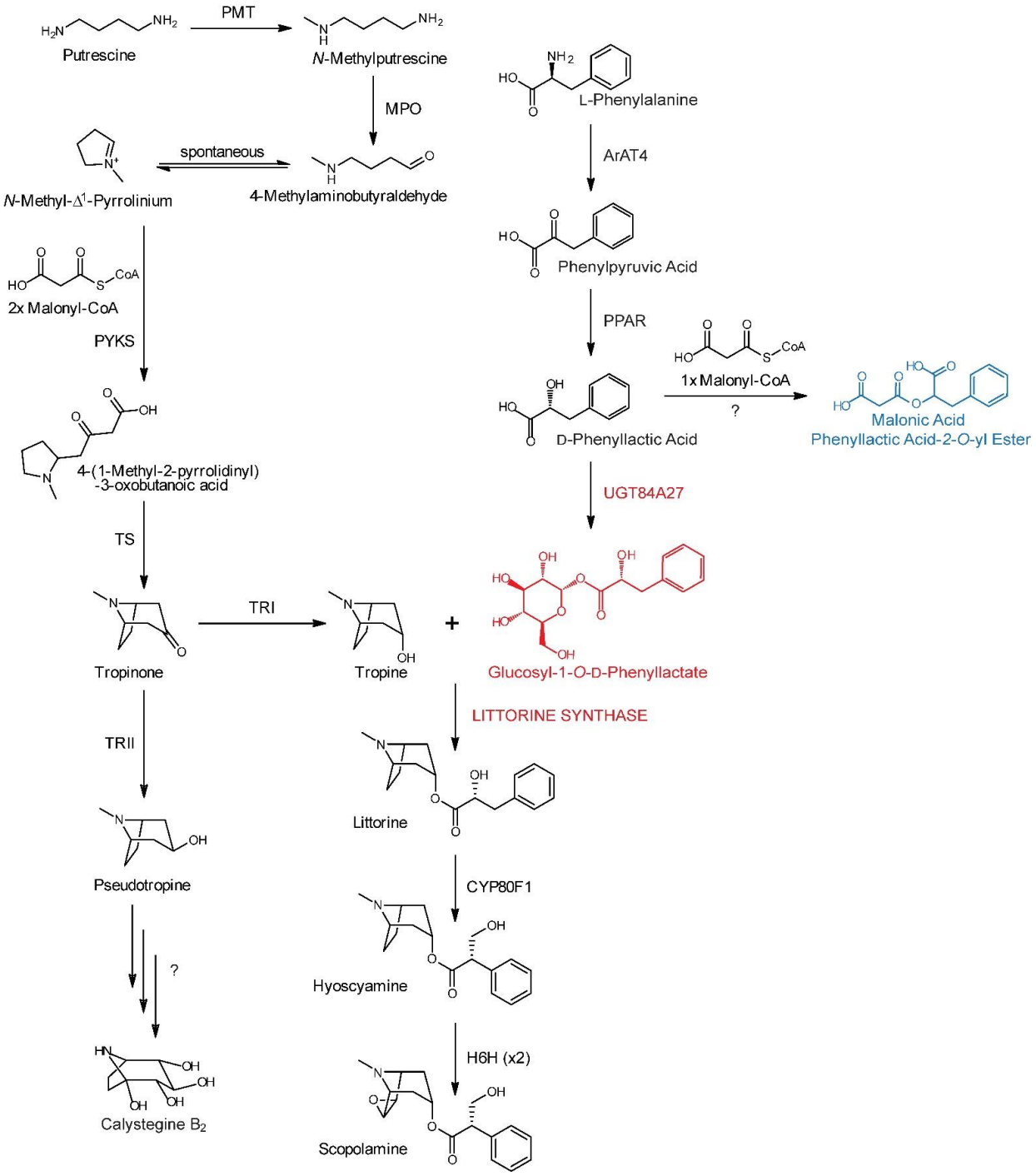

Figure 4.2 The Proposed Pathway of Tropane Alkaloid Biosynthesis in the Solanaceae.

Figure 4.2 (cont'd)

Based on the discoveries presented in this study glucosyl-1-*O*-D-phenyllactate (shown in red) is included as a key intermediate in the synthesis of littorine, a precursor of scopolamine. The enzymes identified in this study, UGT84A27 and LITTORINE SYNTHASE are also shown in red. Enzyme abbreviations: PMT: Putrescine Methyl Transferase, MPO: Methyl Putrescine Oxidase, PYKS: Pyrrolidine Ketide Synthase, TS: Tropinone Synthase, TR I: Tropinone Reductase I, TR II: Tropinone Reductase II, CYP80F1: Littorine Mutase, H6H: Hyoscyamine-6-Hydroxylase, ArAT4: Ab-ArAT4, a Phenylalanine Aminotransferase, PPAR: Phenylpyruvate Reductase. Unknown steps and enzymes are indicated by question marks.

The enzymes catalyzing the formation of tropane esters in the Solanaceae remain undefined; although, acylation through a D-phenyllactoyl-CoA thioester (Figure 4.1) was initially proposed as a mechanism for littorine biosynthesis over twenty years ago (Robins et al., 1994). More recently, additional support for BAHD-mediated tropane ester formation was obtained through the identification and characterization of a cocaine synthase from *Erythroxylum coca* (Schmidt et al., 2015). However, an alternative hypothesis is that littorine formation proceeds through glucose-ester mediated acylation whereby a glucosyl-1-*O*-D-phenyllactate ester intermediate is formed by a UDP-glucosyltransferase, which then serves as the acyl donor in an SCPL-catalyzed reaction that utilizes tropine as the acyl acceptor (Figure 4.1).

Herein, the underlying mechanisms of aromatic tropane ester formation in the Solanaceae are defined. Silencing of BAHD acyltransferases preferentially-expressed in the roots of *Atropa belladonna*, a species that synthesizes aromatic tropane esters, failed to reduce hyoscyamine and scopolamine levels suggesting the hypothesis implicating a coenzyme A thioester-mediated acylation in aromatic tropane ester biosynthesis is unsupported. In contrast, a combination of gene silencing and biochemical characterization of recombinant enzymes reveals that aromatic tropane ester formation proceeds through a 1-*O*-β-glucose-ester mediated acylation pathway. The root preferentially expressed UDP-glucosyltransferase (UGT84A27) catalyzes the formation of a glucosyl-1-*O*-D-phenyllactate ester intermediate using D-phenyllactic acid and UDP-glucose as substrates. The SCPL acyltransferase littorine synthase subsequently catalyzes the transfer of phenyllactate from glucosyl-1-*O*-D-phenyllactate to tropine to

form littorine, the precursor of hyoscyamine and scopolamine. The reaction catalyzed by littorine synthase is stereospecific and uses the α-epimer tropine as the acyl acceptor, but not the β-epimer pseudotropine, which is reflected in the stereochemistry of littorine *in planta*. Together, these data identify the pathway to aromatic tropane ester formation in the Solanaceae and provide further evidence supporting independent evolution of tropane alkaloid biosynthesis in the Erythroxylaceae and the Solanaceae.

Results

Silencing of Root-expressed BAHD Acyltransferases does not Affect Hyoscyamine and Scopolamine Levels in *A. belladonna*

To test the hypothesis that the formation of aromatic tropane esters proceeds through BAHD-mediated acylation, a transcriptome dataset of *A. belladonna* (Bedewitz et al., 2014) was mined for BAHD transcripts that preferentially accumulate in lateral roots, the site of tropane alkaloid biosynthesis. Three transcripts, *Ab-BAHD-12081*, *Ab-BAHD-5228*, and *Ab-BAHD-5896*, display preferential expression in lateral roots (Table 4.1). However, while expression of transcripts corresponding to *Ab-BAHD-12081* and *Ab-BAHD-5896* is relatively high, *Ab-BAHD-5228* transcripts are less abundant. Furthermore, phylogenetic analyses revealed that Ab-BAHD-5228 is a highly conserved protein, with putative orthologs of unknown function present in multiple plant genomes, including species not known to synthesize tropane alkaloids (Figure 4.3). These data suggest that Ab-BAHD-5228 is unlikely to be involved in tropane alkaloid biosynthesis. In contrast, Ab-BAHD-12081 and Ab-BAHD-5896 are highly expressed in lateral roots and belong to BAHD subclade IIIa, which contains enzymes involved in specialized metabolism, including the tropane-related enzyme, cocaine synthase from *E. coca* and acylsugar acyltransferases from tomato (*Solanum lycopersicum*) (Schmidt et al., 2015; Fan et al., 2016). *Ab-BAHD-12081* and *Ab-BAHD-5896* were silenced in *A. belladonna* roots using virus induced gene silencing (VIGS), reducing transcript abundance by 85 – 90% compared to that observed in empty vector controls (Figure 4.4A and B). However, the abundance of hyoscyamine and scopolamine, the major pharmaceutically relevant aromatic tropane esters in *A. belladonna*, are unaltered in both *Ab-BAHD-12081* and *Ab-*

BAHD-5896-silenced lines compared to empty vector controls, suggesting that these genes are unlikely to be involved in aromatic tropane ester biosynthesis (Figure 4.4C - F).

Table 4.1 BAHD Transcript Abundance (Fragments Per Kilobase of Transcript per Million Mapped Reads) in *A. belladonna* Tissues as Determined by RNAseq Analysis (Bedewitz et al., 2014).

Gene identifier	Tissue type									
	Seedling	Taproot	Lateral Root	Stem	Leaf	Flower Buds	Flower	Green Fruit	Ripe Fruit	Seed
Ab-BAHD-12081	77.9	50.3	224.3	21.8	2.9	1.3	18.8	33	0	0
Ab-BAHD-5228	0.6	3.7	36.1	5.6	1.1	2.7	11.9	2.2	10	1.2
Ab-BAHD-5896	49.3	160	346.7	0	0	0	1.2	0	0	0

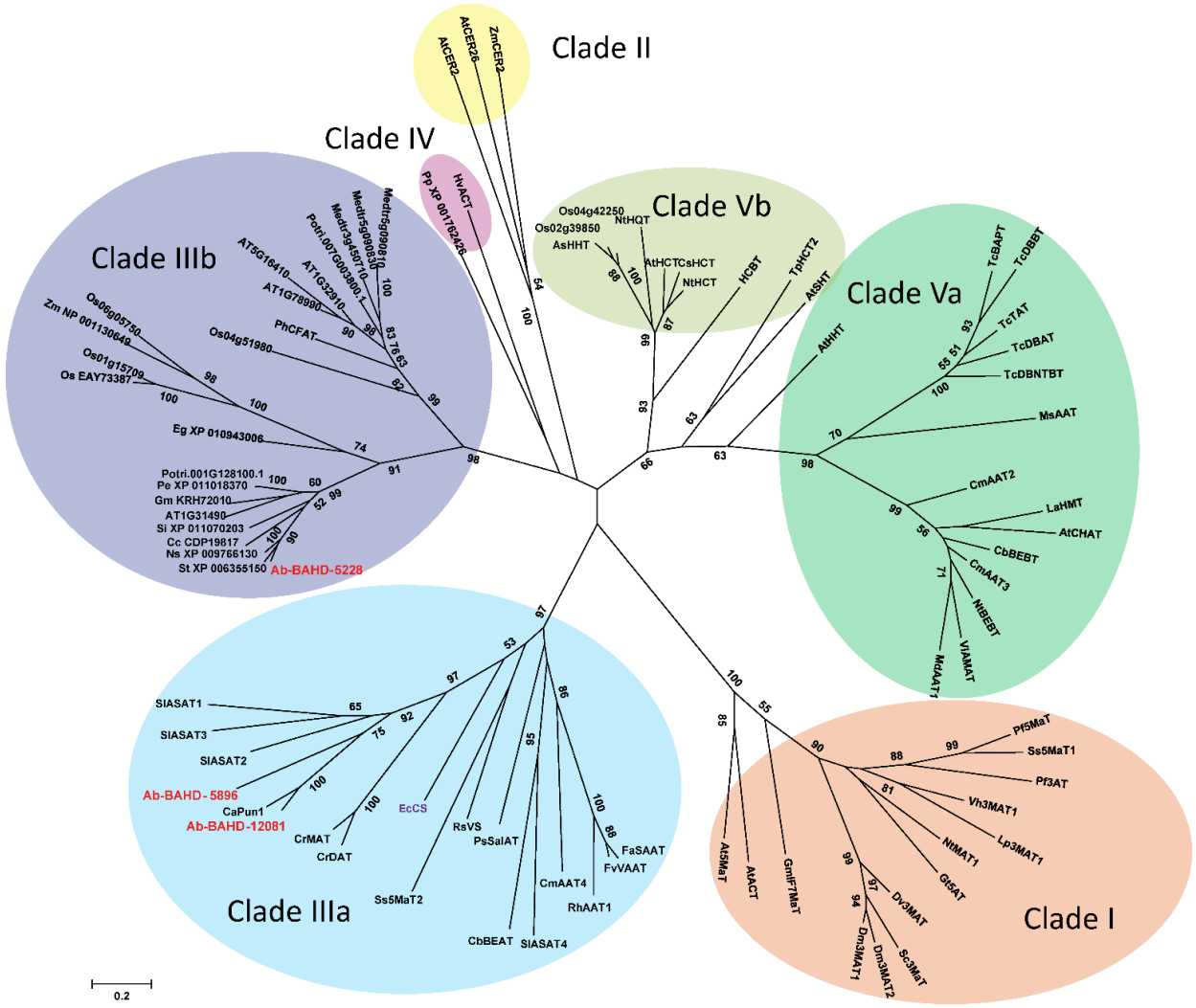

Figure 4.3 Phylogenetic Relationship of Root Preferentially Expressed BAHDs from *A. belladonna*.

An unrooted maximum likelihood phylogenetic tree obtained using a combination of functionally characterized and predicted BAHD amino acid sequences. Bootstrap values greater than 50 derived from 2000 replicates are shown on the nodes of the tree. Shading corresponds to clades as defined by (Tuominen et al., 2011). Root preferentially expressed BAHDs from *A. belladonna* are shown in red. The identities of the proteins are provided in Table 4.2.

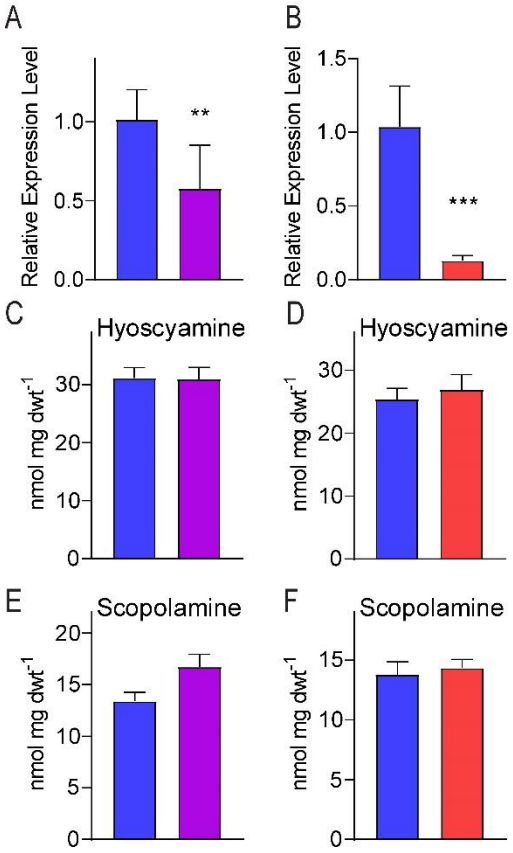

Figure 4.4 Silencing of *Ab-BAHDs* does not affect Scopolamine Levels.

(A and B) Relative expression level of *Ab-BAHDs* in *TRV2* empty vector (Blue) and *Ab-BAHD-12081* (Purple) or *5896* (Red) VIGS lines. Data are presented as the mean of six biological and three technical replicates with the expression level in *TRV2* empty vector control lines set to 1 ± SE. The six plants selected for gene expression analysis represent individuals with scopolamine levels closest to the median values for the given genotypes presented in (Figure 4.3E and F). Asterisks denote significant differences (** $P < 0.01$, *** $P < 0.001$) as determined by Student's *t* test.

(C) Abundance of DL-hyoscyamine in *TRV2* empty vector control lines (Blue) and *Ab-BAHD-12081* VIGS lines (Purple). Data are presented as the mean n = 24 ± SE.

Figure 4.4 (cont'd)

(D) Abundance of DL-hyoscyamine in *TRV2* empty vector control lines (Blue) and *Ab-BAHD-5896* VIGS lines (Red). Data are presented as the mean n = 24 ± SE.

(E) Abundance of scopolamine in *TRV2* empty vector control lines (Blue) and *Ab-BAHD-12081* VIGS lines (Purple). Data are presented as the mean n = 24 ± SE.

(F) Abundance of scopolamine in *TRV2* empty vector control lines (Blue) and *Ab-BAHD-5896* VIGS lines (Red). Data are presented as the mean n = 24 ± SE.

Table 4.2 BAHD Acyltransferases Utilized for Phylogenetic Analyses.

Organism	Sequence Name	Accession
Arabidopsis thaliana	AtCHAT	https://www.ncbi.nlm.nih.gov/protein/15228568
Arabidopsis thaliana	AT1G31490	https://www.ncbi.nlm.nih.gov/protein/15222365
Arabidopsis thaliana	AtCER26	https://www.ncbi.nlm.nih.gov/protein/15236357
Arabidopsis thaliana	AtCER2	https://www.ncbi.nlm.nih.gov/protein/15233851
Arabidopsis thaliana	AtHCT	https://www.ncbi.nlm.nih.gov/protein/15239747
Arabidopsis thaliana	AtHHT	https://www.ncbi.nlm.nih.gov/protein/30693723
Arabidopsis thaliana	AtACT	https://www.ncbi.nlm.nih.gov/protein/15240152
Arabidopsis thaliana	AtSHT	https://www.ncbi.nlm.nih.gov/protein/15224709
Arabidopsis thaliana	At5MaT	https://www.ncbi.nlm.nih.gov/protein/15230013
Arabidopsis thaliana	AT1G78990	https://www.ncbi.nlm.nih.gov/protein/3152598
Arabidopsis thaliana	AT1G32910	https://www.ncbi.nlm.nih.gov/protein/15223333
Arabidopsis thaliana	AT5G16410	https://www.ncbi.nlm.nih.gov/protein/9759123
Atropa belladonna	Ab-BAHD-5896	
Atropa belladonna	Ab-BAHD-12081	
Atropa belladonna	Ab-BAHD-5228	
Avena sativa	AsHHT	https://www.ncbi.nlm.nih.gov/protein/32400291
Capsicum annuum	CaPun1	https://www.ncbi.nlm.nih.gov/protein/55824325
Catharanthus roseus	CrDAT	https://www.ncbi.nlm.nih.gov/protein/4091808
Catharanthus roseus	CrMAT	https://www.ncbi.nlm.nih.gov/protein/27447956
Clarkia breweri	CbBEAT	https://www.ncbi.nlm.nih.gov/protein/3170250
Clarkia breweri	CbBEBT	https://www.ncbi.nlm.nih.gov/protein/75150384
Coffea canephora	Cc CDP19817	https://www.ncbi.nlm.nih.gov/protein/661875909
Cucumis melo	CmAAT3	https://www.ncbi.nlm.nih.gov/protein/1036551250
Cucumis melo	CmAAT2	https://www.ncbi.nlm.nih.gov/protein/18652312
Cucumis melo	CmAAT4	https://www.ncbi.nlm.nih.gov/protein/57472001
Cucumis sativus	CsHCT	https://www.ncbi.nlm.nih.gov/protein/821595324
Dahlia variabilis	Dv3MAT	https://www.ncbi.nlm.nih.gov/protein/75150335
Dendranthema × morifolium	Dm3MAT1	https://www.ncbi.nlm.nih.gov/protein/34305617
Dendranthema × morifolium	Dm3MAT2	https://www.ncbi.nlm.nih.gov/protein/34305619
Dianthus caryophyllus	HCBT	https://www.ncbi.nlm.nih.gov/protein/50400249
Elaeis guineensis	Eg XP_010943006	https://www.ncbi.nlm.nih.gov/protein/743860416
Erythroxylum coca	EcCS	https://www.ncbi.nlm.nih.gov/protein/531033428
Fragaria vesca	FvVAAT	https://www.ncbi.nlm.nih.gov/protein/819231752
Fragaria x ananassa	FaSAAT	https://www.ncbi.nlm.nih.gov/protein/10121328
Gentiana triflora	Gt5AT	https://www.ncbi.nlm.nih.gov/protein/38503267
Glycine max	Gm KRH72010	https://www.ncbi.nlm.nih.gov/protein/947123804
Glycine max	GmIF7MaT	https://www.ncbi.nlm.nih.gov/protein/351722557
Hordeum vulgare	HvACT	https://www.ncbi.nlm.nih.gov/protein/322518394
Lamium purpureum	Lp3MAT1	https://www.ncbi.nlm.nih.gov/protein/45790023
Lupinus albinus	LaHMT	https://www.ncbi.nlm.nih.gov/protein/125634608
Malus domestica	MdAAT1	https://www.ncbi.nlm.nih.gov/protein/52139953
Medicago truncatula	Medtr3g450710	https://www.ncbi.nlm.nih.gov/protein/922378817

Table 4.2 (cont'd)

Medicago truncatula	Medtr5g090830	https://www.ncbi.nlm.nih.gov/protein/357494159
Medicago truncatula	Medtr5g090810	https://www.ncbi.nlm.nih.gov/protein/357494155
Musa acuminata	MsAAT	https://www.ncbi.nlm.nih.gov/protein/XP_009411021.1
Nicotiana sylvestris	Ns XP_009766130	https://www.ncbi.nlm.nih.gov/protein/698541581
Nicotiana tabacum	NtHQT	https://www.ncbi.nlm.nih.gov/protein/1027853209
Nicotiana tabacum	NtHCT	https://www.ncbi.nlm.nih.gov/protein/1027858419
Nicotiana tabacum	NtBEBT	https://www.ncbi.nlm.nih.gov/protein/1027858409
Nicotiana tabacum	NtMAT1	https://www.ncbi.nlm.nih.gov/protein/1027857316
Oryza sativa	Os EAY73387	https://www.ncbi.nlm.nih.gov/protein/125525273
Oryza sativa	Os04g51980	https://www.ncbi.nlm.nih.gov/protein/1002261268
Oryza sativa	Os01g15709	https://www.ncbi.nlm.nih.gov/protein/7228445
Oryza sativa	Os06g05750	https://www.ncbi.nlm.nih.gov/protein/1002277268
Oryza sativa	Os04g42250	https://www.ncbi.nlm.nih.gov/protein/1002262849
Oryza sativa	Os02g39850	https://www.ncbi.nlm.nih.gov/protein/1002244013
Papaver somniferum	PsSalAT	https://www.ncbi.nlm.nih.gov/protein/14861417
Perilla frutescens	Pf5MaT	https://www.ncbi.nlm.nih.gov/protein/17980232
Perilla frutescens	Pf3AT	https://www.ncbi.nlm.nih.gov/protein/75192856
Petunia hybrida	PhCFAT	https://www.ncbi.nlm.nih.gov/protein/110559373
Physcomitrella patens	Pp XP_001762426	https://www.ncbi.nlm.nih.gov/protein/168019788
Populus euphratica	Pe XP_011018370	https://www.ncbi.nlm.nih.gov/protein/743808856
Populus trichocarpa	Potri.001G128100.1	https://www.ncbi.nlm.nih.gov/protein/566146477
Populus trichocarpa	Potri.007G003800.1	https://www.ncbi.nlm.nih.gov/protein/566181413
Rauvolfia serpentina	RsVS	https://www.ncbi.nlm.nih.gov/protein/57635335
Rosa hybrida	RhAAT1	https://www.ncbi.nlm.nih.gov/protein/56967598
Salvia splendens	Ss5MaT2	https://www.ncbi.nlm.nih.gov/protein/75128866
Salvia splendens	Ss5MaT1	https://www.ncbi.nlm.nih.gov/protein/75161989
Senecio cruentus	Sc3MaT	https://www.ncbi.nlm.nih.gov/protein/28396175
Sesamum indicum	Si XP_011070203	https://www.ncbi.nlm.nih.gov/protein/747041003
Solanum lycopersicum	SlASAT2	https://www.ncbi.nlm.nih.gov/protein/970597816
Solanum lycopersicum	SlASAT3	https://www.ncbi.nlm.nih.gov/protein/723745432
Solanum lycopersicum	SlASAT4	https://www.ncbi.nlm.nih.gov/protein/392522210
Solanum lycopersicum	SlASAT1	https://www.ncbi.nlm.nih.gov/protein/970597792
Solanum tuberosum	St XP_006355150	https://www.ncbi.nlm.nih.gov/protein/565377356
Taxus canadensis	TcDBNTBT	https://www.ncbi.nlm.nih.gov/protein/21700317
Taxus cuspidata	TcBAPT	https://www.ncbi.nlm.nih.gov/protein/23534472
Taxus cuspidata	TcDBAT	https://www.ncbi.nlm.nih.gov/protein/6746554
Taxus cuspidata	TcDBBT	https://www.ncbi.nlm.nih.gov/protein/11559716
Taxus cuspidata	TcTAT	https://www.ncbi.nlm.nih.gov/protein/6978038
Trifolium pratense	TpHCT2	https://www.ncbi.nlm.nih.gov/protein/206730711
Verbena hybrida	Vh3MAT1	https://www.ncbi.nlm.nih.gov/protein/45790002
Vitis labrusca	VlAMAT	https://www.ncbi.nlm.nih.gov/protein/56694504
Zea mays	Zm NP_001130649	https://www.ncbi.nlm.nih.gov/protein/212274421
Zea mays	ZmCER2	https://www.ncbi.nlm.nih.gov/protein/949980

Aromatic Tropane Esters Are Synthesized via Glucose-ester Mediated Acylation in *A. belladonna*

Silencing of *BAHD*s preferentially expressed in roots of *A. belladonna* failed to identify a candidate gene required for the formation of hyoscyamine and scopolamine. Thus, based on prior knowledge of the biosynthesis of diverse classes of plant specialized metabolites, and particularly those with aromatic rings (Bontpart et al., 2015), it was hypothesized that the alternative acylation pathway involving a 1-*O*-β-glucose ester intermediate as the acyl donor and an SCPL acyltransferase is required for aromatic tropane ester formation in *A. belladonna* (Figure 4.1). To test this hypothesis, the *A. belladonna* transcriptome was mined for root-preferentially expressed transcripts encoding UDP-glucosyltransferases (UGTs) and SCPLs. In both cases, a single unigene predicted to encode a member of each enzyme class; *Ab-UGT-22777* and *Ab-SCPL-17884* was identified (Figure 4.5A). Phylogenetic analyses revealed Ab-UGT-22777 is closely related to the UGT84A1-4 enzymes of *Arabidopsis thaliana* (Figure 4.6). The UGT84 subfamily includes enzymes that catalyze the transfer of glucose from UDP-glucose to either an alcohol or a carboxylic acid functional group, resulting in production of glucosyl ethers or acyl-glucose esters (Hall and De Luca, 2007; Landmann et al., 2007; Sinlapadech et al., 2007; Babst et al., 2014). For example, UGT84A2 and UGT84A9 from Arabidopsis and *Brassica napus*, respectively, catalyze the synthesis of glucosyl-1-*O*-sinapate, the glucose ester substrate of SCPL acyltransferases that synthesize sinapoylmalate and sinapoylcholine (Lehfeldt et al., 2000; Milkowski et al., 2000; Milkowski et al., 2004; Sinlapadech et al., 2007).

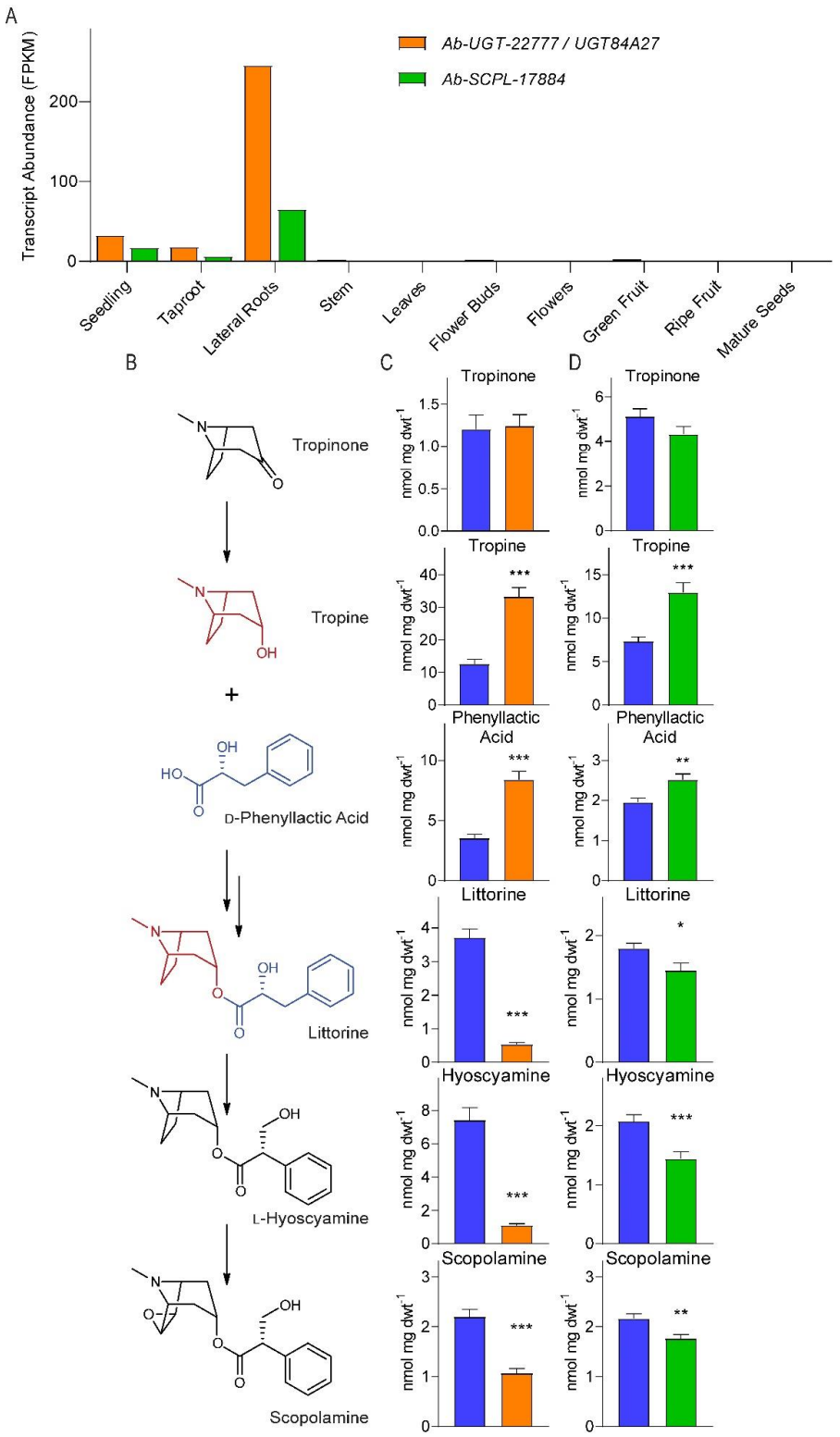

Figure 4.5. Silencing of *UGT84A27* and *Ab-SCPL-17884* Reduces Aromatic Tropane Ester Levels

Figure 4.5 (cont'd)

(A) Transcript abundance of *Ab-UGT-22777* (*UGT84A27*) and *Ab-SCPL-17884* in *A. belladonna* tissues.

(B) Structures and pathway relation of select quantified metabolites.

(C) Abundance of the tropane alkaloids and selected precursors in *TRV2* empty vector control (Blue) and *UGT84A27* VIGS lines (Orange). Data are presented as the mean n = 24 ± SE. Asterisks denote significant differences (*** $P < 0.001$) as determined by Student's *t* test.

(D) Abundance of tropane alkaloids and selected precursors in *TRV2* empty vector control (Blue) and *Ab-SCPL-17884* VIGS lines (Green). Data are presented as the mean n = 24 ± SE. Asterisks denote significant differences (* $P < 0.05$, ** $P < 0.01$, *** $P < 0.001$) as determined by Student's *t* test.

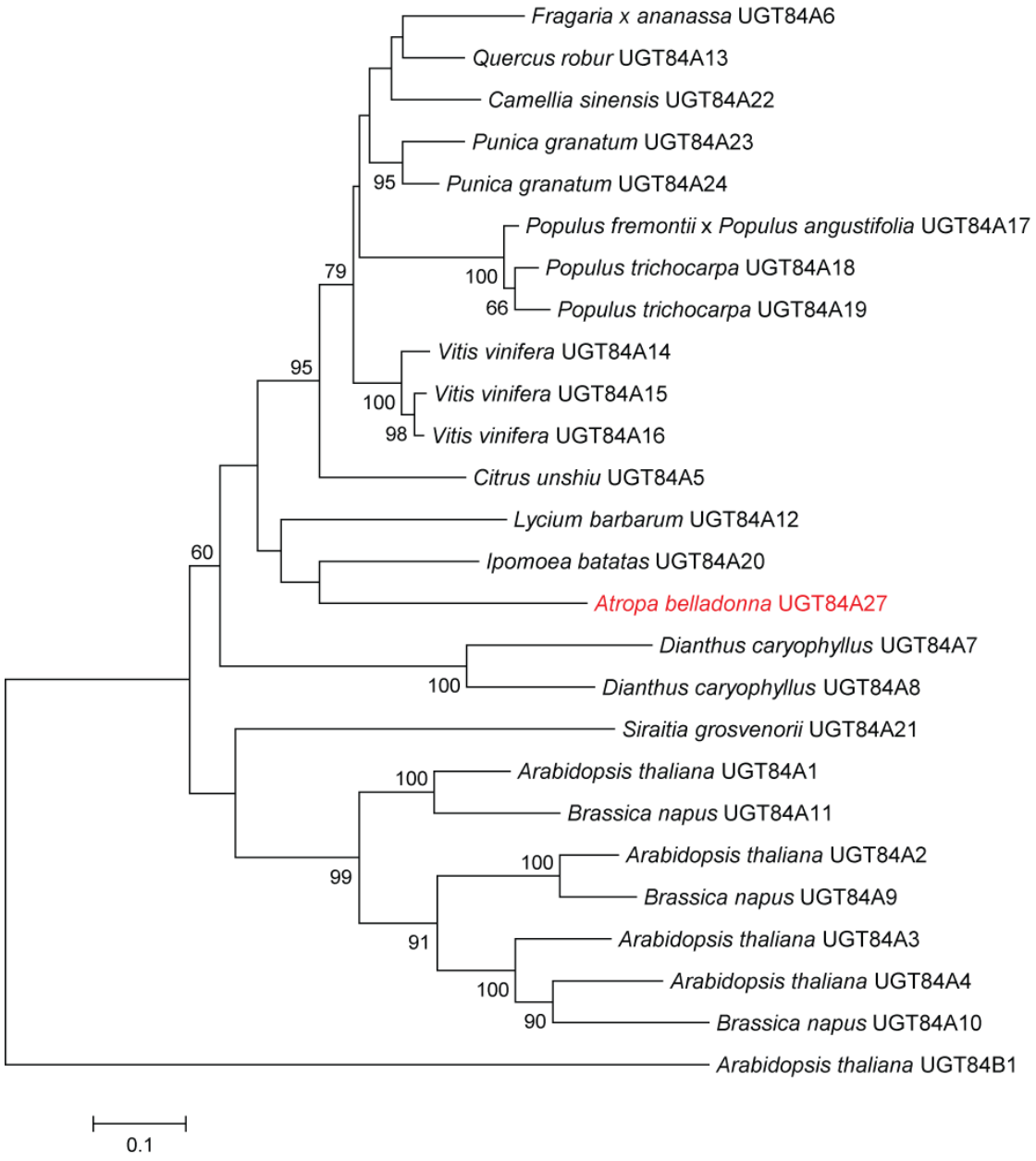

Figure 4.6 Phylogenetic Relationship of *A. belladonna* UGT84A27 with Additional Proteins of the UGT84A Subfamily.

An unrooted maximum likelihood phylogenetic tree constructed using MEGA version 5 is shown. Bootstrap values greater than 50 derived from 2000 replicates are shown on the nodes of the tree. The identities of the proteins are provided in Table 4.3.

Table 4.3 UGT84A Subfamily Members Utilized for Phylogenetic Analyses.

Organism	Sequence Name	Accession
Arabidopsis thaliana	UGT84A1	http://www.ncbi.nlm.nih.gov/protein/CAB10326.1
Arabidopsis thaliana	UGT84A2	http://www.ncbi.nlm.nih.gov/protein/BAB02351.1
Arabidopsis thaliana	UGT84A3	http://www.ncbi.nlm.nih.gov/protein/CAB10327.1
Arabidopsis thaliana	UGT84A4	http://www.ncbi.nlm.nih.gov/protein/CAB10328.1
Arabidopsis thaliana	UGT84B1	http://www.ncbi.nlm.nih.gov/protein/AAB87119.1
Atropa belladonna	UGT84A27	
Brassica napus	UGT84A9	http://www.ncbi.nlm.nih.gov/protein/9794913
Brassica napus	UGT84A10	http://www.ncbi.nlm.nih.gov/protein/88999675
Brassica napus	UGT84A11	http://www.ncbi.nlm.nih.gov/protein/88999677
Camellia sinensis	UGT84A22	http://www.ncbi.nlm.nih.gov/nuccore/KA279970.1
Citrus unshiu	UGT84A5	http://www.ncbi.nlm.nih.gov/protein/BAA93039.1
Dianthus caryophyllus	UGT84A7	http://www.ncbi.nlm.nih.gov/protein/156138785
Dianthus caryophyllus	UGT84A8	http://www.ncbi.nlm.nih.gov/protein/156138771
Fragaria x ananassa	UGT84A6	http://www.ncbi.nlm.nih.gov/protein/51705411
Ipomoea batatas	UGT84A20	http://www.ncbi.nlm.nih.gov/protein/1049013395
Lycium barbarum	UGT84A12	http://www.ncbi.nlm.nih.gov/protein/209954699
Populus fremontii x Populus angustifolia	UGT84A17	http://www.ncbi.nlm.nih.gov/protein/670609967
Populus trichocarpa	UGT84A18	https://phytozome.jgi.doe.gov/phytomine/report.do?id=218476194
Populus trichocarpa	UGT84A19	https://phytozome.jgi.doe.gov/phytomine/report.do?id=218476198
Punica granatum	UGT84A23	http://www.ncbi.nlm.nih.gov/protein/1039217158
Punica granatum	UGT84A24	http://www.ncbi.nlm.nih.gov/protein/1039217162
Quercus robur	UGT84A13	http://www.ncbi.nlm.nih.gov/protein/558480484
Siraitia grosvenorii	UGT84A21	http://www.ncbi.nlm.nih.gov/protein/343466223
Vitis vinifera	UGT84A14	http://www.ncbi.nlm.nih.gov/protein/XP_002274256
Vitis vinifera	UGT84A15	http://www.ncbi.nlm.nih.gov/protein/XP_002285379
Vitis vinifera	UGT84A16	http://www.ncbi.nlm.nih.gov/protein/NP_001267849

Therefore, if aromatic tropane esters of *A. belladonna* are formed by SCPL-mediated acylation, then a glucose ester of D-phenyllactic acid is the likely acyl donor that undergoes condensation with tropine to form littorine, the precursor of hyoscyamine and scopolamine (Figure 4.1). Based on current nomenclature standards, the root-expressed UGT from *A. belladonna* was designated UGT84A27. Compared to UGTs, few SCPLs are functionally characterized but sequence analysis revealed that Ab-SCPL-17884 shares common features with several well characterized SCPLs (Stehle et al., 2006), including a signature catalytic triad, a leader sequence for targeting to the secretory system, and a linker sequence that is ultimately cleaved to yield a mature enzyme (Figure 4.7). Phylogenetic analyses placed Ab-SCPL-17884 within a clade of several uncharacterized SCPLs from tomato, and potato (*Solanum tuberosum*) that each share between 50-60% amino acid identity with Ab-SCPL-17884 (Figure 4.8).

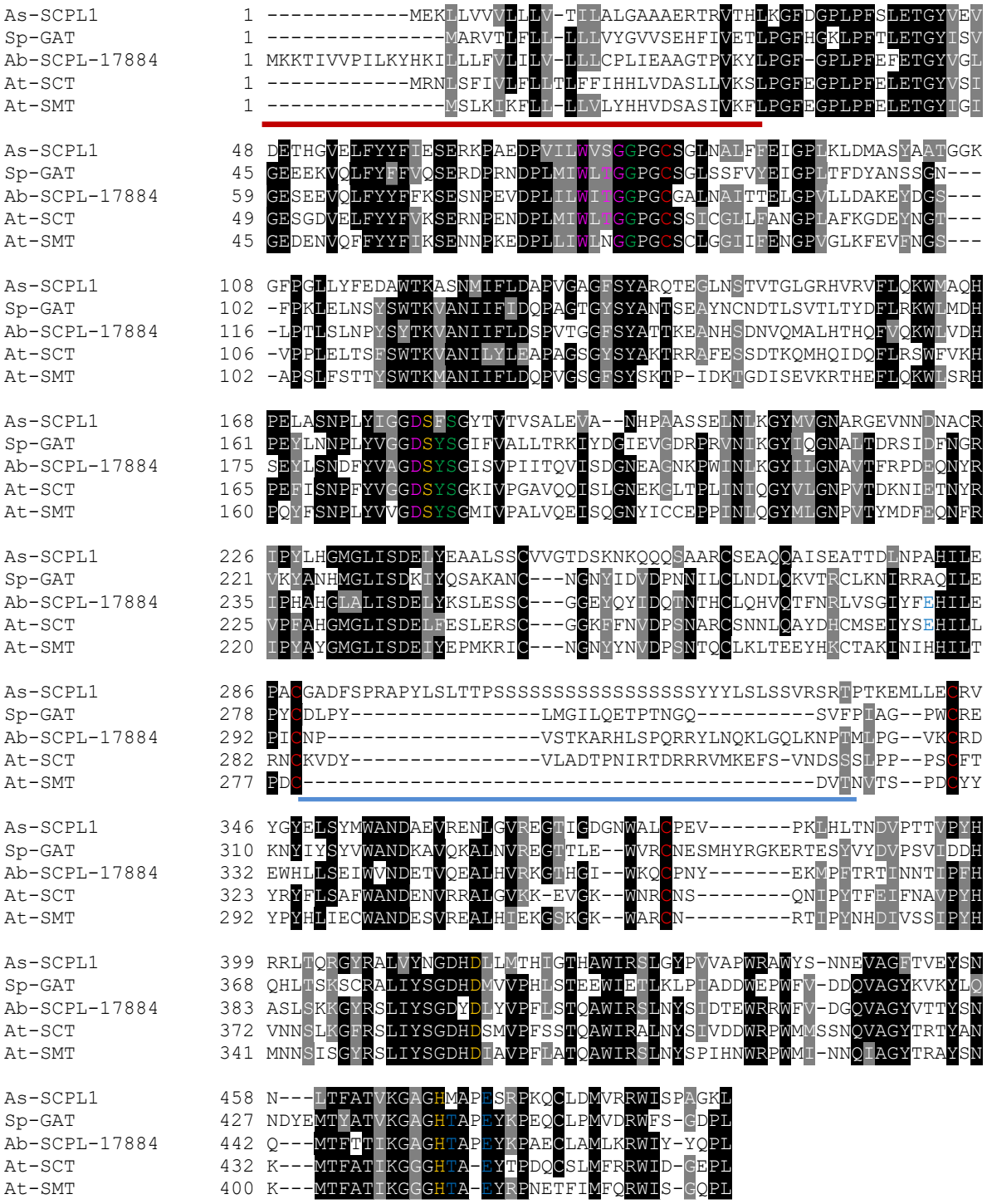

Figure 4.7 Amino Acid Alignment of Ab-SCPL-17884 and Related SCPL Acyltransferases.

Figure 4.7 (cont'd)

A full-length amino acid alignment was generated using MUSCLE (Edgar, 2004) with Ab-SCPL-17884 and well characterized SCPLs from *A. thaliana* (At-SCT, At-SMT), *A. strigosa* (As-SCPL1), and *S. pennellii* (Sp-GAT). Boxshade was used to indicate conserved residues with a threshold of 0.7 (black shading). Amino acid residues with similar properties are shown in gray. The putative catalytic triad is shown in gold. Cysteines putatively involved in cross-subunit disulfide bonds are shown in red. Highlighted are residues putatively forming the oxyanion hole (Green), those involved in forming a hydrogen bond network for the active site (Pink), and residues putatively interacting with the choline moiety of AtSCT (Blue). Underlined regions predicted to be removed from the processed enzyme and constitute the leader sequence (red line) and the linker sequence (blue line), respectively. For details, refer to Stehle et al., 2006.

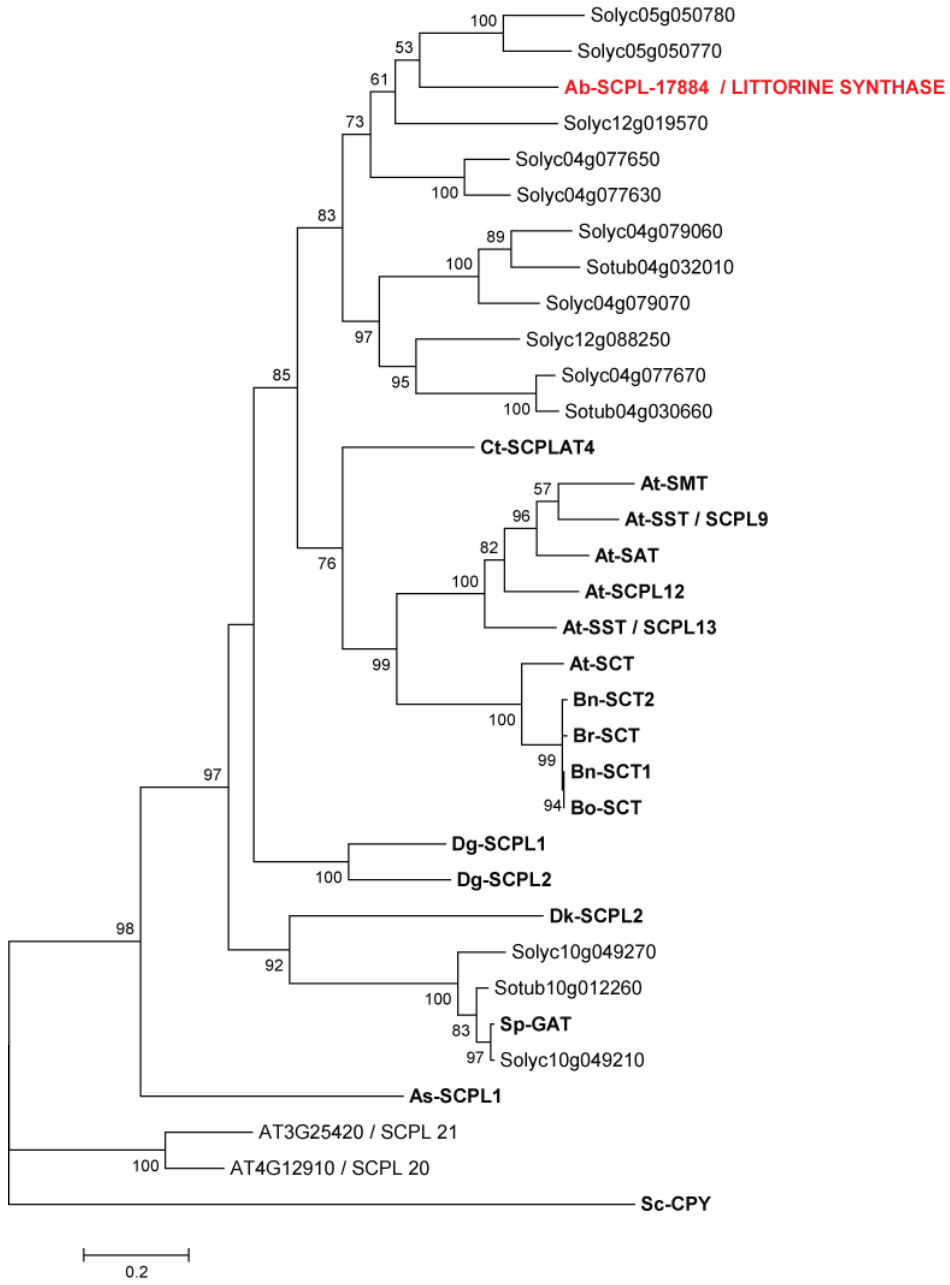

Figure 4.8 Phylogenetic Relationship of Ab-SCPL-17884 and Related SCPL Acyltransferases.

A maximum likelihood phylogenetic tree constructed using MEGA version 5 is shown. Bootstrap values greater than 50 derived from 2000 replicates are shown on the nodes of the tree. Proteins shown in bold represent biochemically characterized SCPLs. The identities of the proteins are provided in Table 4.4.

Table 4.4 SCPL Acyltransferases Utilized for Phylogenetic Analyses.

Organism	Sequence Name	Accession
Arabidopsis thaliana	AtSCT	http://www.genome.jp/dbget-bin/www_bget?uniprot:SCP19_ARATH
Arabidopsis thaliana	AtSMT	http://www.ncbi.nlm.nih.gov/protein/Q8RUW5.2
Arabidopsis thaliana	AtSAT	http://www.uniprot.org/uniprot/O64810
Arabidopsis thaliana	AtSST (AtSCPL9)	http://www.uniprot.org/uniprot/O64811
Arabidopsis thaliana	AtSCPL12	http://www.uniprot.org/uniprot/O81009
Arabidopsis thaliana	AtSST (AtSCPL13)	http://www.ncbi.nlm.nih.gov/protein/NP_179881
Arabidopsis thaliana	AtSCPL20	http://www.ncbi.nlm.nih.gov/protein/AEE83202.1
Arabidopsis thaliana	AtSCPL21	http://www.ncbi.nlm.nih.gov/protein/NP_189169.1
Atropa belladonna	Littorine Synthase	
Avena strigosa	AsSCPL1	http://www.uniprot.org/uniprot/C8YJB5
Brassica napus	BnSCT1	http://www.ncbi.nlm.nih.gov/protein/AAQ91191
Brassica napus	BnSCT2	http://www.uniprot.org/uniprot/A4VB85
Brassica oleracea	BoSCT	http://www.uniprot.org/uniprot/A4VB82
Brassica rapa	BrSCT	http://www.uniprot.org/uniprot/B0JDI4
Clitorea terneata	CtSCPLAT4	http://www.genome.jp/dbget-bin/www_bget?uniprot:B0I1H8_CLITE
Delphinium grandiflorum	DgSCPL1	http://www.ncbi.nlm.nih.gov/protein/557357632
Delphinium grandiflorum	DgSCPL2	http://www.ncbi.nlm.nih.gov/protein/557357634
Diospyros kaki	DkSCPL2	http://www.uniprot.org/uniprot/C6L1N2
Saccharomyces cerevisiae	ScCPY	http://www.uniprot.org/uniprot/P00729
Solanum lycopersicum		Solyc10g049210
Solanum lycopersicum		Solyc10g049270
Solanum lycopersicum		Solyc05g050780
Solanum lycopersicum		Solyc05g050770
Solanum lycopersicum		Solyc12g019570
Solanum lycopersicum		Solyc04g077630
Solanum lycopersicum		Solyc04g077650
Solanum lycopersicum		Solyc04g079060
Solanum lycopersicum		Solyc04g079070
Solanum lycopersicum		Solyc12g088250
Solanum lycopersicum		Solyc04g077670

Table 4.4 (cont'd)

Solanum pennellii	SpGAT	http://www.ncbi.nlm.nih.gov/protein/AAF64227
Solanum tuberosum		Sotub10g012260
Solanum tuberosum		Sotub04g032010
Solanum tuberosum		Sotub04g030660

Silencing of *UGT84A27* and *Ab-SCPL-17884* was performed to determine whether they are involved in tropane alkaloid biosynthesis. Silencing resulted in an approximate 90% reduction in transcript abundance in *UGT84A27*-silenced lines and an 80% reduction in transcript abundance in *Ab-SCPL-17884*-silenced lines (Figure 4.9). The aromatic tropane esters littorine, hyoscyamine, and scopolamine were significantly reduced ($P < 0.001$; Student's *t*-test) in *UGT84A27*-silenced lines compared to *TRV2* empty vector control lines (Figure 4.5B and C). This was accompanied by an ~2.5-fold increase in tropine and phenyllactic acid, the precursors of littorine. Silencing of *Ab-SCPL-17884* similarly affected the abundance of tropane-related metabolites, although the magnitude of the difference between *TRV2* and *Ab-SCPL-17884* lines was less (Figure 4.5D). This difference may result from the reduced silencing efficiency of *Ab-SCPL-17884* compared to that observed in *UGT84A27*-silenced lines (Figure 4.9).

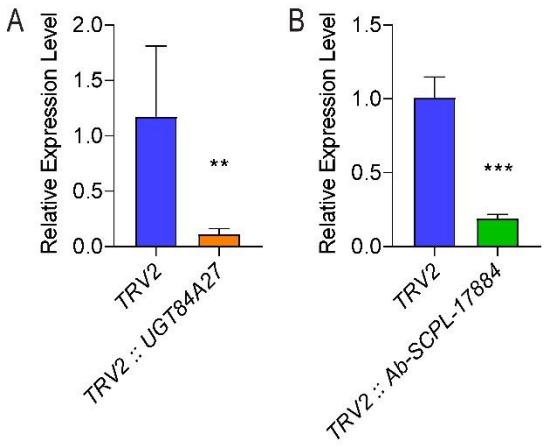

Figure 4.9 Efficiency of RNAi in *UGT84A27* and *Ab-SCPL-17884* VIGS lines.

(A and B) Relative expression level of *UGT84A27* (A) and *Ab-SCPL-17884* (B) in *TRV2* empty vector control lines and *UGT84A27* or *Ab-SCPL-17884* VIGS lines. Data are presented as the mean of six biological and three technical replicates with the expression level in *TRV2* empty vector control lines set to 1 ± SE. The six plants selected for gene expression analysis represent individuals with scopolamine levels closest to the median values for the given genotypes presented in (**Figure 4.5C** and **D**). Asterisks denote significant differences (** $P < 0.01$) as determined by Student's *t* test.

Based on the phenotypes of the *UGT84A27* and *Ab-SCPL-17884* silenced lines, it was predicted that a hexosyl-D-phenyllactate (*m/z* 327.1 $[M-H]^-$) or its formate adduct (*m/z* 373.1, $[M+HCOO]^-$) would be detectable by LC/MS in *Ab-SCPL-17884* silenced lines. Further, by comparison, we hypothesized the metabolite abundances of the glycoside and its formate adduct would be reduced in the *UGT84A27* silenced lines relative to that of *TRV2* controls. This hypothesis was substantiated by analyzing the metabolites from these lines for a pseudomolecular ion *m/z* 373.1 that yielded a fragment ion *m/z* 165.05, corresponding to phenyllactic acid carboxylate anion, upon collision-induced dissociation at elevated collision potentials (Figure 4.10A and B). Attempts to purify the hexosyl D-phenyllactic acid ester for structural elucidation were unsuccessful due to its low abundance and propensity for hydrolysis and acyl group rearrangement on the glycoside to form multiple isomers. Together, these data suggest that littorine formation occurs through hexose-ester mediated acylation, involving *UGT84A27* and *Ab-SCPL-17884*.

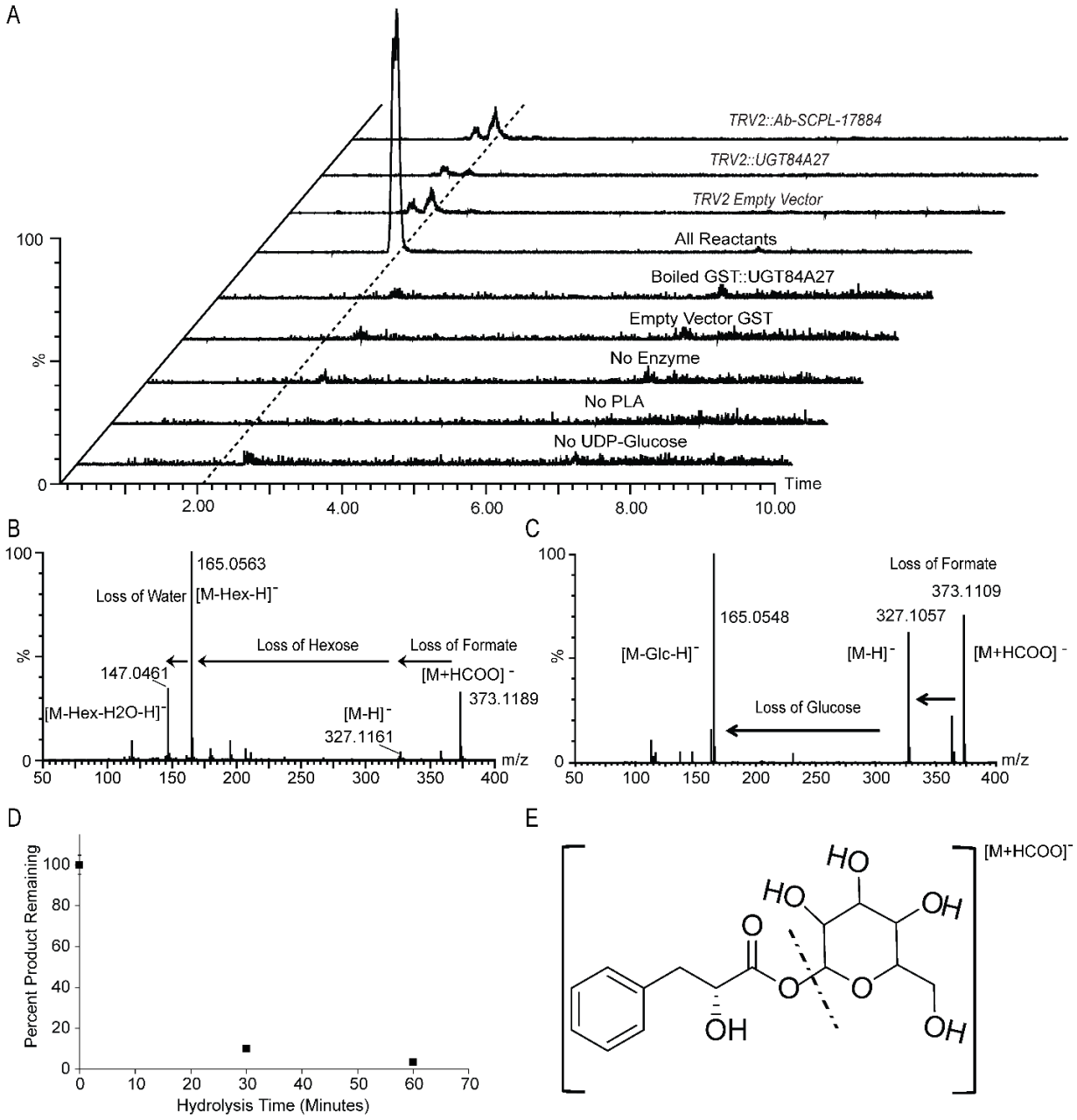

Figure 4.10 Accumulation of a glucosyl phenyllactate in *UGT84A27* and *Ab-SCPL-17884* silenced lines and characterization of the Ab-UGT84A27 product.

Figure 4.10 (cont'd)

(A) Extracted ion chromatograms (*m/z* 327.1, $[M-H]^-$) of the product mixtures from UGT84A27-mediated catalysis of glucosyl phenyllactate, various control assays lacking a key ingredient, a boiled enzyme control, or from in representative *TRV2* empty vector control lines, *UGT84A27* VIGS lines, and *Ab-SCPL-17884* VIGS lines. The Y-axes indicate arbitrary signal units and percent signal compared to maximum.

(B) Mass spectrum of glucosyl phenyllactate in a representative *Ab-SCPL-17884* VIGS line under MS^E as described in METHODS.

(C) Mass spectrum of the UGT84A27-catalyzed reaction containing 'All Reactants' shown in panel *A*.

(D) Hydrolysis of the UGT84A27-catalyzed reaction product under mild alkaline conditions as described in METHODS.

(E) Predicted structure of the formate adduct of glucosyl-1-*O*-D-phenyllactate. The dashed line indicates where fragmentation occurs to release a fragment ion corresponding to phenyllactate.

UGT84A27 Possesses UDP-Glucose:Phenyllactic Acid Glucosyltransferase Activity

LC/MS analyses predict that hexosyl phenyllactate is an intermediate in littorine biosynthesis (Figure 4.10). As all known acyl donor substrates for SCPL acyltransferases are glucose esters, the product of UGT84A27 is predicted to be a glucose ester of D-phenyllactic acid (Figure 4.1). To test if UGT84A27 catalyzes the formation of glucosyl-1-*O*-D-phenyllactate, the enzyme was expressed as an *N*-terminal GST fusion protein in *E. coli*. Initial assays using purified recombinant fusion protein were performed at pH 6.0 due to the potential for hydrolysis and acyl group migration on the predicted glucosyl-1-*O*-D-phenyllactate ester product at higher pH. A pseudomolecular ($[M+HCOO]^-$) ion of *m/z* 373.1109 of a glucosyl-1-*O*-D-phenyllactate was observed in assay mixtures incubated with UGT84A27 and all reactants. This signal was absent in assays when the enzyme was omitted or denatured, or substrates were excluded (Figure 4.10A). In addition, the glucosyl-1-*O*-D-phenyllactate synthesized through UGT84A27 catalysis co-retains with the predicted hexosyl phenyllactate detected *in planta* while collision-induced fragmentation of the pseudomolecular ions yields identical mass spectra to reveal the phenyllactic acid fragment ion: *m/z* 165.05 (Figure 4.10A – C).

As D-phenyllactic acid is an α-hydroxy acid, the signal annotated as glucosyl-1-*O*-D-phenyllactate formed by UGT84A27 could be a glucose ester, a glucose ether, or a combination of both compounds that are unresolved by chromatography. However, only glucose esters are known to be substrates of SCPLs and these can be distinguished from glucose ethers through their propensity for hydrolysis under mild alkaline conditions

(Babst et al., 2014). Thus the biosynthetic products formed by UGT84A27 catalysis were subjected to mild alkaline hydrolysis (pH 10) for one hour at room temperature, and the resulting products analyzed by LC/MS/MS (Figure 4.10D). Mild alkaline hydrolysis led to ~95% reduction in the ion abundance of a compound consistent with a glucosyl phenyllactate isomer, suggesting that the majority of the enzymatically produced compound is a glucose ester. The instability of the glucosyl-1-*O*-D-phenyllactate product toward base hydrolysis and potential for acyl group migration necessitated acidic conditions to stabilize the ester formed after UGT84A27 catalysis, and thus confounded accurate characterization of enzyme properties at higher pH by quantifying glucosyl-1-*O*-D-phenyllactate using LC/MS. Hence, an alternative assay based on direct measurement of UDP released during catalysis was utilized, allowing for quantitative assessment of UGT84A27 kinetic parameters. Utilizing this alternative assay, UGT84A27 was found to have a pH optimum of ~8.0 and the apparent K_m and V_{max} for UDP-glucose were 230 µM and 0.12 nmol sec^{-1} mg^{-1}, respectively, while the apparent K_m and V_{max} for D-phenyllactic acid were 790 µM and 0.11 nmol sec^{-1} mg^{-1}, respectively (Table 4.5 and Figure 4.11).

Table 4.5 Kinetic Properties of Ab-UGT84A27

Variable Substrate (Concentration in Assay)	Co-substrate (Concentration in Assay)	K_m (μM)	V_{max} (nmol sec^{-1} mg^{-1})	K_i (μM)	k_{cat} (sec^{-1})	k_{cat}/K_m (mM^{-1} sec^{-1})
UDP-Glucose (0.031 - 2 mM)	D-Phenyllactic Acid (10 mM)	230 ± 40[a]	0.12 ± 0.002	N/A	0.0095 ± 0.0002	0.046 ± 0.01
D-Phenyllactic Acid (0.15 - 10 mM)	UDP-Glucose (2 mM)	790 ± 60	0.11 ± 0.01	N/A	0.0091 ± 0.0008	0.011 ± 0.0003
4-Coumaric Acid (0.061 - 250 μM)	UDP-Glucose (1 mM)	0.075 ± 0.004	7.91 ± 0.16	22.8 ± 3.9	0.66 ± 0.01	8657.8 ± 268.7
Caffeic Acid (0.061 - 250 μM)	UDP-Glucose (1 mM)	2.27 ± 0.08	8.66 ± 0.05	325.2 ± 29.5	0.71 ± 0.004	312.4 ± 12.4
Ferulic Acid (0.061 - 250 μM)	UDP-Glucose (1 mM)	0.30 ± 0.03	8.27 ± 0.24	892.6 ± 2.4	0.68 ± 0.02	2256.8 ± 168.8
UDP-Glucose (0.00049 - 1 mM)	4-Coumaric Acid (2 μM)	4.79 ± 0.65	7.67 ± 0.09	N/A	0.63 ± 0.007	136.6 ± 22.0

[a] All data are presented as the mean ± SE of three replicates.

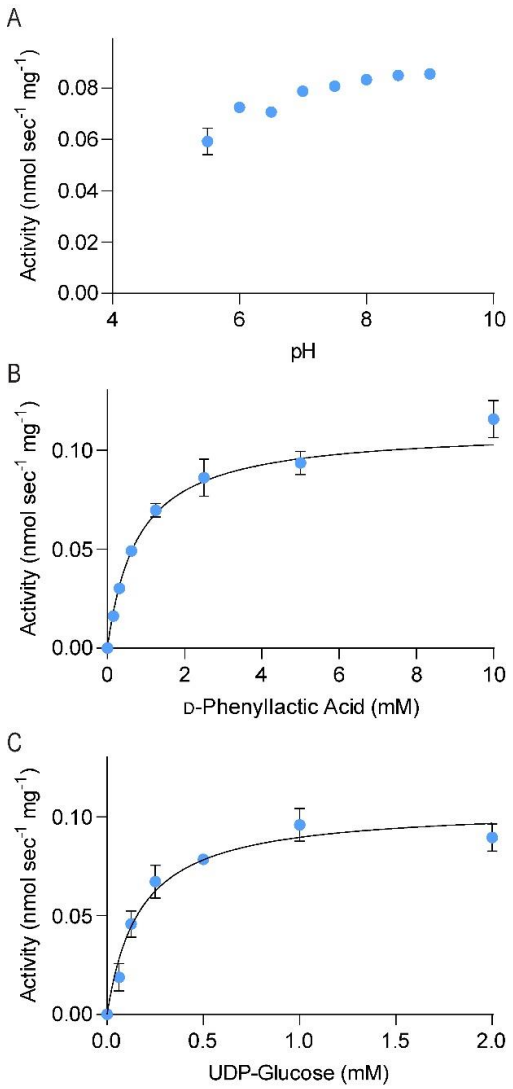

Figure 4.11 Characterization of UGT84A27 activity using D-phenyllactic acid and UDP-glucose.

(A) Determination of the pH optimum of UGT84A27.

(B) Determination of the apparent K_m of UGT84A27 for D-phenyllactic acid using 2 mM UDP-glucose as the co-substrate.

(C) Determination of the apparent K_m of UGT84A27 for UDP-glucose with 10 mM D-phenyllactic acid as co-substrate. Data are presented as the mean of three replicates ± SE.

Ab-SCPL-17884 Possesses Littorine Synthase Activity

Results of metabolite profiling following silencing of *Ab-SCPL-17884* suggest a direct role for this enzyme in littorine biosynthesis through condensation of tropine with the glucosyl-1-*O*-D-phenyllactate formed by UGT84A27 (Figure 4.5D). Plant SCPLs undergo several post-translational modifications, including those leading to translocation to the endoplasmic reticulum, proteolytic cleavage of both a leader peptide and a variable endopeptide, formation of several disulfide bonds, and presumptive asparagine glycosylation with the mature enzyme transported to the vacuole (Bontpart et al., 2015). The variety and type of post-translational modifications makes heterologous expression of full-length SCPLs in *E. coli* challenging. Therefore, to test the hypothesis that Ab-SCPL-17884 possesses littorine synthase activity, a full-length untagged version of Ab-SCPL-17884 was transiently expressed in leaves of *Nicotiana benthamiana* and the resulting crude protein extracts utilized in coupled assays together with the glucosyl-1-*O*-D-phenyllactate formed by recombinant UGT84A27. Utilizing this approach, LC/MS analysis of the product of the assay yielded a pseudomolecular ($[M+H]^+$) ion at *m/z* 290.17, which is consistent with littorine. A signal at this mass was only present when UDP-glucose, D-phenyllactic acid, tropine, UGT84A27, and leaf protein extracted from *N. benthamiana* expressing Ab-SCPL-17884 were included in the reaction mix (Figure 4.12A). The reaction product formed by Ab-SCPL-17884 catalysis has a retention time and fragmentation pattern that matched an authentic littorine standard (Figure 4.12B-E). Furthermore, this reaction was highly stereospecific as no product was observed when pseudotropine was substituted for tropine (Figure 4.12F). This stereoselectivity is consistent with the stereochemistry of littorine *in planta*. Attempts to determine the kinetic

parameters of the littorine synthase enzyme were thwarted by the inability to synthesize sufficient quantities of the glucosyl-1-*O*-D-phenyllactate ester for use as a substrate. Together, these data demonstrate that *Ab-SCPL-17884* encodes littorine synthase, an enzyme that possesses strong stereospecificity for tropine as the acyl acceptor. This is consistent with the role of this α-epimer in hyoscyamine and scopolamine biosynthesis (Figure 4.1).

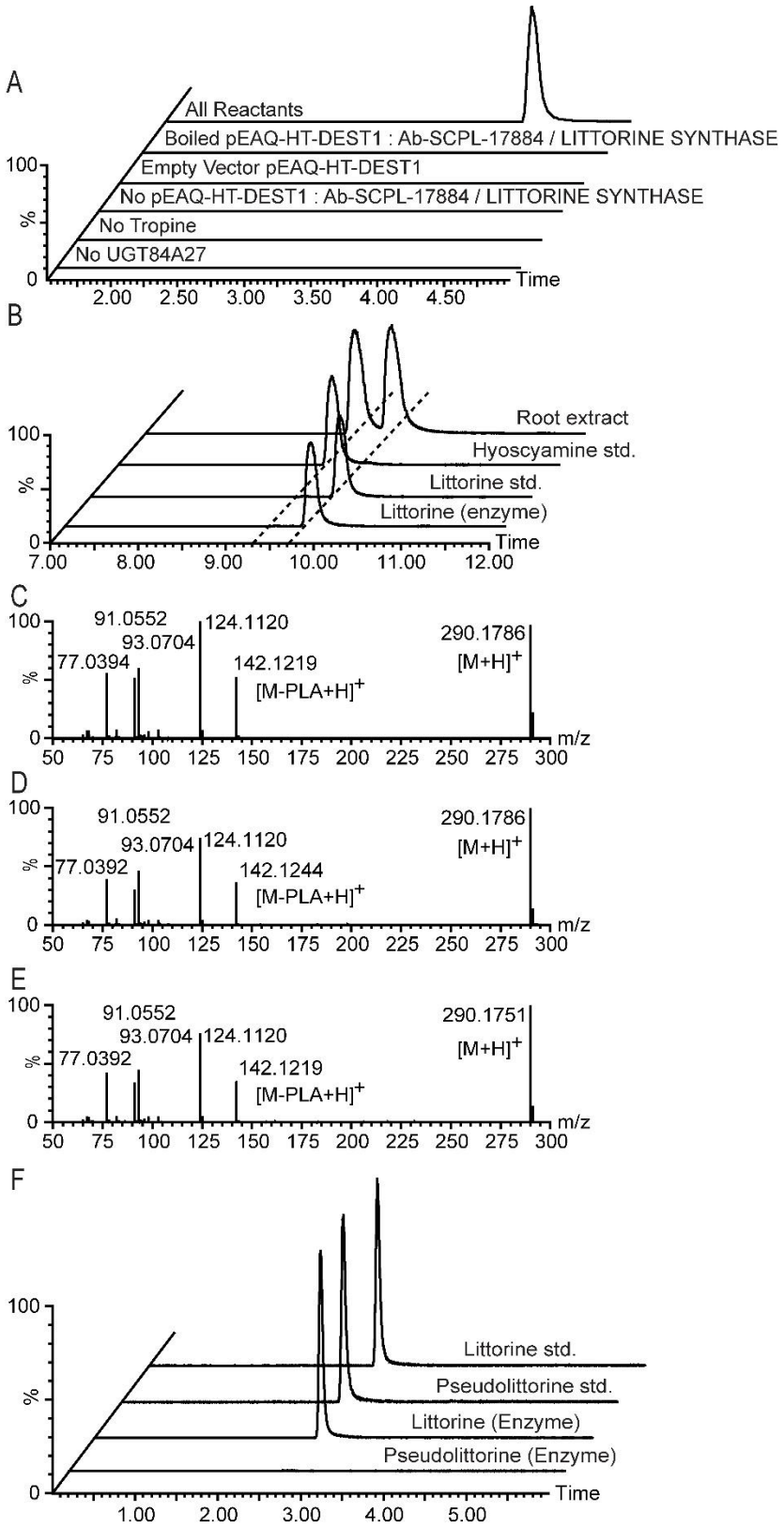

Figure 4.12 *Ab-SCPL-17884* encodes LITTORINE SYNTHASE.

Figure 4.12 (cont'd)

(A) Extracted ion LC/MS chromatograms (*m/z* 290.17, $[M+H]^+$) of product mixtures isolated from UGT84A27 and Ab-SCPL-17884-mediated *in vitro* production of littorine, various control assays lacking a key ingredient, or a boiled enzyme control. The Y-axes indicate arbitrary signal units and percent signal compared to maximum.

(B) Extracted ion LC/MS chromatograms (*m/z* 290.17, $[M+H]^+$) for hyoscyamine (RT 9.38 min), and littorine (RT 9.79 min) identified in product mixtures isolated from *A. belladonna* (labeled as 'Root Extract', authentic standards of hyoscyamine and littorine (each labeled accordingly), and products of an *in vitro* coupled enzyme reaction of UGT84A27 and Ab-SCPL-17884 using tropine to produce littorine (labeled as 'Littorine (enzyme)'.

(C) The mass spectrum of littorine from the *A. belladonna* root extract shown in Panel B. The $[M+H]^+$ and $[M\text{-}PLA+H]^+$ (PLA: phenyllactoyl fragment of littorine) ions are shown.

(D) The mass spectrum of authentic littorine shown in Panel B.

(E) The mass spectrum of littorine formed in the coupled *in vitro* enzyme reaction containing UGT84A27 and Ab-SCPL-17884 catalysts labeled as 'Littorine (enzyme)' in Panel B.

(F) Extracted ion LC/MS chromatograms (*m/z* 290.17, $[M+H]^+$) of product mixtures isolated from UGT84A27 and Ab-SCPL-17884-mediated *in vitro* production of littorine or pseudolittorine, using tropine or pseudotropine as the acyl acceptor, respectively. Enzyme reactions and authentic standards are labeled accordingly. The Y-axis indicates arbitrary signal units and percent signal compared to maximum.

Catalytic Promiscuity of UGT84A27

Enzymes of the UGT84A subfamily typically exhibit catalytic promiscuity and are able to use diverse phenolic and benzoic acid substrates (Bowles et al., 2006). To determine whether such catalytic promiscuity is also a property of UGT84A27, the *in vitro* activity of the enzyme was tested with 29 phenolic substrates that were grouped into seven structural classes: group 1, phenylpropanoic acids without an α-substitution; group 2, phenylpropanoic acids with an α-substitution; group 3 benzoic acids without an *ortho*-substitution; group 4, benzoic acids with an *ortho*-substitution; group 5, phenylacetic acids without an α-substitution; group 6, phenylacetic acids with an α-substitution; group 7, flavonoids (Figure 4.13 and Figure 4.14). These experiments revealed that UGT84A27 exhibited a wide range of glucosyltransferase activity with 28 out of the 29 substrates tested, while activity below the limits of detection was only observed when β-resorcylic acid was used as a substrate (Figure 4.13). Furthermore, even though gene-silencing indicates **D**-phenyllactic acid is a substrate of UGT84A27 *in planta*, the velocity of the enzyme with this substrate is relatively poor when compared to others tested. For example, UGT84A27 exhibits less than one percent of the relative activity with **D**-phenyllactic acid as compared to 4-methoxybenzoic acid. The classification of the substrates into different groups based on structural characteristics revealed potential insights into the substrate preferences of UGT84A27 (Figure 4.13 and Figure 4.14). For example, UGT84A27 has clear preferences for phenylpropionic and phenylacetic acids that lack α-substitutions (Group 1 and Group 5) compared to those that possess these substitutions (Group 2 and Group 6). Similarly, the enzyme is active with benzoic acids that lack an *ortho*-substitution but either has no detectable activity, or very low activity

with those that possess an *ortho*-substitution. These data suggest that UGT84A27 displays preference for phenolic substrates that do not possess additional functional groups adjacent to the carboxylic acid group.

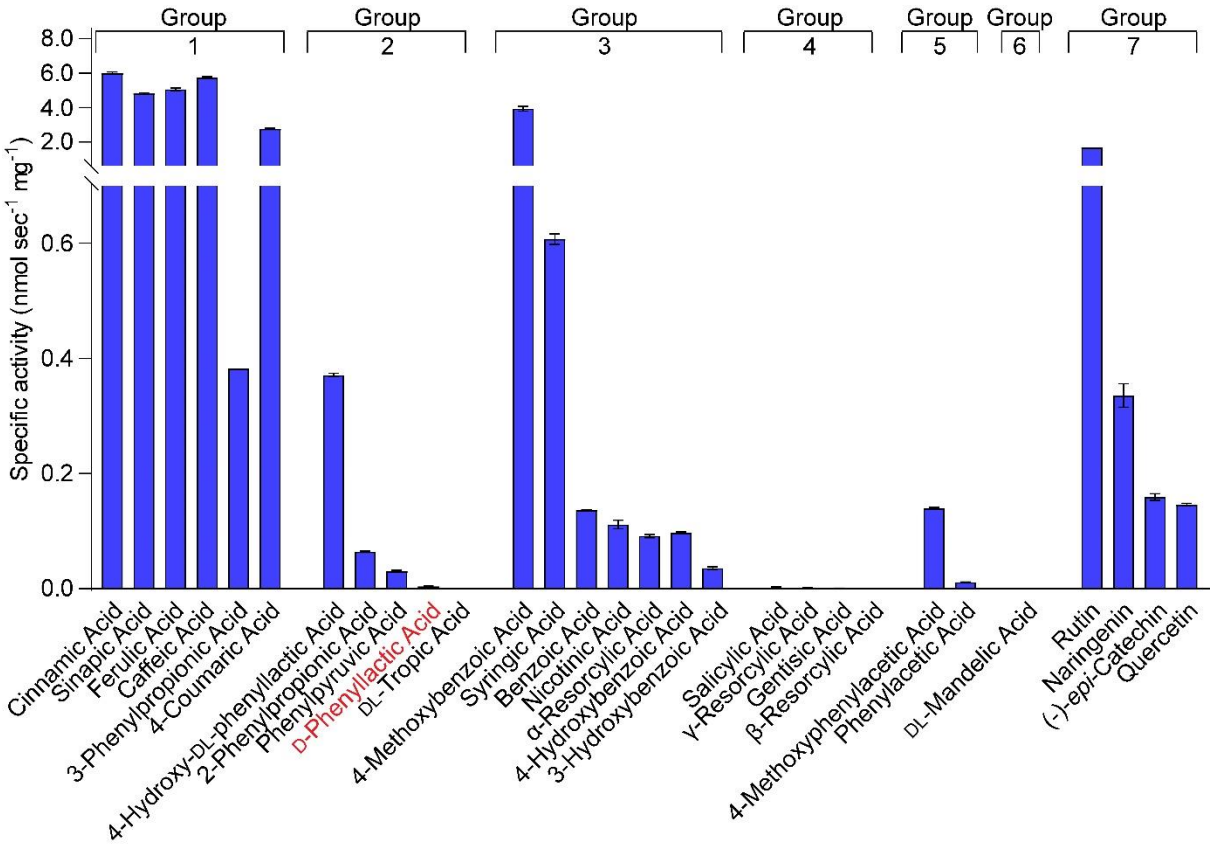

Figure 4.13 Substrate promiscuity of UGT84A27.

Determination of the crude specific activity of UGT84A27 using 1 mM UDP-glucose with 1 mM of the indicated glucose acceptor substrate. Glucose acceptors are grouped by structural similarity. Data are presented as the mean of two replicates ± SE.

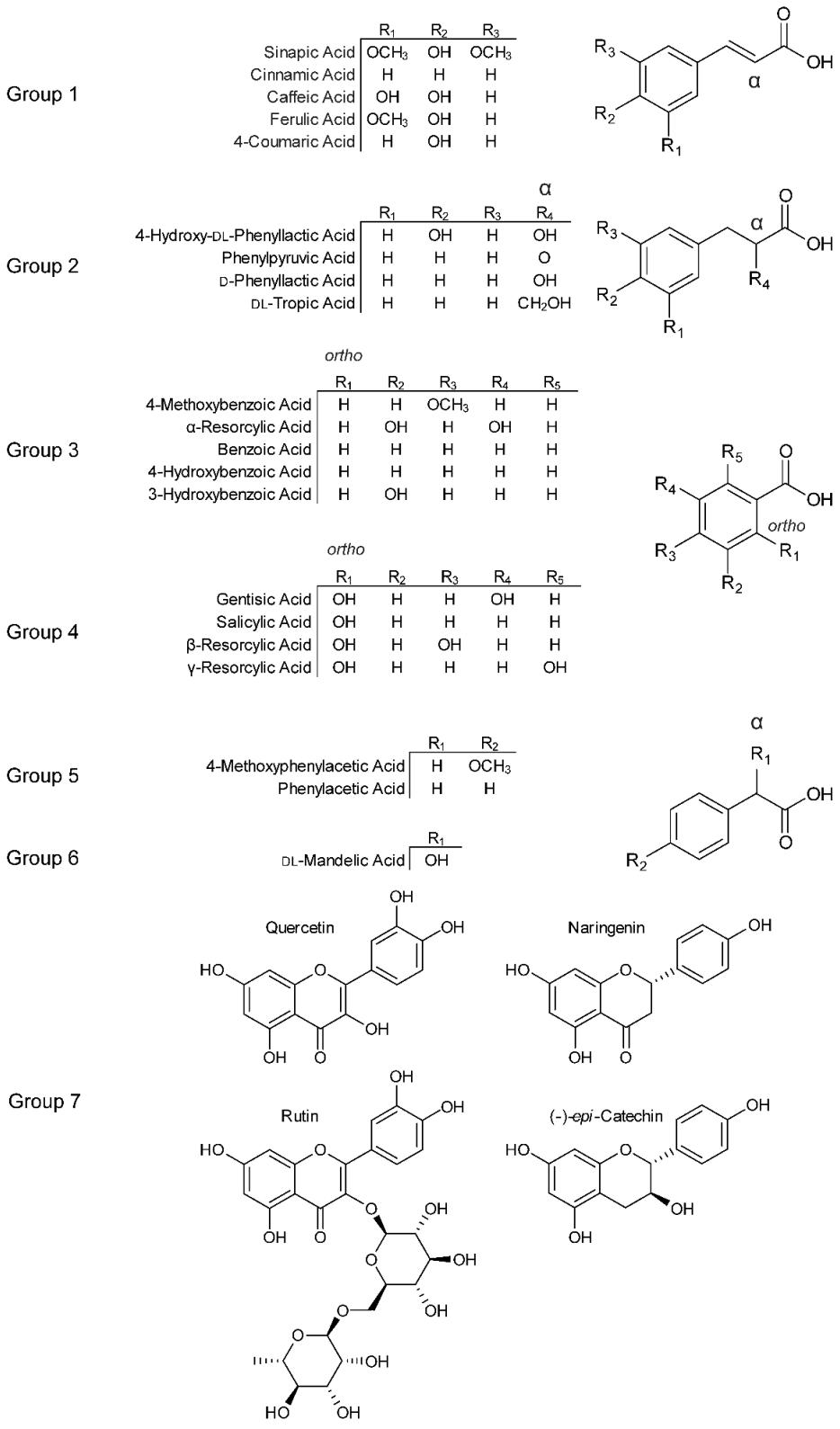

Figure 4.14 Structures of select UGT84A27 glucose acceptors.

Substitution patterns refer to substrate groupings illustrated in **Figure 4.13**.

Given the relatively high specific activity of UGT84A27 with substrates other than D-phenyllactic acid, the potential exists for additional phenolic acids to act as *in planta* substrates of the enzyme. To investigate this hypothesis, LC/MS data from *TRV2* empty vector control and *TRV2::UGT84A27* silenced lines were scanned for *m/z* ratios and mass spectra consistent with phenolic acids conjugated to a hexose. This approach revealed the existence of metabolites in *A. belladonna* roots with *m/z* ratios and mass spectra consistent with putative coumaroyl hexose, caffeoyl hexose, and feruloyl hexose. The abundance of these metabolites is reduced in *TRV2::UGT84A27* silenced lines, which is consistent with the catalytic activity of UGT84A27 when supplied with these phenolic acids and UDP-glucose as substrates (Figure 4.15A - C). Furthermore, the retention times of these phenolic hexoses in plant extracts matches those of *in vitro* reactions catalyzed by UGT84A27 (Figure 4.15D - F). Given that 4-coumaric acid, caffeic acid, and ferulic acid appear to represent *in vivo* substrates of UGT84A27, the kinetic properties of the enzyme were determined with each of these substrates (Figure 4.16 and Table 4.5). The apparent K_m of UGT84A27 with these three substrates ranges from 0.075 µM to 2.27 µM while the V_{max} of the enzyme is fairly consistent and lies between 7.91 and 8.66 nmol sec^{-1} mg^{-1} enzyme. For multisubstrate enzymes, kinetic properties of the enzyme for one substrate can be influenced by the second substrate. Therefore, the kinetic properties of UGT84A27 for UDP-glucose were re-examined using 4-coumaric acid as co-substrate. This analysis revealed greatly improved kinetic parameters for UDP-glucose with 4-coumaric acid as the co-substrate compared to when D-phenyllactic acid is the co-substrate (Table 4.5).

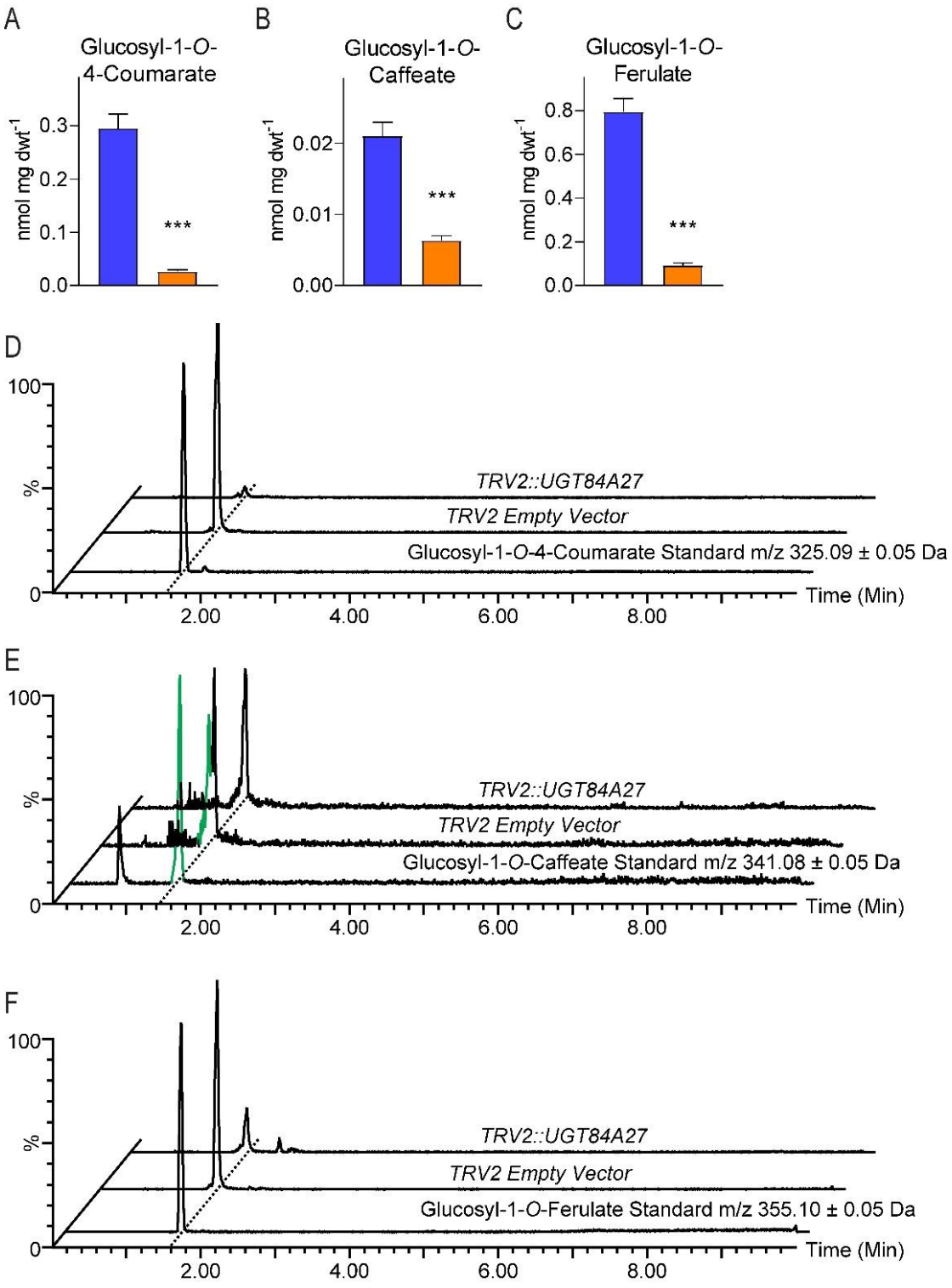

Figure 4.15 Depletion of glucosyl-1-*O*-4-coumarate, glucosyl-1-*O*-caffeate, and glucosyl-1-*O*-ferulate in *UGT84A27* VIGS Lines

Figure 4.15 (cont'd)

(A) Abundance of glucosyl-1-*O*-4-coumarate in *TRV2* empty vector control lines (Blue) and *UGT84A27* VIGS lines (Orange). Data are presented as the mean n = 19 and 14, respectively ± SE. Asterisks denote significant differences (*** P < 0.001) as determined by Student's *t* test.

(B) Abundance of glucosyl-1-*O*-4-caffeate in *TRV2* empty vector control lines (Blue) and *UGT84A27* VIGS lines (Orange). Data are presented as the mean n = 19 and 14, respectively ± SE. Asterisks denote significant differences (*** P < 0.001) as determined by Student's *t* test.

(C) Abundance of glucosyl-1-*O*-4-ferulate in *TRV2* empty vector control lines (Blue) and *UGT84A27* VIGS lines (Orange). Data are presented as the mean n = 19 and 14, respectively ± SE. Asterisks denote significant differences (*** P < 0.001) as determined by Student's *t* test.

(D) Extracted ion chromatograms (*m/z* 325.09, $[M-H]^-$) of the product from UGT84A27-mediated catalysis of glucosyl-1-*O*-4-coumarate, from a representative *TRV2*empty vector control line, or from a representative *UGT84A27* VIGS line. The Y-axes indicate arbitrary signal units and percent signal compared to maximum, which was set by the enzymatic product at 1.0 µM.

(E) Extracted ion chromatograms (*m/z* 341.08, $[M-H]^-$) of the product from UGT84A27-mediated catalysis of glucosyl-1-*O*-4-caffeate, from a representative *TRV2*empty vector control line, or from a representative *UGT84A27* VIGS line. The Y-axes indicate arbitrary signal units and percent signal compared to maximum, which was set by the enzymatic

Figure 4.15 (cont'd)

product at 0.1 µM. The glucosyl-1-*O*-4-caffeate peak *in planta* which co-retains with the enzymatic product is noted in green.

(F) Extracted ion chromatograms (*m/z* 355.1, $[M-H]^-$) of the product from UGT84A27-mediated catalysis of glucosyl-1-*O*-4-ferulate, from a representative *TRV2*empty vector control line, or from a representative *UGT84A27* VIGS line. The Y-axes indicate arbitrary signal units and percent signal compared to maximum, which was set by the enzymatic product at 2.5 µM.

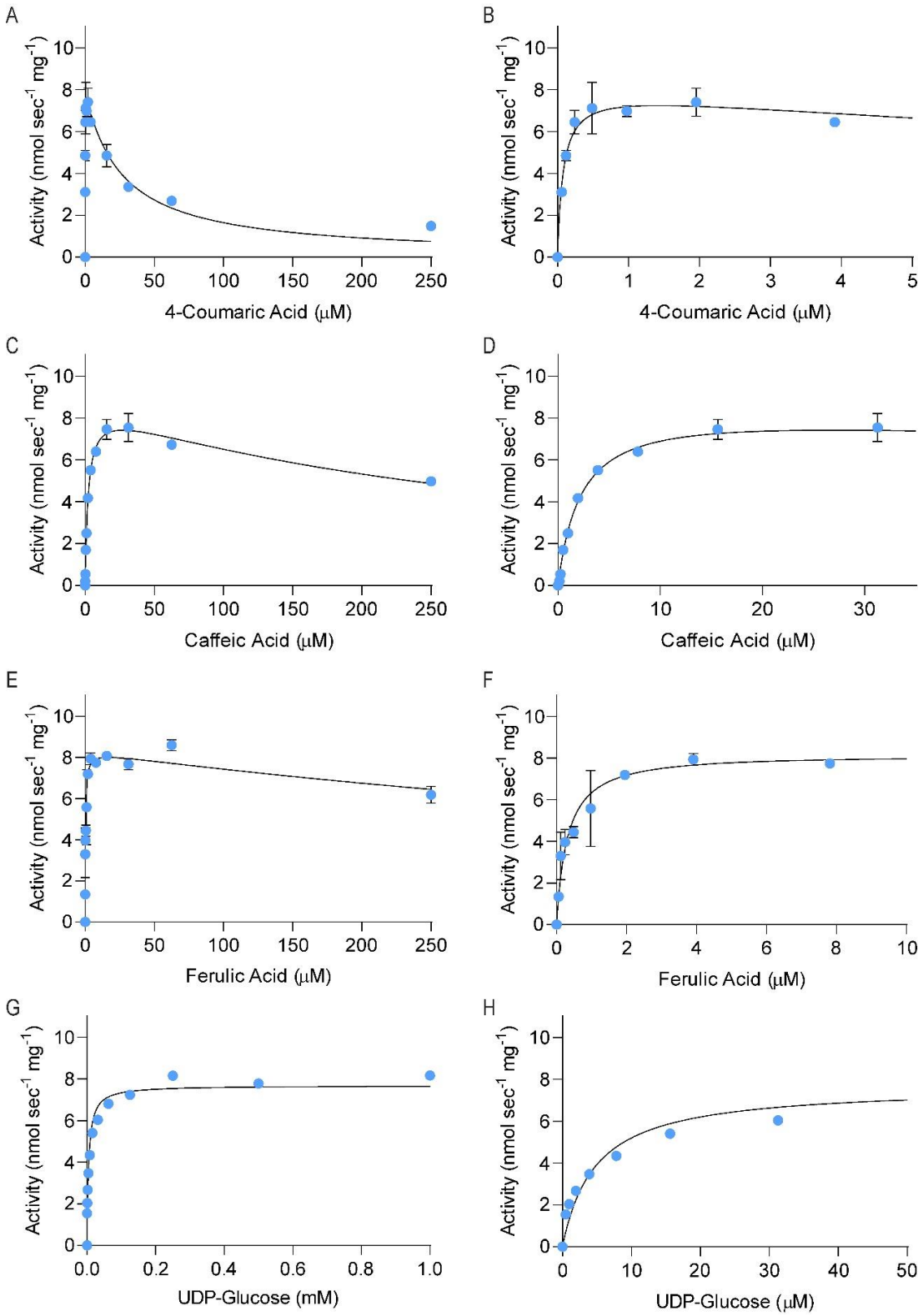

Figure 4.16 Characterization of UGT84A27 activity using a selection of phenolic acids.

Figure 4.16 (cont'd)

(A) Determination of the apparent K_m of UGT84A27 for 4-coumaric acid using 1 mM UDP-glucose as the co-substrate, with the concentration of 4-coumaric acid shown over the full range tested. Data are presented as the mean of two replicates ± SE.

(B) Determination of the apparent K_m of UGT84A27 for 4-coumaric acid using 1 mM UDP-glucose as the co-substrate, with the concentration of 4-coumaric acid shown only to 5 µM. Data are presented as the mean of two replicates ± SE.

(C) Determination of the apparent K_m of UGT84A27 for caffeic acid using 1 mM UDP-glucose as the co-substrate, with the concentration of caffeic acid shown over the full range tested. Data are presented as the mean of two replicates ± SE.

(D) Determination of the apparent K_m of UGT84A27 for caffeic acid using 1 mM UDP-glucose as the co-substrate, with the concentration of caffeic acid shown only to 35 µM. Data are presented as the mean of two replicates ± SE.

(E) Determination of the apparent K_m of UGT84A27 for ferulic acid using 1 mM UDP-glucose as the co-substrate, with the concentration of ferulic acid shown over the full range tested. Data are presented as the mean of two replicates ± SE.

(F) Determination of the apparent K_m of UGT84A27 for ferulic acid using 1 mM UDP-glucose as the co-substrate, with the concentration of ferulic acid shown only to 10 µM. Data are presented as the mean of two replicates ± SE.

(G) Determination of the apparent K_m of UGT84A27 for UDP-Glucose using 2 µM 4-coumaric acid as the co-substrate, with the concentration of 4-coumaric acid shown over the full range tested. Data are presented as the mean of three replicates ± SE.

Figure 4.16 (cont'd)

(H) Determination of the apparent K_m of UGT84A27 for UDP-Glucose using 2 µM 4-coumaric acid as the co-substrate, with the concentration of UDP-glucose shown only to 50 µM. Data are presented as the mean of three replicates ± SE.

Silencing of UGT84A27 Redirects Phenyllactic Acid Flux

Mass spectrometry based metabolite profiling coupled with genetic perturbation of enzymes involved in the synthesis of plant specialized metabolites can reveal unexpected flux that helps identify novel metabolites (Sinlapadech et al., 2007; Bottcher et al., 2008). While analyzing LC/MS data for ions corresponding to the glucosyl-1-*O*-D-phenyllactate ester, it became apparent that a second metabolite with a major fragment anion consistent with phenyllactate (*m/z* 165.05 $[M-H]^-$) is also present at greater abundance in *UGT84A27*-silenced lines compared to *TRV2* empty vector control lines (Figure 4.17A). This fragment ion does not co-elute with authentic standards of D-phenyllactic acid or DL-tropic acid and is also reduced in abundance in *Ab-ArAT4* VIGS lines (Figure 4.17B), which contain reduced levels of phenyllactic acid and aromatic tropane esters due to reduced flux of L-phenylalanine into the tropane pathway (Bedewitz et al., 2014). Further analysis of the mass spectra revealed that this peak possesses a fragmentation pattern consistent with a malonate ester of phenyllactic acid (Figure 4.17C). For example, an ion with *m/z* 251.0549 $[M-H]^-$ is observed, consistent with an unfragmented malonic acid phenyllactic acid-2-*O*-yl ester. Neutral loss of 44 Da yields an ion of *m/z* 207.0652 $[M-H-CO_2]^-$, in agreement with facile loss of CO_2 from a malonyl group. A loss of 86 Da also occurs, in accordance with neutral loss of an entire malonate group to yield the phenyllactic acid anion, *m/z* 165.0548 $[M-H]^-$, the major observed fragment ion for this compound (Figure 4.17C and D). Due to the presence of multiple carboxylic acid groups, a monosodium salt is also observed *m/z* 273.0367 $[M+Na-2H]^-$, as well as dimeric *m/z* 525.1013 $[2M+Na-2H]^-$ and trimeric ion clusters *m/z* 799.1462 $[3M+2Na-3H]^-$ (Figure 4.17E and 9F). The identification and structure of the proposed malonic acid phenyllactic

acid-2-*O*-yl ester was confirmed following purification from *A. belladonna* roots and NMR analyses (Table 4.6). The abundance of malonic acid phenyllactic acid-2-*O*-yl ester is increased approximately 3-fold in *UGT84A27*-silenced lines compared to *TRV2* empty vector controls (Figure 4.17G). Malonylation is a decoration common to many plant specialized metabolites that is frequently catalyzed by BAHD acyltransferases (Bontpart et al., 2015). To test a hypothesis that one of the previously identified root-preferentially expressed BAHDs, *Ab-BAHD-12081* and *Ab-BAHD-5896*, is responsible for the malonylation of phenyllactic acid, the malonic acid phenyllactic acid-2-*O*-yl ester was quantified in VIGS lines. However, the levels of this metabolite were not reduced in *Ab-BAHD-12081* and *Ab-BAHD-5896*-silenced lines compared to *TRV2* empty vector controls, suggesting that an as-yet unidentified acyltransferase is responsible for this activity (Figure 4.17H and I).

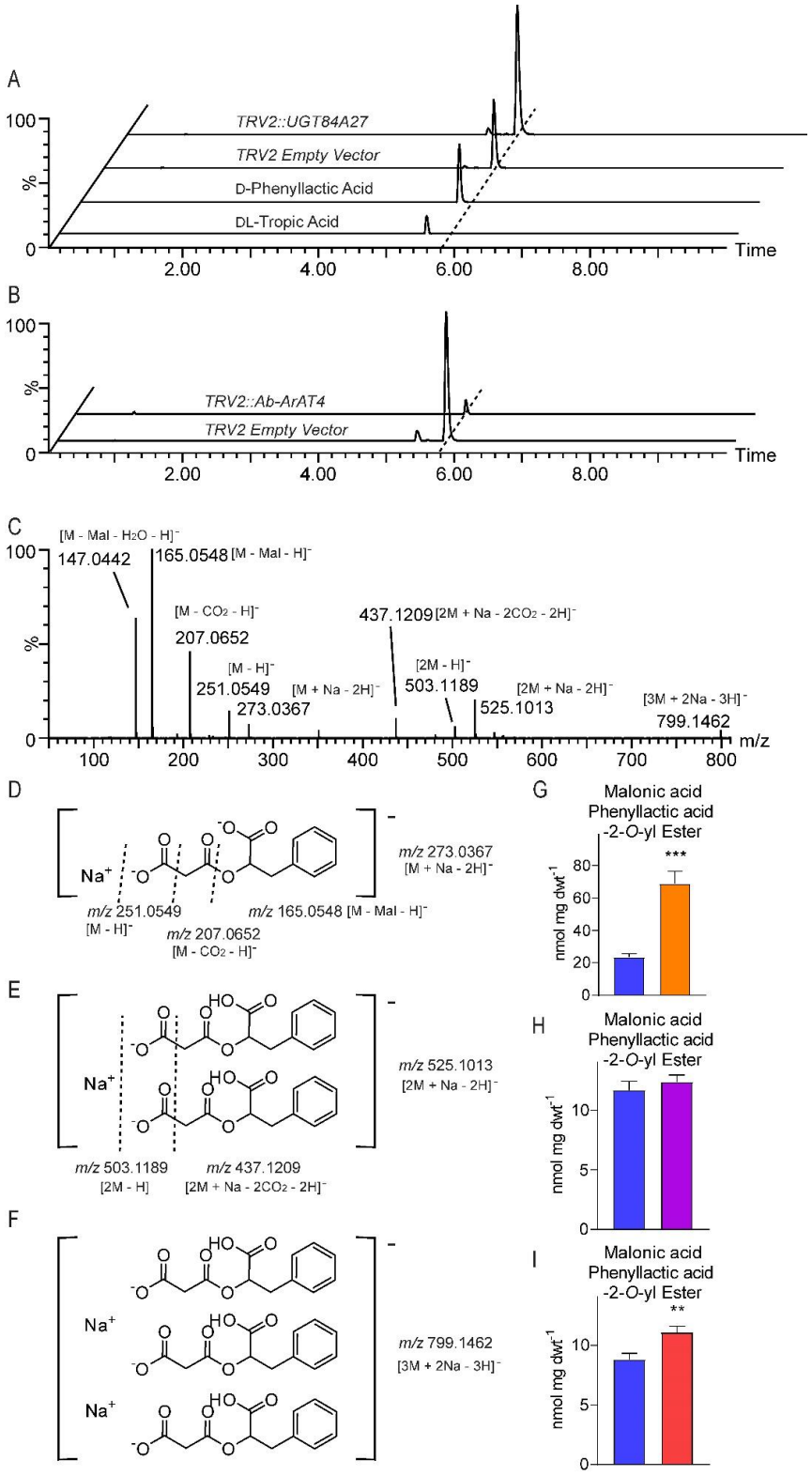

Figure 4.17 Identification of Malonic acid Phenyllactic acid-2-*O*-yl Esters in *A. belladonna* Roots.

Figure 4.17 (cont'd)

(A) Extracted ion LC/MS chromatograms in negative-ion mode (*m/z* 165.05) for the phenyllactate fragment ion from conjugates of phenyllactic acid and malonic acid (*m/z* 251.0549, $[M-H]^-$) in representative *TRV2* empty vector control lines and *UGT84A27* VIGS lines. Unconjugated phenyllactic acid is also presented as an extracted ion chromatogram of (*m/z* 165.05). Tropic acid is presented as an extracted ion chromatogram of (*m/z* 353.09 $[2M+Na-2H]^-$).

(B) Extracted ion LC/MS chromatograms in negative-ion mode (*m/z* 165.05) for the phenyllactate fragment ion from conjugates of phenyllactic acid and malonate (*m/z* 251.0549, $[M-H]^-$) in representative *TRV2* empty vector control lines and *Ab-ArAT4* VIGS lines.

(C) Mass spectrum of the phenyllactic acid glucoside in a representative *UGT84A27* VIGS line with ion-source fragmentation.

(D-F) Predicted structures of the observed sodium salts of malonic acid phenyllactic acid-2-*O*-yl ester. The dashed lines indicate where fragmentations occur to release carbon dioxide(s) and malonate.

(**G**) Abundance of malonic acid phenyllactic acid-2-*O*-yl ester in *TRV2* empty vector control lines (Blue) and *UGT84A27* VIGS lines (Orange). Data are presented as the mean n = 19 and 14, respectively ± SE.

(H) Abundance of malonic acid phenyllactic acid-2-*O*-yl ester in *TRV2* empty vector control lines (Blue) and *Ab-BAHD-12081* VIGS lines (Purple). Data are presented as the mean n = 24 and 23, respectively ± SE.

Figure 4.17 (cont'd)

(I) Abundance of malonic acid phenyllactic acid-2-*O*-yl ester in *TRV2* empty vector control lines (Blue) and *Ab-BAHD-5896* VIGS lines (Red). Data are presented as the mean n = 20 and 22, respectively ± SE.

Table 4.6 NMR Chemical Shift Data for malonic acid phenyllactic acid-2-*O*-yl ester.

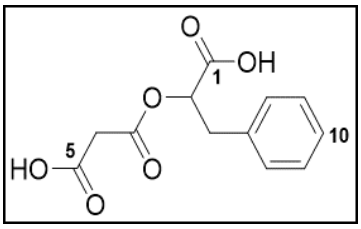

NMR Solvent: CD_3CN (δ_H = 1.94, δ_C = 118.70 ppm)

Position	**^{1}H (ppm)**	**^{13}C (ppm)**
1		171.0
H-2	5.23	74.7
3		167.8*
H_2-4	3.38 (d, *J* = 16.1 Hz)	
	3.36 (d, J = 16.1 Hz)	
5		168.2*
H_2-6	3.19 (dd, J = 4.5, 14.5 Hz)	38.0
	3.11 (dd, J = 8.1, 14.5 Hz)	
C_6H_5	7.32 – 7.23 (m, 5H)	137.5 (7)
		130.9 (8 &12)
		129.7 (9 & 11)
		128.3 (10)

*Starred values indicate that the chemical shift assignments may be interchanged

The pool of phenyllactic acid is larger than the pools of alternative UGT84A27 substrates *in planta*

Upon identification of a major derivative of phenyllactic acid, the abundance of the characterized apparent *in planta* UGT84A27 substrates were quantified in lateral roots of wild-type *A. belladonna* plants. There is approximately one order of magnitude more malonic acid phenyllactic acid-2-*O*-yl ester than unconjugated phenyllactic acid, and an additional three orders of magnitude more phenyllactic acid than the most abundant phenolic acid, which was caffeic acid (Figure 4.18). A direct comparison between phenyllactic acid and 4-coumaric acid, which is the most favorable UGT84A27 substrate by affinity, reveals that the lateral root pool of phenyllactic acid is ~33,000 fold greater than the pool of 4-coumaric acid. The greater pool size of phenyllactic acid suggests that the kinetically unfavorable tropane pathway reaction of UGT84A27 may be able to coexist with much more kinetically favorable phenylpropanoid reactions through variation in the size of the respective substrate pools, where poorer substrates have a larger pool size.

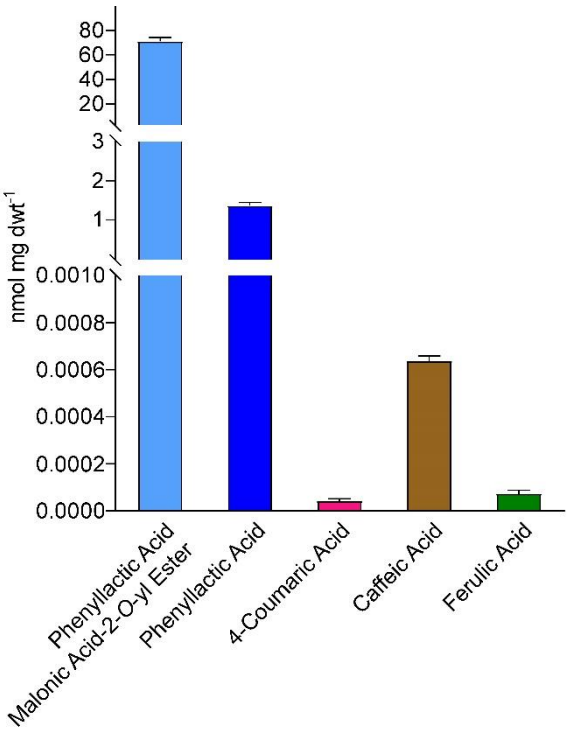

Figure 4.18 Abundance of select phenolic acids, phenyllactic acid, and phenyllactic acid-malonic acid-2-*O*-yl ester in *A. belladonna* lateral roots.

Data are presented as the mean n = 3 ± SE.

Littorine synthase displays restricted substrate preferences

Given the catalytic promiscuity of UGT84A27, we explored whether any of the reaction products generated by UGT84A27 catalysis are substrates for littorine synthase that potentially could lead to the formation of additional tropane alkaloids. For example, although littorine is the initial aromatic tropane ester formed in *A. belladonna* and other species that synthesize hyoscyamine and scopolamine, aromatic groups other than D-phenyllactic acid can also be incorporated into tropane esters, including 4-methoxybenzoate, 4-methoxyphenylacetate, and *t*-cinnamate groups that are incorporated into datumetine, physochlaine, and 3α–cinnamoyloxytropane in *Datura metel*, *Physochlaina alaica*, and *Latua pubiflora*, respectively (Mirzamatov et al., 1974; Siddiqui et al., 1986; Munoz and Casale, 2003). The enzymes catalyzing the synthesis of these minor aromatic tropane esters are unknown, but UGT84A27 is able to catalyze the formation of glucose esters using either 4-methoxybenzoic acid, 4-methoxyphenylacetic acid, or *t*-cinnamic acid as acceptor substrates together with UDP-glucose as the donor (Table 4.7). However, in coupled assays in which these glucose ester products of UGT84A27 catalysis were provided as acyl donors and tropine was supplied as the acyl acceptor to littorine synthase, the resulting SCPL acyltransferase activity was only a small percentage of that observed when **D**-phenyllactic acid and tropine were used to synthesize littorine (Table 4.7). Similarly, upon extending this study to include a further eleven phenolic glucose-ester substrates generated by UGT84A27 catalysis (note; some UGT84A27 products are glucose-ethers and are therefore not suitable as putative substrates of SCPL acyltransferases), failed to detect the formation of any novel tropane esters when tropine was used as the acyl acceptor substrate (Table

4.7). This included DL-tropic acid, which previous *in vivo* labelling experiments with *Datura* and *Brugmansia* root cultures revealed was not an intermediate in tropane alkaloid biosynthesis (Robins et al., 1994)**.** DL-tropic acid is a poor substrate of UGT84A27 and the resulting glucosyl-1-*O*-DL-tropate ester is inactive with littorine synthase. These data suggest that while UGT84A27 is a highly promiscuous enzyme, the activity of littorine synthase is more catalytically restricted.

Table 4.7 Formation of diverse aromatic tropane esters by UGT84A27 and littorine synthase in coupled assays.

Aromatic acid substrate	Tropane ester formed using tropine as a co-substrate[a]	UGT84A27 activity (nmol sec^{-1} mg^{-1})[c]	Percent of UGT84A27 reaction product loss following hydrolysis[d]	AbSCPL-17884 activity (percent of littorine synthase activity)[f]
D-Phenyllactic Acid	Littorine	0.0044	-84	100
DL-Tropic Acid	DL-Hyoscyamine	0.00042	-83	0
t-Cinnamic Acid	3α-Cinnamoyl tropine	6	Not applicable[e]	0.6
4-Methoxybenzoic Acid	Datumetine	3.93	Not applicable	5.4
4-Methoxyphenylacetic Acid	6-Deoxyphysochlaine[b]	0.14	Not applicable	3.2
Caffeic Acid	-	5.74	-9	- [g]
Ferulic Acid	-	5.07	-36	0
Sinapic Acid	-	4.82	0	-
4-Coumaric Acid	-	2.76	-	-
Rutin	-	1.68	-30	0
Syringic Acid	-	0.61	Not applicable	0
3-Phenylpropionic Acid	-	0.38	0	-
4-Hydroxy-DL-phenyllactic Acid	-	0.37	Not applicable	-
Naringenin	-	0.34	-	-
(-)-epi-Catechin	-	0.16	Not applicable	0
Quercetin	-	0.15	Not applicable	-
Benzoic Acid	-	0.14	-8	0
Nicotinic Acid	-	0.11	Not applicable	-
4-Hydroxybenzoic Acid	-	0.097	-70	0
α-Resorcylic Acid	-	0.091	Not applicable	-
2-Phenylpropionic Acid	-	0.064	Not applicable	0
3-Hydroxybenzoic Acid	-	0.036	Not applicable	0
Phenylpyruvic Acid	-	0.031	Not applicable	-
Phenylacetic Acid	-	0.011	Not applicable	0
Salicylic Acid	-	0.0023	-	0
γ-Resorcylic Acid	-	0.0017	-	-
Gentisic Acid	-	0.00071	-	-
DL-Mandelic Acid	-	0.00062	-	-
β-Resorcylic Acid	-	0	-	-

Data are presented as the mean of two replicates.
[a] Aromatic tropane esters identified in planta.
[b] An aromatic tropane ester thus far not identified in planta but potentially the immediate precursor of physochlaine.
[c] Activity determined by UDP-Glo assay using 1.0 mM UDP-Glucose and 0.1 mM of each aromatic acid substrate.
[d] Percent of product degraded following alkaline hydrolysis at pH 10 for 1 h.
[e] Hydrolysis assay not applicable as either a glucose ester or an ether formation are the only possible outcomes from the corresponding acceptor substrates.
[f] Aromatic tropane esters formed by AbSCPL-17884 activity from tropine and UGT84A27 derived aromatic glucose-esters.
[g] Substrate not tested.

Discussion

Transcriptome-guided pathway discovery is a powerful approach for dissecting the biosynthesis of plant specialized metabolites, particularly when the target metabolites are synthesized in a specific tissue, cell type, or induced by a stimulus (Xiao et al., 2013). In this study, two genes involved in the synthesis of scopolamine, a medicinally important tropane alkaloid, were identified based on their preferential expression in the lateral roots of *A. belladonna*. The data presented reveal that the aromatic tropane ester littorine is synthesized through 1-*O*-β-glucose ester-mediated acylation rather than through a coenzyme A thioester intermediate as previously proposed (Robins et al., 1994). This alternative route involves a two-step process; first, the UDP-glucosyltransferase (UGT84A27) utilizes D-phenyllactic acid and UDP-glucose as co-substrates to synthesize glucosyl-1-*O*-D-phenyllactate (Figure 4.10). Silencing of the corresponding gene reduces the abundance of this compound together with the downstream aromatic tropane esters, littorine, hyoscyamine and scopolamine (Figures 4 and 5). Second, the resulting glucosyl-1-*O*-D-phenyllactate serves as the acyl donor in an SCPL acyltransferase-catalyzed reaction that utilizes tropine as the acyl acceptor to form littorine (Figure 4.12). As observed for *UGT84A27*, silencing of *Ab-SCPL-17884* / *LITTORINE SYNTHASE* reduces aromatic tropane ester synthesis (Figure 4.5).

A general role for UGT84A27 in phenylpropanoid metabolism

Plant specialized metabolism embodies tremendous chemical diversity, which occurs through the catalytic activities of enzymes that typically evolve faster and possess greater promiscuity than those of primary metabolism (Milo and Last, 2012; Weng et al., 2012;

Chae et al., 2014). The UGT84A subfamily of glucosyltransferases display catalytic promiscuity with the ability to use multiple phenolic acids as substrates (Lunkenbein et al., 2006; Babst et al., 2014; Ono et al., 2016). This catalytic promiscuity is shared by UGT84A27 which, in addition to catalyzing the formation of glucosyl-1-*O*-D-phenyllactate, also catalyzes the formation of glucosyl-1-*O*-4-coumarate, glucosyl-1-*O*-caffeate, and glucosyl-1-*O*-ferulate in *A. belladonna* roots (Figure 4.15). Indeed, these three phenylpropanoid metabolites accumulate in diverse species, including *Arabidopsis thaliana*, tomato (*Solanum lycopersicum*), strawberry (*Fragaria x ananassa*), and *Populus* spp. (Lunkenbein et al., 2006; Carrillo-Lopez and Yahia, 2013; Babst et al., 2014; Sundin et al., 2014). These metabolites are also the catalytic products of several UGT84A enzymes, suggesting that their formation represents possible conserved ancestral activities of the UGT84A subfamily.

In contrast, phenyllactic acid and its glucose ester are not widely reported in plants outside members of the Solanaceae family that synthesize the aromatic tropane esters, littorine, hyoscyamine, and scopolamine. For example, phenyllactic acid biosynthesis, and its subsequent incorporation into aromatic tropane esters in *A. belladonna* roots requires L-phenylalanine:4-hydroxyphenylpyruvate aminotransferase activity (Bedewitz et al., 2014). This enzyme is encoded by *Ab-ArAT4*, a gene that is absent in members of the Solanaceae family such as tomato and potato that do not synthesize aromatic tropane esters. Based on the broad catalytic activities of UGT84A27, it appears this enzyme has been recruited into tropane alkaloid biosynthesis from a more general role in phenylpropanoid metabolism. This hypothesis is supported by both the relatively poor

activity of UGT84A27 when using D-phenyllactic acid (k_{cat} 0.009 sec^{-1}) as a substrate compared to either 4-coumaric acid, caffeic acid, or ferulic acid (k_{cat} 0.66 - 0.71 sec^{-1}) (Figure 4.11, Figure 4.16 and Table 4.5). Indeed, even though several UGT84A subfamily enzymes possess apparent K_m values for phenolic substrates in the same range as that of UGT84A27 for D-phenyllactic acid, in general the turnover numbers lie within a similar range as those observed for UGT84A27 with 4-coumaric acid, caffeic acid, or ferulic acid (Lim et al., 2001; Lunkenbein et al., 2006; Hall and De Luca, 2007; Babst et al., 2014; Ono et al., 2016).

Insight into the mechanism underlying the substrate preferences of UGT84A27 was achieved through comparison of the relative activity of the enzyme with diverse phenolic substrates. These data revealed clear preferences of UGT84A27 for phenolic acids that lack an α-substitution and benzoic acids that lack an *ortho*-substitution, suggesting that access to the carboxylic acid group is a key determinant of catalytic efficiency (Figure 4.13 and Table 4.7). Therefore, as D-phenyllactic acid possesses an α-substitution it is a relatively poor substrate for UGT84A27 compared to others that were tested. Such preferences are reversed in UGT74F1 and UGT74F2 that utilize salicylic acid (*ortho*-substituted) or benzoic acid, but exhibit reduced or no activity using 3- or 4-hydroxybenzoic acid (*meta*- and *para*-, respectively) (Lim et al., 2002).

Even though gene-silencing clearly indicates the importance of UGT84A27 in tropane alkaloid biosynthesis, the catalytic properties of the enzyme, coupled with substrate and product pools suggest that it may be rate limiting for tropane biosynthesis. For example,

glucosyl-1-*O*-D-phenyllactate does not accumulate to high levels in *A. belladonna* roots whereas pools of free phenyllactic acid and malonic acid phenyllactic acid-2-*O*-yl ester are abundant (Figure 4.5 and 10). The high abundance of the phenyllactic acid pool in *A. belladonna* roots relative to that of 4-coumaric acid, caffeic acid, and ferulic acid (Figure 4.18), may promote high levels of tropane alkaloid biosynthesis in this species despite the relatively poor kinetic properties of UGT84A27 with D-phenyllactic acid. Directed evolution of UGT84A27 toward improved recognition of, and velocity with, α-hydroxy acids could be utilized as a component of a metabolic engineering strategy to improve flux toward scopolamine biosynthesis (McArthur and Chen, 2016). Furthermore, it will also be informative to determine the kinetic properties of UGT84A27 orthologs from scoploamine and non-scopolamine producing members of the Solanaceae. This will allow the evolutionary trajectory of UGT84A27-like enzymes to be tracked to establish whether each possesses the ability to synthesize glucosyl-1-*O*-D-phenyllactate or whether this activity has evolved specifically in scopolamine producing species like *A. belladonna* that also synthesize large amounts of phenyllactic acid due to the presence of *ArAT4* orthologs and associated L-phenylalanine:4-hydroxyphenylpyruvate aminotransferase activity.

Evolution of Tropane Alkaloid Biosynthesis

Although plant specialized metabolites often display lineage-specific distribution, numerous examples exist whereby similar compounds have evolved independently several times within diverse plant families (Pichersky and Lewinsohn, 2011). Tropane alkaloid biosynthesis represents an excellent example of convergent evolution of plant

specialized metabolism. Tropanes accumulate in 10 divergent plant families but their biosynthesis has been most widely studied in the Solanaceae and the Erythroxylaceae, revealing both differential spatial localization of synthesis as well as recruitment of different classes of enzymes for similar biochemical reactions (Kim et al., 2016). For example, while tropane alkaloid biosynthesis is predominantly localized in roots in members of the Solanaceae, in *E. coca* (Erythroxylaceae), biosynthesis occurs mainly in young leaf tissues (Jirschitzka et al., 2012; Bedewitz et al., 2014; Schmidt et al., 2015). In addition, in the Solanaceae, reduction of the key pathway intermediate, tropinone to form the epimers tropine and pseudotropine is catalyzed by members of the short-chain dehydrogenase/reductase family while the analogous reaction in *E. coca*, the NADPH-dependent reduction of methylecgonone to methylecgonine is catalyzed by an enzyme belonging to the aldo-keto reductase family (Jirschitzka et al., 2012). The finding that aromatic tropane ester formation in *A. belladonna* proceeds through SCPL-mediated acylation rather than through BAHD-acyltransferase catalysis observed for cocaine biosynthesis (Schmidt et al., 2015), provide further evidence of independent evolution of tropane alkaloid biosynthesis in the Solanaceae and the Erythroxylaceae.

The phenomenon whereby both BAHD acyltransferase and SCPL-mediated acylations participate in creating tropane ester diversity is seen in other classes of plant specialized metabolites, most notably anthocyanins and additional phenylpropanoids (Bontpart et al., 2015). However, although the identification of littorine synthase and cocaine synthase reveals key steps in the biosynthesis of two of the most abundant and widely studied tropane esters, little is known regarding the relative contribution of BAHD acyltransferase

and SCPL-mediated acylations to the overall chemical diversity of tropanes that exist *in planta*. For example, approximately 200 tropane structures are known and much of the observed chemical variation is due to the formation of different tropane esters at the C3 hydroxyl group of the tropanol skeleton (see Figure 4.2 for numbering) (Eich, 2008; Jirschitzka et al., 2013). This chemical diversity is manifest in part by the incorporation of different aliphatic and aromatic acyl donors into C3 tropane esters. However, chemical complexity is enhanced in *Datura* and *Schizanthus* spp. due to the formation diacylated tropane esters that contain an additional acyl group at either the C6 or C7 position (Doncheva et al., 2006; Reina et al., 2010; Nguyen et al., 2015). The genes encoding the catalysts responsible for this chemical diversity remain unknown.

UGT84A27 is able to synthesize glucose esters from phenolic acids that, in some species, are incorporated into tropane esters, including 4-methoxybenzoic acid, 4-methoxyphenylacetic acid, and *t*-cinnamic acid (Figure 4.13; Table 4.7) (Mirzamatov et al., 1974; Siddiqui et al., 1986; Munoz and Casale, 2003). While *A. belladonna* does not accumulate tropane alkaloids containing these phenolic acids, it is possible that they are formed through 1-*O*-β-glucose ester-mediated acylation, as coupled assays with both UGT84A27 and littorine synthase resulted in the synthesis of datumetine, 6-deoxyphysochlaine, and 3α-cinnamoyl tropine *in vitro*, albeit at far lower activity than observed for littorine formation (Table 4.7). However, direct experimental evidence obtained through identification and characterization of the corresponding enzymes from *D. metel*, *P. alaica*, and *L. pubiflora* is needed to confirm the mechanisms underlying the synthesis of these diverse tropane esters *in planta*.

The substrate promiscuity of UGT84A27 and littorine synthase highlight the potential to directly engineer the biosynthesis of novel and non-natural tropanes with altered bioactivities. For example, there is considerable interest in synthesizing halogenated variants of medicinally important metabolites (Runguphan et al., 2010) and earlier *in vivo* labeling studies in *D. stramonium* demonstrated that synthetic fluorinated derivatives of D-phenyllactic acid could be biocatalytically incorporated into tropane esters (O'Hagan et al., 1999). This suggests that both UGT84A27 and littorine synthase can utilize fluorinated substrates.

The potential role of transport in tropane alkaloid biosynthesis

The identification of littorine synthase as an SCPL acyltransferase raises intriguing, and as-yet unanswered, questions related to the potential subcellular localization of tropane alkaloid biosynthesis and the transport of intermediate metabolites. The SCPL acyltransferases, 1-*O*-sinapoylglucose:malate sinapoyltransferase of Arabidopsis and As-SCPL1 from *Avena strigosa* are localized in the vacuole (Hause et al., 2002; Mugford et al., 2013; Bontpart et al., 2015) and while the cellular and subcellular localization of littorine synthase has yet to be determined, it shares sequence features with vacuole targeted SCPLs, including a leader sequence that is proposed to facilitate targeting via the secretory pathway (Figure 4.8). The next most probable localization would be the apoplast, which is the default destination for proteins processed using the secretory pathway (Pedrazzini et al., 2013). Either vacuolar or apoplastic localization of littorine synthase would add complexity to the multi-enzyme tropane pathway, including the need

to transport tropine and glucosyl-1-*O*-D-phenyllactate substrates into the vacuole on one hand or move them to the apoplast on the other. An apoplastic branch could additionally facilitate littorine transport through a major facilitator superfamily protein, as is the case for nicotine in *N. tabacum* (Hildreth et al., 2011). In addition, once littorine is formed, is it transported out of the vacuole for subsequent conversion to scopolamine through steps catalyzed by LITTORINE MUTASE and HYOSCYAMINE-6-HYDROXYLASE (H6H) (Hashimoto et al., 1991; Li et al., 2006)? LITTORINE MUTASE is a cytochrome P450, which are generally functionally associated with the endoplasmic reticulum. These questions are further complicated when the cellular localization of tropane-related proteins within the root is also considered. For example, the reductase TRI from *Hyoscyamus niger* synthesizes tropine preferentially in the endodermis and outer cortex and is absent in the pericycle (Nakajima and Hashimoto, 1999). Similarly, PHENYLPYRUVIC ACID REDUCTASE (PPAR), the enzyme producing phenyllactic acid, is localized to the pericycle and endodermis in *A. belladonna*, meaning that it overlaps at the cellular level with TRI location in the endodermis, assuming that *A. belladonna* TRI is produced in the same cells as *H. niger* TRI (Qiu et al., 2018). By comparison, hyoscyamine-6-hydroxylase, that catalyzes the final step in scopolamine biosynthesis is exclusively localized to the pericycle (Hashimoto et al., 1991). Thus, it is suggested that tropane alkaloids are assembled in different cell types and in distinct subcellular compartments. Physical separation of specialized metabolism at the cellular and subcellular levels is a common feature in plant alkaloid biosynthesis as both monoterpene indole alkaloid and benzylisoquinoline alkaloid biosynthesis occurs in different cell types and subcellular localizations (Onoyovwe et al., 2013; Courdavault et al., 2014). As

additional tropane-related genes are identified, creating a comprehensive cellular and subcellular map of tropane-related proteins and metabolites in distinct tropane producing species will become feasible.

The identification of *A. belladonna* enzymes that catalyze the synthesis of littorine from tropine and D-phenyllactic acid reveals the mechanisms of tropane ester formation in the Solanaceae and creates a foundation to further explore the evolution of tropane alkaloid biosynthesis across diverse plant families. In particular, it will be of interest to assess the relative contribution of BAHD acyltransferase- and SCPL-mediated acylation in creating tropane alkaloid diversity both within and between individual species as well as across different plant families.

Methods

Chemicals Utilized in this Study

The chemicals utilized in this study, including tropane alkaloids and their precursors used as substrates and authentic standards, were purchased through commercial vendors, including Sigma-Aldrich and Santa Cruz Biotechnology.

Chemical Synthesis

Due to a lack of commercial sources the tropane esters pseudolittorine, 6-deoxyphsochlaine, and datumetine were synthesized in-house. Pseudolittorine was synthesized via Fischer esterification as follows. Pseudotropine (10 mmol) and D-phenyllactic acid (5 mmol) were dissolved in a solution of 4 M HCl in *p*-dioxane (10 mL). Reactions were refluxed with vigorous stirring for 16 hours at 85°C and cooled to room temperature. Unreacted pseudotropine was filtered out and the *p*-dioxane was evaporated, leaving a thick, yellow paste. This mixture was dissolved in 10 mL of H_2O and saturated sodium carbonate was added until the pH reached ~11. The mixture was repeatedly extracted with hexanes until no further alkaloidal constituent was extracted from the aqueous phase by monitoring the pH of the organic phase following evaporation of the solvent and reconstitution in H_2O. The organic phase was dried over sodium sulfate and filtered. HCl (5 mmol) in *p*-dioxane (1.25 mL) was added, to precipitate pseudolittorine as a white solid.

6-Deoxyphysochlaine was synthesized by allowing 1 mmol tropine and 1.1 mmol *p*-methoxyphenylacetoyl chloride to react in 0.5 mL chloroform for 2 hours at 20°C. The

reaction mixture was partitioned between hexanes (5 mL) and H_2O (5 mL). 6-deoxyphysochlaine was recovered from the aqueous phase as a white precipitate by adding saturated sodium carbonate. Datumetine was synthesized using the same approach as 6-deoxyphysochlaine except that reactants were incubated for 16 hours at 40°C, and the product was recovered as a pale yellow precipitate.

The crude precipitates of all three compounds were dissolved at 40 mg/mL in 0.1% formic acid and purified using solid phase extraction cartridges (Supelco C18, 3 mL, 500 mg) as follows. The cartridges were equilibrated with 10 mL methanol and 10 mL 0.1% formic acid, in 2 mL additions with centrifugation at 150 x *g* for 3 min after each addition. Compounds were applied to the cartridge in 40 mg batches, and eluted using 4 mL each of increasing concentration of methanol (0%, 10%, 20% and 30%) in 0.1% formic acid solution in H_2O. The elution solvents were added in 1 mL aliquots and collected separately by centrifugation. To determine purity, fractions from each batch were pooled and screened at 1:100 dilution by flow-injection mass spectrometry on a Waters Xevo G2-XS Q-TOF mass spectrometer (1:1 0.1% formic acid: methanol (v/v) mobile phase). Fractions containing less than 1% impurities were pooled, sodium carbonate added to pH ~11, extracted with hexanes, and HCl in *p*-dioxane was added to precipitate the compound. The precipitates were collected, dried under vacuum, and dissolved in methanol-d_4 (99.95 atom % D) and transferred into NMR tubes for analysis. ^{1}H (500 MHz),^{13}C (126 MHz), gHSQCAD, gCOSY, and HOMO2DJ NMR spectra were collected at 25°C using Agilent DDR2 500 MHz NMR spectrometers at the Michigan State University Max T. Rogers NMR facility and processed using MestReNova software. Chemical shift assignments

(Tables 4.8 – 4.10) were compared to those of previously characterized tropane esters (Taha and Rucker, 1978; Nakanishi et al., 1998; Jenett-Siems et al., 2005).

Table 4.8 NMR Chemical Shift Data for 6-Deoxyphysochlaine-HCl.

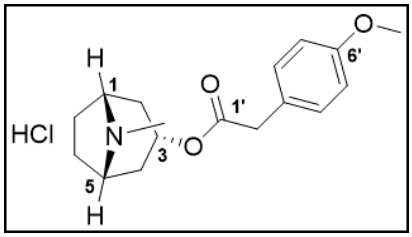

NMR Solvent: CD_3OD ($\delta_H = 3.31$, $\delta_C = 47.8$ ppm)

Position	^{1}H (ppm)	^{13}C (ppm)
H-6b, H-7b	1.95 – 1.90 (m, 2H)	23.3
H-2b, H-4b	1.98 – 1.93 (m, 2H)	34.4
H-6a, H-7a	2.14 – 2.07 (m, 2H)	23.3
H-2a, H-4a	2.54 – 2.46 (m, 2H)	34.4
N-CH_3	2.71 (s, 3H)	38.3
H_2-2'	3.61 (s, 2H)	40.3
O-CH_3	3.75 (s, 3H)	54.6
H-1, H-5	3.80 – 3.76 (m, 2H)	62.3
H-3	4.98 (t, J = 5.0 Hz, 1H)	64.6
H-5', H-7'	6.92 – 6.86 (m, 2H)	113.8
H-4', H-8'	7.24 – 7.18 (m, 2H)	130.3
3'		126.1
6'		158.9
1'		170.8

Table 4.9 NMR Chemical Shift Data for Datumetine-HCl.

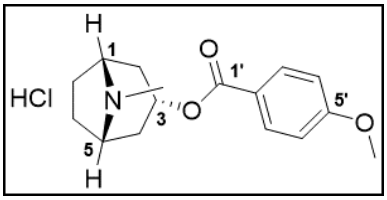

NMR Solvent: CD_3OD ($\delta_H = 3.31$, $\delta_C = 47.8$ ppm)

Position	^{1}H (ppm)	^{13}C (ppm)
H-2b, H-4b	2.25 (d, *J* = 16.3 Hz, 2H)	34.7
H_2-6, H_2-7	2.51 – 2.35 (m, 4H)	23.7
H-2a, H-4a	2.55 (dt, *J* = 16.4, 4.3 Hz, 2H)	34.7
N-CH_3	2.86 (s, 3H)	38.1
O-CH_3	3.88 (s, 3H)	54.7
H-1, H-5	3.99 – 3.92 (m, 2H)	62.4
H-3	5.27 (t, *J* = 5.1 Hz, 1H)	64.5
H-4', H-6'	7.06 – 7.01 (m, 2H)	113.7
H-3', H-7'	8.00 – 7.95 (m, 2H)	131.2
2'		121.9
5'		164.0
1'		165.2

Table 4.10 NMR Chemical Shift Data for Pseudolittorine-HCl.

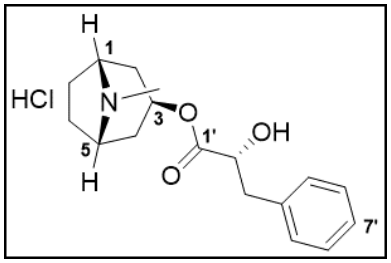

NMR Solvent: CD_3OD (δ_H = 3.31, δ_C = 47.8 ppm)

Position	^{1}H (ppm)	^{13}C (ppm)
H-2b, H-4b	1.90 (ddd, *J* = 14.0, 10.9, 3.0 Hz, 1H)	34.7
	1.98 (ddd, *J* = 14.0, 10.9, 2.9 Hz, 1H)	34.8
H_2-6, H_2-7	2.12 – 2.05 (m, 2H)	23.6
	2.39 – 2.30 (m, 2H)	
H-2a, H-4a	2.16 – 2.10 (m, 1H)	34.7
	2.25 (ddt, *J* = 14.1, 5.8, 2.7 Hz, 1H)	34.8
N-CH_3	2.77 (s, 3H)	37.6
H-3'a, H-3'b	3.03 (dd, *J* = 13.7, 5.6 Hz, 1H)	40.2
	2.94 (dd, *J* = 14.0, 7.4 Hz, 1H)	
H-1, H-5	3.95 (m, 2H)	63.2
		63.3
H-2'	4.36 (dd, *J* = 7.4, 5.5 Hz, 1H)	71.6
H-3	5.13 (tt, J = 10.9, 6.2 Hz, 1H)	64.1
C_6H_5	7.32 – 7.16 (m, 5H)	125.9 (7')
		127.9 (5' & 9')
		129.2 (6' & 8')
4'		136.8
1'		173.0

Growth of Plant Material and Virus-Induced Gene Silencing

A. belladonna plants were grown, and VIGS experiments performed as previously described using the two-component tobacco rattle virus system with target gene constructs assembled by ligation independent cloning in the TRV2-LIC vector (Dong et al., 2007; Bedewitz et al., 2014). Wild type *A. belladonna* plants for phenolic pool analysis were grown as previously described (Bedewitz et al., 2018). Fragments of *Ab-BAHDs*, *UGT84A27*, and *Ab-SCPL-17884* utilized for silencing were amplified from cDNA synthesized from *A. belladonna* lateral root RNA using primer pairs described in Table 4.11.

Table 4.11 Oligonucleotide Primers Utilized in this Study.

Primer	Sequence	Function
UGT84A27 VF	5'-CGACGACAAGACCCTTGACAGCCTTGGTATACCTTGTGC-3'	VIGS construct assembly
UGT84A27 VR	5'-GAGGAGAAGAGCCCTGTAGGCGATCTCATCAACTTGTTC-3'	VIGS construct assembly
Ab-SCPL-17884 VF	5'-CGACGACAAGACCCTGTGGTTAGTTGACCATTCGGAGTA-3'	VIGS construct assembly
Ab-SCPL-17884 VR	5'-GAGGAGAAGAGCCCTTCTTGAACAGTTTCATCATTAACC-3'	VIGS construct assembly
Ab-BAHD-12081 VF	5'-CGACGACAAGACCCTCCTTAATCATCCCCATGCAGCTCA-3'	VIGS construct assembly
Ab-BAHD-12081 VR	5'-GAGGAGAAGAGCCCTGCTGCTACCTTAGCTCGAAGAGC-3'	VIGS construct assembly
Ab-BAHD-5896 VF	5'-CGACGACAAGACCCTCCACGGAGGAGGTGAAGAAGAGAAC-3'	VIGS construct assembly
Ab-BAHD-5896 VR	5'-GAGGAGAAGAGCCCTTAAATTTTTGGAGAGAGAATTTTCA-3'	VIGS construct assembly
UGT84A27 QF	5'-TGTGACAGAGAACAGGGTTATTCC-3'	RT-qPCR
UGT84A27 QR	5'-TCGTCACGTCATGCAAAGATC-3'	RT-qPCR
Ab-SCPL-17884 QF	5'-CCATTAAGGGTGCAGGACATACT-3'	RT-qPCR
Ab-SCPL-17884 QR	5'-TGAGCATGGCCAGACACTCA-3'	RT-qPCR
Ab-BAHD-12081 QR	5'-GAATGGTCGAATTATGCATGCA-3'	RT-qPCR
Ab-BAHD-12081 QF	5'-CACAATCACAACAGAAATGAAATCC-3'	RT-qPCR
Ab-BAHD-5896 QF	5'-GCAATTTTCAATTGATTGGGCAACATT-3'	RT-qPCR
Ab-BAHD-5896 QR	5'-GTGTCACTTATGTAATAAGGTGGAATT-3'	RT-qPCR
UGT84A27 BamH1 F	5'-TTGGATCCATGGGATCTCAAGGTACCAATATA-3'	Expression construct assembly
UGT84A27 Sal1 R	5'-TTGTCGACCTAATTGGATAGAGGTGCTAACTT-3'	Expression construct assembly
Ab-SCPL-17884 ENT-F	5'-CACCATGAAGAAAACAATTGTGGTTC-3'	Expression construct assembly
Ab-SCPL-17884 ENT-R	5'-TTATAGAGGTTGATAATATATCCA-3'	Expression construct assembly
Ab-SCPL-17884 INT1	5'-GTACAAATGGCTCTACACACTCATC-3'	Sequencing Primer
Ab-SCPL-17884 INT2	5'-TGATTAAGATATCTTCTCTGAGGAGAC-3'	Sequencing Primer
Ab-BAHD-5896 INT1	5'-GGGTGTTGAGTTCTTGAATGTACAC-3'	Sequencing Primer
UGT84A27 INT1	5'-TGCCTAACATGCCAATTCTCAA-3'	Sequencing Primer
UGT84A27 INT2	5'-TGTCCAAATAGCCTTGTGGCAA-3'	Sequencing Primer

RNA Isolation, cDNA Synthesis and Quantitative RT-PCR

Total RNA was isolated from roots of *A. belladonna* using the RNeasy Plant Mini Kit with the on-column DNase treatment (Qiagen). cDNA synthesis was accomplished using the SuperScript III first-strand synthesis kit (Invitrogen) and 1 µg of total RNA as template. The quantity and quality of all products were determined by UV absorbance. Gene-specific primers (Table 4.11), were designed using Primer Express 3.0 software (Applied Biosystems). PCR efficiency was determined for each set of primers by using standard curves derived from serial dilutions of cDNA and only primer pairs that had an absolute value of the slope of ΔC_T versus log of the input cDNA concentration of ≤ 0.1 were utilized. Quantitative PCR was performed in 10 µL reactions using FAST SYBR master mix (Applied Biosystems) with 300 nM of each primer and 20 ng of cDNA template for *UGT84A27,* and 50 ng of cDNA template for *Ab-BAHD-5896*, *Ab-BAHD-12081*, and *Ab-SCPL-17884*. Reactions were assembled, DNAs amplified, and relative transcript levels determined as described previously (Bedewitz et al., 2014).

Plant Metabolite Extractions and the Identification and Quantification of Tropane Alkaloids

Tropane alkaloids, phenyllactic acid, and its corresponding glucose ester were extracted as described previously (Bedewitz et al., 2018). Phenolic compounds were extracted using the same technique, with use of 80% methanol, 10 mM ammonium formate, 10 µM telmisartan and 0.1% formic acid as the solvent. The identification and quantification of tropane alkaloids in plant extracts were performed using a Waters Quattro Micro API mass spectrometer coupled to a Shimadzu LC-20AD HPLC using an Waters Symmetry C18 column (2.1 x 100 mm with 3.5 µm particle size) with an oven temperature of 50°C

and an injection volume of 10 µL as previously described (Bedewitz et al., 2014). MRM parameters are provided in Table 4.12. Quantification of tropane alkaloids was achieved using standard curves of commercially available authentic standards.

Table 4.12 Multiple-reaction Monitoring Parameters Utilized and Transition Ions Observed for LC-MS/MS Analyses of Tropane Alkaloids.

Compound	Precursor ion > product ion (*m*/*z*)	Cone voltage (V)	Collision voltage (V)	Retention time (min)
Tropinone	140.1 > 98	40	22	2.77
Tropine	142.1 > 98	46	22	2.73
Cinnamoyl Tropine	272.15 > 124.1	40	22	4.04
Datumetine	276.15 > 124.1	40	22	4.00
Hyoscyamine	290.17 > 124.1	40	22	3.76
Littorine	290.17 > 124.1	40	22	3.90
Pseudolittorine	290.17 > 124.1	40	22	3.99
6-Deoxyphysochlaine	290.17 > 124.1	40	22	4.11
Scopolamine	304.15 > 103	34	40	3.51
Telmisartan[a]	515.2 > 276.1	42	52	3.51

Data was analyzed in positive ion mode using a Waters Quattro Micro API mass spectrometer.

[a] Telmisartan (1 μM) is included as an internal standard.

Identification and Characterization of a D-Phenyllactic Acid Glucose and Malonate Esters

Free DL-3-phenyllactic acid and glucosylated D-phenyllactate were detected in plant extracts using a Waters Quattro Premier XE Mass Spectrometer coupled to an Acquity UPLC system as previously described (Bedewitz et al., 2014). DL-3-phenyllactic acid was quantified using a standard curve of a commercially available authentic standard. MRM parameters are provided in Table 4.13. Glucosylated D-phenyllactate was characterized by generating product ion MS/MS spectra using a Waters Xevo G2-XS Q-TOF Mass Spectrometer equipped with an Acquity UPLC system and an Ascentis Express F5 column (2.1 x 100 mm with 2.7 µm particle size). Spectra were acquired using electrospray ionization in negative-ion mode using the following parameters: 2.7 kV capillary voltage, source temperature of 100°C, desolvation temperature of 350°C, desolvation gas flow of 600 L/h, 30 V cone voltage, and a mass range of *m/z* 50 to 400 with centroided spectra accumulated in resolution mode at 0.5 seconds/function. Mass correction was performed using leucine encephalin as lock mass. MS/MS product ion spectra were generated using a precursor ion of *m/z* 373.1 representing the formate adduct ($[M+formate]^-$) of the glucosylated phenyllactate, with collision potential ramped from 10 - 60 V. Chromatographic separation was performed using the gradient described in Table 4.14 with a flow rate of 0.3 mL/min.

Table 4.13 Multiple-reaction Monitoring Parameters Utilized and Transition Ions Observed for LC/MS/MS Determination of Phenyllactic Acid and its Glucose Ester Metabolites.

Compound	Precursor ion > product ion (*m/z*)	Cone Voltage (V)	Collision voltage (V)	Retention time (min)
Phenyllactic Acid	165.05 > 103	-30	-20	2.41
D-Phenyllactic Acid Glucose Ester	327.1 > 165.05	-22	-12	2.08
D-Phenyllactic Acid Glucose Ester Formate Adduct	373.1 > 165.05	-22	-18	2.08

Table 4.14 UPLC Mobile Phase Gradients Utilized for LC-TOF-MS Analyses of Phenyllactic Acid and the Glucosyl Phenyllactate Ester.

Time (min)	Mobile phase A (%)	Mobile phase B (%)
0.00	98	2
1.50	98	2
2.80	60	40
3.00	0	100
4.00	0	100
4.01	98	2
5.00	98	2

Mobile phase A = 0.1% aqueous formic acid. Mobile phase B = methanol.

Identification of malonic acid phenyllactic acid-2-O-yl ester was performed using a Waters Xevo G2-XS Q-TOF Mass Spectrometer equipped with an Acquity UPLC system and an Ascentis Express C18 column (2.1 x 100 mm with 1.7 µm particle size). Root extracts were analyzed for identity using MS^E acquisition in sensitivity mode using negative-ion mode electrospray ionization with the following parameters: 2.5 kV capillary voltage, source temperature of 100°C, desolvation temperature of 350°C, desolvation gas flow of 600 L/h, 40 V cone voltage, and a mass range of *m/z* 50 to 1200 with spectra accumulated at 0.2 seconds/function. Low energy spectra were acquired without applied collision potential, and high energy spectra were acquired using a collision potential ramp of 20-80 V. Mass correction was performed using leucine encephalin as lock mass. Chromatographic separation employed the gradient described in Table 4.15 with a flow rate of 0.3 mL/min.

Table 4.15 UPLC Mobile Phase Gradients Utilized for LC-TOF-MS Analyses of the Malonic Acid Phenyllactic Acid-2-*O*-yl Ester and Phenolics Using a Waters Xevo G2-XS QTOF Mass Spectrometer.

Time (min)	Mobile phase A (%)	Mobile phase B (%)
0.00	98	2
0.40	98	2
0.60	60	40
5.60	0	100
9.00	0	100
9.02	98	2
10.00	98	2

Mobile phase A = 0.15% formic acid in water. Mobile phase B = methanol.

Malonic acid phenyllactic acid-2-O-yl ester, phenolic acids, and glucosyl phenolic esters were quantified in root extracts using a Waters Xevo G2-XS Q-TOF Mass Spectrometer equipped with an Acquity UPLC system and an Ascentis Express C18 column (2.1 x 100 mm with 1.7 µm particle size). Root extracts were analyzed for identity using MS^E acquisition in sensitivity mode using negative-ion mode electrospray ionization with the following parameters: 2.5 kV capillary voltage, source temperature of 100°C, desolvation temperature of 350°C, desolvation gas flow of 600 L/h, 40 V cone voltage, and a mass range of *m/z* 50 to 600 with spectra accumulated at 0.1 seconds/function. Low energy spectra were acquired without applied collision potential, and high energy spectra were acquired using a collision potential ramp of 20-80 V. Mass correction was performed using leucine encephalin as lock mass. Chromatographic separation employed the gradient described in Table 4.15 with a flow rate of 0.4 mL/min.

Purification and Structural Elucidation of Malonic acid phenyllactic acid-2-O-yl ester

Frozen *A. belladonna* root tissue from 10 month-old plants (450 g) was extracted in four equal batches in methanol : water (1:1, v/v) by pulverizing in a blender until thawed and free-flowing (total volume ~1.4 L). The solution was filtered under vacuum using Whatman No. 1 filter paper and Celite® 545 filter aid. 500 mL of the filtrate was dried in aliquots under vacuum. The residue was resuspended and extracted in 8 mL 20% methanol containing 1 mM ammonium formate (pH = 7.6). Following mixing, insoluble material was removed by centrifugation at 10,000 × *g* for 10 min, the supernatant was transferred to 15 mL conical tubes and stored at ~2 °C.

An anion exchange purification method was developed for purifying malonic acid phenyllactic acid-2-O-yl ester. Supelclean™ LC-SAX (Part No. 57017, Cl^- counterion, 3 mL, bed wt. 500 mg) solid phase extraction (SPE) cartridges were conditioned with 4 mL of MilliQ water, methanol and conditioning solvent (80% water: methanol with 1 mM ammonium formate, pH 7.6) in sequence. Approximately 4 mL of extract was loaded onto the column, followed by several washings. First washing, 4 mL of conditioning solvent. Second washing, 4 mL of 80% water: methanol (4:1, v/v) with 0.35 % formic acid. Third washing, 4 mL of 50% water methanol (1:1, v/v) with 0.35% formic acid. Fourth washing, 4 mL methanol with 0.088% formic acid. The malonic acid phenyllactic acid-2-O-yl ester was eluted into a 15 mL centrifuge tube using 4 mL water : methanol (1:1, v/v) containing 0.1 M sulfuric acid. The eluate was transferred to 50 mL centrifuge tubes and diluted to 90% water: methanol (9:1, v/v, 0.02 M sulfuric acid) by adding 16 mL of water. The sample was further purified using J.T. Baker Bakerbond™ Octadecyl SPE cartridges (Part. No. 7020-03, C18, 3 mL, bed wt. 500 mg). The SPE cartridges were conditioned with 4 mL of MilliQ water, methanol and MilliQ water in sequence. All 20 mL of diluted eluate from the anion exchange step was loaded onto the column. The column was washed with 4 mL of 0.088% formic acid to remove sulfuric acid. The malonic acid phenyllactic acid-2-O-yl ester was eluted using 4 mL of methanol, and transferred to a Pyrex culture tube and concentrated to dryness under vacuum.

The sample was dissolved in 300 µL of Acetonitrile-d_3 (99.96 atom % D), and transferred to solvent matched Shigemi tubes for NMR analysis. ^1H, ^{13}C and gHSQC experiments were performed using a Bruker Avance 900 spectrometer equipped with a TCI triple

resonance probe. All spectra were referenced to non-deuterated solvent signals (δ_H = 1.94 and δ_C = 118.70 ppm).

Heterologous Expression and Characterization of UGT84A27

The predicted full-length open reading frame of *UGT84A27* was amplified from root cDNA with *Kod* DNA polymerase using the primers UGT84A27-*Bam*HI-F and UGT84A27-*Sal*I-R (Table 4.11). Fragments were cloned into the pCR™4-TOPO® vector and their identity confirmed by DNA sequencing. UGT84A27 was subcloned into the pGEX4T-1 vector to create an N-terminal GST-fusion. The GST::UGT84A27 construct was transformed into *E. coli* strain BL21 (DE3). A fresh transformant was selected and used to inoculate 1 L selective autoinducer medium ZYP-20052 (Studier, 2005). The cells were grown for 40 hours at 18°C and harvested by centrifugation for 15 minutes at 4,750 *g* at 4°C. The GST-fusion protein was purified according to manufacturer's instructions (GE Healthcare). The eluate was exchanged for a solution of 1x phosphate buffered saline (PBS) pH 7.4, 1 mM dithiothreitol, and 1 mM EDTA using an Amicon Ultra-30 module (EMD Millipore). Protein fractions were quantified by the Bradford assay (Bio-Rad Laboratories), separated by SDS-PAGE using 10% polyacrylamide gels, and visualized with Coomassie Brilliant Blue R-250 stain. Glycerol was added to the enzyme solution to a final concentration of 40% v/v and was stored at -20°C for up to 3 weeks with no loss of activity. This enzyme stock solution was diluted as needed into ice-cold 1x phosphate-buffered saline (pH 8.0) immediately prior to use.

Standard activity assays contained UGT84A27 (2 µg) in 25 mM potassium phosphate buffer pH 6.0, containing 1 mM UDP-glucose, and 50 mM D-phenyllactic acid in 100 µL. Reactions were stopped using 20 µL 5% formic acid (125 mM). Reaction products from standard assays were measured as described above for the plant extracts using a Waters Quattro Premier XE Mass Spectrometer coupled to an Acquity UPLC system using the MRM parameters provided in Table 4.13. Hydrolysis of UGT84A27 reaction products was performed as follows: standard assays were split into two equal aliquots, and sodium carbonate buffer (pH 10.0) was added to one aliquot (test sample) to a final concentration of 250 mM. The sample was incubated at room temperature for 1 hour, at which point formic acid was added to 500 mM. To the second aliquot (control sample), the formic acid and sodium carbonate solutions were mixed and then added to the UGT84A27 reaction products and incubated at room temperature for 1 hour (Babst et al., 2014). Products of hydrolysis were analyzed using a Waters Xevo G2-S Q-TOF Mass Spectrometer coupled to an Acquity UPLC system in sensitivity mode. Parameters for negative-ion mode electrospray ionization were as follows: 1.96 kV capillary voltage, source temperature of 90°C, desolvation temperature of 350°C, desolvation gas flow of 600 L/h, 30 V cone voltage, and a mass range of *m/z* 50 to 1500 with spectra accumulated at 0.5 seconds/function. Chromatographic separation used the gradient described in Table 4.14 with a flow rate of 0.4 mL/min. Chromatographic separations were performed using an Acquity BEH C18 column (2.1 × 100 mm with 1.7-µm particle size) with a column temperature of 50°C and an injection volume of 10 µL.

For determination of the optimum pH of UGT84A27, enzyme assays were performed at room temperature for 1 hour in 25-µL reaction mixes in 96-well plates using the UDP-Glo Assay kit (Promega) according to manufacturer's instructions. Reactions contained potassium phosphate buffer (pH 5.5 – 9), 1.25 mM ultra-pure UDP-glucose (Promega), 1 mM D-phenyllactic acid and 600 ng of purified enzyme. UDP-Glo kit assays were measured in a Centro XS^3 LB 960 luminometer, measured for 0.1 seconds and quantified using a standard curve. The kinetic parameters of UGT84A27 for D-phenyllactic acid and UDP-glucose with D-phenyllactic acid as a co-substrate were determined using a standard UDP-Glo assay containing 25 mM potassium phosphate buffer pH 8.0, and specified amounts of D-phenyllactic acid and ultra-pure UDP-glucose in 25 µL. Reactions were performed at room temperature for 1 hour using 600 ng of recombinant enzyme and were stopped and measured as described. Kinetic parameters of UGT84A27 for 4-coumaric acid, caffeic acid, and ferulic acid, as well as UDP-Glucose with 4-coumaric acid as the co-substrate, were determined using a standard UDP-Glo assay containing 25 mM potassium phosphate buffer pH 8.0, and specified amounts of phenolic acid and ultra-pure UDP-glucose in 25 µL. Reactions were performed at room temperature for 1 hour using 100 pg of recombinant enzyme for caffeic acid and ferulic acid, 50 pg of recombinant enzyme for 4-coumaric acid, and 300 pg of recombinant enzyme for UDP-glucose and were stopped and measured as described. Apparent V_{max} and K_m values were determined using nonlinear regression of the Michaelis-Menten equation using the Solver add-on of Microsoft Excel 2010. A calculated molecular weight of 81.61 kDa was used for determination of k_{cat}. Relative activity assays were performed in the same manner with the following specifications: 100 µM of each acid substrate and 1 mM ultra-

pure UDP-glucose, with enzyme use as follows: cinnamic acid, 4-coumaric acid, caffeic acid, ferulic acid, sinapic acid, 4-methoxybenzoic acid and 3-phenylpropionic acid, used 1 ng of recombinant enzyme, 4-hydroxy-DL-phenyllactic acid, benzoic acid, 4-methoxyphenylacetic acid, 2-phenylpropionic acid, nicotinic acid, α-resorcylic acid, syringic acid, rutin, quercetin, naringenin, and (-)-*epi*-catechin used 10 ng of recombinant enzyme, D-phenyllactic acid, phenylpyruvic acid, 3-hydroxybenzoic acid, 4-hydroxybenzoic acid, and phenylacetic acid used 100 ng of recombinant enzyme, and β-resorcylic acid, gentisic acid, γ-resorcylic acid, DL-tropic acid, salicylic acid, and DL-mandelic acid used 1 µg of recombinant enzyme. All substrates were suspended in water at 10 mM and neutralized with 10 M sodium hydroxide until dissolved.

Glucosyl-1-*O*-4-coumarate, glucosyl-1-*O*-caffeate, and glucosyl-1-*O*-ferulate were produced for use as LC/MS standards in 250 µL reactions with 25 mM potassium phosphate pH 6.0 using 2 mM UDP-glucose, 10 mM of each acid, and 10 µg of recombinant enzyme. A 5 µL aliquot was taken from each reaction and diluted 1 to 10 in 25 mM potassium phosphate pH 6.0 for quantitation as described.

Heterologous Expression of Littorine Synthase

The predicted full-length open reading frame of *Ab-SCPL-17884* (*LITTORINE SYNTHASE*) was amplified from root cDNA with *Kod* DNA polymerase using the primers Ab-SCPL-17884 ENT-F and Ab-SCPL-17884 ENT-R (Table 4.11) and cloned into the pEntr D-TOPO vector (Invitrogen). Following sequence verification, the insert was recombined into the pEAQ-HT-DEST1 vector (Sainsbury et al., 2009) using LR Clonase

(Invitrogen). The resulting destination construct was transformed into *Agrobacterium tumefaciens* strain LBA4404. Recombinant protein was generated by infiltrating *N. benthamiana* plants with this *A. tumefaciens* strain as described (Sainsbury et al., 2009). Inoculated leaves were harvested 9 days after infiltration, frozen and ground in liquid N_2. A crude leaf protein preparation was generated by extracting 10 g of ground leaves in 40 mL of an extraction buffer containing 100 mM potassium phosphate pH 6.0, 100 mM KCl, 10 mM EDTA, 10% glycerol, 1 mM 1,10-phenanthroline, 1 µM bestatin, 10 µM leupeptin, 1 µM pepstatin A, and 1 µM E-64. This crude extract was centrifuged in falcon tubes for 10 minutes at 10,000 x g to remove most of the macroscopic particles. The supernatant was decanted and cold, dry, ammonium sulfate powder was added to saturation. The precipitate was collected by repeating the centrifugation, and the supernatant was collected and discarded. The pellet was dissolved in 5 mL 50 mM potassium phosphate buffer pH 6.0 containing 10 mM EDTA. The redissolved protein was centrifuged again, and passed through a 0.2 µm filter before desalting with PD-10 desalting columns. Protein concentration was quantified using the Bradford assay (Bio-Rad Laboratories), and directly used for assays.

Littorine Synthase Activity Assays

For coupled assays of UGT84A27 and littorine synthase, the UGT reaction was performed concurrently with littorine synthase, generating glucose-ester products for immediate acylation reactions. Coupled reactions were performed for 1 hour in a 50 µL mixture containing 25 mM potassium phosphate buffer pH 6.0, 1 mM UDP-glucose, 1 mM of each acid indicated in Table 4.5, 1 mM Tropine, and 50 µg crude *N. benthamiana* leaf

protein from plants expressing littorine synthase or the pEAQ empty vector construct. Those pairings possessing acylation activity were assayed sequentially.

For sequential assays of UGT84A27 and littorine synthase, large scale UGT reactions were performed to generate sufficient glucose-ester products for subsequent acylation reactions. UGT reactions were performed in a mixture containing 25 mM potassium phosphate buffer pH 6.0, 1 mM UDP-glucose, 1 mM of *t*-cinnamic, *p*-methoxyphenylacetic, or *p*-methoxybenzoic acids, and 200 µg of purified UGT84A27 in a 200 µL volume for 1 hour. The reaction for D-phenyllactic acid used 5 mg of purified UGT84A27 in a volume of 500 µL, and the reaction for tropic acid used 10 mg of purified UGT84A27 in a volume of 300 µL. The enzyme was removed using an Amicon Ultra-10 module (EMD Millipore) and glucose ester products were quantified as previously described using UDP-Glo Assay kit (Promega).

The subsequent acylation reactions were performed in 25 µL reactions containing 50 µM of each glucose ester, 1 mM tropine or pseudotropine, and crude *N. benthamiana* leaf protein from plants expressing littorine synthase or the pEAQ empty vector construct. Assays contained 10 µg of crude *N. benthamiana* leaf protein for all substrate pairings. Products were analyzed using a Waters Acquity TQD mass spectrometer coupled to an Acquity UPLC system and an Ascentis Express F5 column (2.1 x 100 mm with 2.7 µm particle size) at a 50°C oven temperature. Liquid chromatography separations were performed using a 10 µL injection volume with a flow rate of 0.3 mL/min using the gradient in Table 4.16. Quantitative analyses were performed using electrospray ionization in

positive-ion mode with multiple reaction monitoring MS/MS using the parameters in Table 4.17. Capillary voltage, extractor voltage, and radio frequency lens settings were 2.99 kV, 2.20 V, and 0.1, respectively. Flow rates of cone gas and desolvation gas were 40 and 700 L/h, respectively with the source temperature at 130°C and desolvation temperature at 350°C. Argon was used as the collision gas for collision-induced dissociation at a manifold pressure of 2×10^{-3} mbar, with collision energies and source cone potentials optimized for each metabolite using Waters QuanOptimize software. To assess co-retention of enzyme products with natural products, reactions were also analyzed using a Waters Xevo G2-S Q-TOF Mass Spectrometer equipped with an Acquity UPLC system and an Ascentis Express F5 column (2.1 x 100 mm; 2.7 µm particle size). Products were analyzed using MS^E in sensitivity mode using positive-ion mode electrospray ionization with the following parameters: 2.7 kV capillary voltage, source temperature of 90°C, desolvation temperature of 350°C, desolvation gas flow of 600 L/h, 30 V cone voltage, and a mass range of *m/z* 50 to 1500 with spectra accumulated at 0.5 seconds/function. Chromatographic separation used the gradient described in Table 4.18 with a flow rate of 0.25 mL/min. Comparison of the fragment ion masses generated by the high energy MS^E function of the littorine standard with products from enzyme assays were performed under the same conditions except that the instrument was run in resolution mode and fragmentation was performed with MS^E with a collision potential ramp from 10-60 V.

Table 4.16 HPLC Mobile Phase Gradients Utilized for LC-MS-MS Analyses of Littorine Synthase Reaction Products Using Waters Acquity TQD Mass Spectrometer.

Time (min)	Mobile phase A (%)	Mobile phase B (%)
0	99	1
0.50	62.5	37.5
2	50	50
4	0	100
5	0	100
5.01	99	1
6	99	1

Mobile phase A = 100 mM ammonium formate + 1% formic acid. Mobile phase B = 80% methanol + 100 mM ammonium formate + 1% formic acid.

Table 4.17 Multiple-reaction Monitoring Parameters Utilized and Transition Ions Observed for LC-MS-MS Analyses of Littorine Synthase Reaction Products.

Compound	Precursor ion > product ion (*m/z*)	Cone voltage (V)	Collision voltage (V)	Retention time (min)
Cinnamoyl Tropine	272.15 > 124.1	40	22	4.36
Datumetine	276.15 > 124.1	40	22	4.12
Hyoscyamine	290.17 > 124.1	40	22	2.68
Littorine	290.17 > 124.1	40	22	2.75
6-Deoxyphysochlaine	290.17 > 124.1	40	22	3.97
Telmisartan[a]	515.2 > 276.1	42	52	5.31

Data was analyzed in positive ion mode using a Waters Acquity TQD mass spectrometer.

[a] Telmisartan (0.1 μM) is included as an internal standard.

Table 4.18 HPLC Mobile Phase Gradients Utilized for LC-TOF-MS Co-retention Analyses of Littorine Synthase Reaction Products Using Waters Xevo G2-S QTOF Mass Spectrometer.

Time (min)	Mobile phase A (%)	Mobile phase B (%)
0.00	99	1
3.00	99	1
5.00	70	30
9.00	55	45
13.00	35	65
15.00	30	70
15.01	99	1
20.00	99	1

Mobile phase A = 10 mM ammonium formate. Mobile phase B = methanol.

Multiple Sequence Alignments and Phylogenetic Analyses

Multiple sequence alignments and phylogenetic analyses were performed as previously described using version 5 of the MEGA package (Tamura et al., 2011; Bedewitz et al., 2014). The accession numbers of the sequences included in the phylogenetic trees are available in Tables 4.2 – 4.4.

REFERENCES

REFERENCES

Anarat-Cappillino, G., and Sattely, E.S. (2014). The chemical logic of plant natural product biosynthesis. Curr. Opin. Plant Biol. **19,** 51-58.

Babst, B.A., Chen, H.Y., Wang, H.Q., Payyavula, R.S., Thomas, T.P., Harding, S.A., and Tsai, C.J. (2014). Stress-responsive hydroxycinnamate glycosyltransferase modulates phenylpropanoid metabolism in *Populus*. J. Exp. Bot. **65,** 4191-4200.

Bedewitz, M.A., Jones, A.D., D'Auria, J.C., and Barry, C.S. (2018). Tropinone synthesis via an atypical polyketide synthase and P450-mediated cyclization. Nat. Commun. **9,** article number 5281.

Bedewitz, M.A., Gongora-Castillo, E., Uebler, J.B., Gonzales-Vigil, E., Wiegert-Rininger, K.E., Childs, K.L., Hamilton, J.P., Vaillancourt, B., Yeo, Y.S., Chappell, J., DellaPenna, D., Jones, A.D., Buell, C.R., and Barry, C.S. (2014). A root-expressed L-phenylalanine:4-hydroxyphenylpyruvate aminotransferase is required for tropane alkaloid biosynthesis in *Atropa belladonna*. Plant Cell **26,** 3745-3762.

Bontpart, T., Cheynier, V., Ageorges, A., and Terrier, N. (2015). BAHD or SCPL acyltransferase? What a dilemma for acylation in the world of plant phenolic compounds. New Phytol. **208,** 695-707.

Bottcher, C., von Roepenack-Lahaye, E., Schmidt, J., Schmotz, C., Neumann, S., Scheel, D., and Clemens, S. (2008). Metabolome analysis of biosynthetic mutants reveals a diversity of metabolic changes and allows identification of a large number of new compounds in Arabidopsis. Plant Physiol. **147,** 2107-2120.

Bowles, D., Lim, E.K., Poppenberger, B., and Vaistij, F.E. (2006). Glycosyltransferases of lipophilic small molecules. Ann. Rev. Plant Biol. **57,** 567-597.

Carrillo-Lopez, A., and Yahia, E. (2013). HPLC-DAD-ESI-MS analysis of phenolic compounds during ripening in exocarp and mesocarp of tomato fruit. Journal of Food Science **78,** C1839-C1844.

Chae, L., Kim, T., Nilo-Poyanco, R., and Rhee, S.Y. (2014). Genomic signatures of specialized metabolism in plants. Science **344,** 510-513.

Cheynier, V., Comte, G., Davies, K.M., Lattanzio, V., and Martens, S. (2013). Plant phenolics: Recent advances on their biosynthesis, genetics, and ecophysiology. Plant Physiol. Bioch. **72,** 1-20.

Courdavault, V., Papon, N., Clastre, M., Giglioli-Guivarc'h, N., St-Pierre, B., and

Burlat, V. (2014). A look inside an alkaloid multisite plant: the *Catharanthus* logistics. Curr. Opin. Plant Biol. **19,** 43-50.

D'Auria, J.C. (2006). Acyltransferases in plants: a good time to be BAHD. Curr. Opin. Plant Biol. **9,** 331-340.

Doncheva, T., Berkov, S., and Philipov, S. (2006). Comparative study of the alkaloids in tribe Datureae and their chemosystematic significance. Biochem. Syst. Ecol. **34,** 478-488.

Dong, Y., Burch-Smith, T.M., Liu, Y., Mamillapalli, P., and Dinesh-Kumar, S.P. (2007). A ligation-independent cloning tobacco rattle virus vector for high-throughput virus-induced gene silencing identifies roles for *NbMADS4-1* and *-2* in floral development. Plant Physiol. **145,** 1161-1170.

Drager, B. (2004). Chemistry and biology of calystegines. Nat. Prod. Rep. **21,** 211-223.

Eich, E. (2008). Solanaceae and Convolvulaceae: Secondary Metabolites: Biosynthesis, Chemotaxonomy, Biological and Economic Significance: A Handbook. (Berlin/Heidelberg, DEU: Springer).

Fan, P.X., Miller, A.M., Schilmiller, A.L., Liu, X.X., Ofner, I., Jones, A.D., Zamir, D., and Last, R.L. (2016). In vitro reconstruction and analysis of evolutionary variation of the tomato acylsucrose metabolic network. Proc. Natl. Acad. Sci. USA **113,** E239-E248.

Galanie, S., Thodey, K., Trenchard, I.J., Interrante, M.F., and Smolke, C.D. (2015). Complete biosynthesis of opioids in yeast. Science **349,** 1095-1100.

Gomez, C., Terrier, N., Torregrosa, L., Vialet, S., Fournier-Level, A., Verries, C., Souquet, J.M., Mazauric, J.P., Klein, M., Cheynier, V., and Ageorges, A. (2009). Grapevine MATE-type proteins act as vacuolar H^+-dependent acylated anthocyanin transporters. Plant Physiol. **150,** 402-415.

Graham, I.A., Besser, K., Blumer, S., Branigan, C.A., Czechowski, T., Elias, L., Guterman, I., Harvey, D., Isaac, P.G., Khan, A.M., Larson, T.R., Li, Y., Pawson, T., Penfield, T., Rae, A.M., Rathbone, D.A., Reid, S., Ross, J., Smallwood, M.F., Segura, V., Townsend, T., Vyas, D., Winzer, T., and Bowles, D. (2010). The genetic map of *Artemisia annua* L. identifies loci affecting yield of the antimalarial drug artemisinin. Science **327,** 328-331.

Hall, D., and De Luca, V. (2007). Mesocarp localization of a bi-functional resveratrol/hydroxycinnamic acid glucosyltransferase of Concord grape (*Vitis labrusca*). Plant J. **49,** 579-591.

Hashimoto, T., Hayashi, A., Amano, Y., Kohno, J., Iwanari, H., Usuda, S., and

Yamada, Y. (1991). Hyoscyamine 6b-hydroxylase, an enzyme involved in tropane alkaloid biosynthesis, is localized at the pericycle of the root. J. Biol. Chem. **266,** 4648-4653.

Hause, B., Meyer, K., Viitanen, P.V., Chapple, C., and Strack, D. (2002). Immunolocalization of 1-*O*-sinapoylglucose:malate sinapoyltransferase in *Arabidopsis thaliana*. Planta **215,** 26-32.

Hibi, N., Higashiguchi, S., Hashimoto, T., and Yamada, Y. (1994). Gene expression in tobacco low-nicotine mutants. Plant Cell **6,** 723-735.

Hildreth, S.B., Gehman, E.A., Yang, H., Lu, R.-H., Ritesh, K.C., Harich, K.C., Yu, S., Lin, J., Sandoe, J.L., Okumoto, S., Murphy, A.S., and Jelesko, J.G. (2011). Tobacco nicotine uptake permease (NUP1) affects alkaloid metabolism. Proc. Natl. Acad. Sci. U. S. A. 108: 18179–18184.

Jenett-Siems, K., Weigl, R., Bohm, A., Mann, P., Tofern-Reblin, B., Ott, S.C., Ghomian, A., Kaloga, M., Siems, K., Witte, L., Hilker, M., Muller, F., and Eich, E. (2005). Chemotaxonomy of the pantropical genus *Merremia* (Convolvulaceae) based on the distribution of tropane alkaloids. Phytochemistry **66,** 1448-1464.

Jirschitzka, J., Dolke, F., and D'Auria, J.C. (2013). Increasing the pace of new discoveries in tropane alkaloid biosynthesis. Adv. Bot. Res. **68,** 39-72.

Jirschitzka, J., Schmidt, G.W., Reichelt, M., Schneider, B., Gershenzon, J., and D'Auria, J.C. (2012). Plant tropane alkaloid biosynthesis evolved independently in the Solanaceae and Erythroxylaceae. Proc. Natl. Acad. Sci. USA **109,** 10304-10309.

Kim, N., Estrada, O., Chavez, B., Jr., Stewart, C., and D'Auria, J.C. (2016). Tropane and granatane alkaloid biosynthesis: A systematic analysis. Molecules **21,** Article Number 1510.

Kitamura, Y., Taura, A., Kajiya, Y., and Miura, H. (1992). Conversion of phenylalanine and tropic acid into tropane alkaloids by *Duboisia leichhardtii* root cultures. J. Plant Physiol. **140,** 141-146.

Landmann, C., Fink, B., and Schwab, W. (2007). FaGT2: a multifunctional enzyme from strawberry (*Fragaria x ananassa*) fruits involved in the metabolism of natural and xenobiotic compounds. Planta **226,** 417-428.

Landry, L.G., Chapple, C.C.S., and Last, R.L. (1995). Arabidopsis mutants lacking phenolic sunscreens exhibit enhanced ultraviolet-B injury and oxidative damage. Plant Physiol. **109,** 1159-1166.

Lau, W., and Sattely, E.S. (2015). Six enzymes from mayapple that complete the

biosynthetic pathway to the etoposide aglycone. Science **349,** 1224-1228.

Lehfeldt, C., Shirley, A.M., Meyer, K., Ruegger, M.O., Cusumano, J.C., Viitanen, P.V., Strack, D., and Chapple, C. (2000). Cloning of the *SNG1* gene of Arabidopsis reveals a role for a serine carboxypeptidase-like protein as an acyltransferase in secondary metabolism. Plant Cell **12,** 1295-1306.

Li, A.X., and Steffens, J.C. (2000). An acyltransferase catalyzing the formation of diacylglucose is a serine carboxypeptidase-like protein. Proc. Natl. Acad. Sci. USA **97,** 6902-6907.

Li, R., Reed, D.W., Liu, E.W., Nowak, J., Pelcher, L.E., Page, J.E., and Covello, P.S. (2006). Functional genomic analysis of alkaloid biosynthesis in *Hyoscyamus niger* reveals a cytochrome P450 involved in littorine rearrangement. Chem. Biol. **13,** 513-520.

Lim, E.K., Li, Y., Parr, A., Jackson, R., Ashford, D.A., and Bowles, D.J. (2001). Identification of glucosyltransferase genes involved in sinapate metabolism and lignin synthesis in Arabidopsis. J. Biol. Chem. **276,** 4344-4349.

Lim, E.K., Doucet, C.J., Li, Y., Elias, L., Worrall, D., Spencer, S.P., Ross, J., and Bowles, D.J. (2002). The activity of Arabidopsis glycosyltransferases toward salicylic acid, 4-hydroxybenzoic acid, and other benzoates. J. Biol. Chem. **277,** 586-592.

Lunkenbein, S., Bellido, M., Aharoni, A., Salentijn, E.M.J., Kaldenhoff, R., Coiner, H.A., Munoz-Blanco, J., and Schwab, W. (2006). Cinnamate metabolism in ripening fruit. Characterization of a UDP-glucose: Cinnamate glucosyltransferase from strawberry. Plant Physiol. **140,** 1047-1058.

McArthur, J.B., and Chen, X. (2016). Glycosyltransferase engineering for carbohydrate synthesis. Biochemical Society Transactions **44,** 129-142.

Milkowski, C., Baumert, A., and Strack, D. (2000). Identification of four Arabidopsis genes encoding hydroxycinnamate glucosyltransferases. FEBS Lett. **486,** 183-184.

Milkowski, C., Baumert, A., Schmidt, D., Nehlin, L., and Strack, D. (2004). Molecular regulation of sinapate ester metabolism in Brassica napus: expression of genes, properties of the encoded proteins and correlation of enzyme activities with metabolite accumulation. Plant J. **38,** 80-92.

Milo, R., and Last, R.L. (2012). Achieving diversity in the face of constraints: Lessons from metabolism. Science **336,** 1663-1667.

Mirzamatov, R.T., Lutfullin, K.L., Malikov, V.M., and Yunusov, S.Y. (1974).

Physochlaine - A new alkaloid from *Physochlaina alaica*. Chem. Nat. Compd. **10,** 426-426.

Mugford, S.T., Louveau, T., Melton, R., Qi, X.Q., Bakht, S., Hill, L., Tsurushima, T., Honkanen, S., Rosser, S.J., Lomonossoff, G.P., and Osbourn, A. (2013). Modularity of plant metabolic gene clusters: A trio of linked genes that are collectively required for acylation of triterpenes in oat. Plant Cell **25,** 1078-1092.

Mugford, S.T., Qi, X.Q., Bakht, S., Hill, L., Wegel, E., Hughes, R.K., Papadopoulou, K., Melton, R., Philo, M., Sainsbury, F., Lomonossoff, G.P., Roy, A.D., Goss, R.J.M., and Osbourn, A. (2009). A serine carboxypeptidase-like acyltransferase is required for synthesis of antimicrobial compounds and disease resistance in oats. Plant Cell **21,** 2473-2484.

Munoz, O., and Casale, J.F. (2003). Tropane alkaloids from *Latua pubiflora*. Z. Naturforsch. C **58,** 626-628.

Nakajima, K., and Hashimoto, T. (1999). Two tropinone reductases, that catalyze opposite stereospecific reductions in tropane alkaloid biosynthesis, are localized in plant root with different cell-specific patterns. Plant Cell Physiol. **40,** 1099-1107.

Nakajima, K., Hashimoto, T., and Yamada, Y. (1993). Two tropinone reductases with different stereospecificities are short-chain dehydrogenases evolved from a common ancestor. Proc. Natl. Acad. Sci. USA **90,** 9591-9595.

Nakanishi, F., Sasaki, K., and Shimomura, K. (1998). Isolation and identification of littorine from hairy roots of *Atropa belladonna*. Plant Cell Rep. **18,** 249-251.

Nguyen, T.-K.-O., Jamali, A., Lanoue, A., Gontier, E., and Dauwe, R. (2015). Unravelling the architecture and dynamics of tropane alkaloid biosynthesis pathways using metabolite correlation networks. Phytochemistry **116,** 94-103.

Nishizaki, Y., Yasunaga, M., Okamoto, E., Okamoto, M., Hirose, Y., Yamaguchi, M., Ozeki, Y., and Sasaki, N. (2013). *p*-Hydroxybenzoyl-glucose is a zwitter donor for the biosynthesis of 7-polyacylated anthocyanin in Delphinium. Plant Cell **25,** 4150-4165.

O'Hagan, D., Robins, R.J., Wilson, M., Wong, C.W., Berry, M., and Zabetakis, I. (1999). Fluorinated tropane alkaloids generated by directed biosynthesis in transformed root cultures of *Datura stramonium*. J. Chem. Soc. Perk. T.1**,** 2117-2120.

Ono, N.N., Qin, X.Q., Wilson, A.E., Li, G., and Tian, L. (2016). Two UGT84 family glycosyltransferases catalyze a critical reaction of hydrolyzable tannin biosynthesis in pomegranate (*Punica granatum*). PLoS One **11,** e0156319.

Onoyovwe, A., Hagel, J.M., Chen, X., Khan, M.F., Schriemer, D.C., and Facchini, P.J. (2013). Morphine biosynthesis in opium poppy involves two cell types: sieve elements and laticifers. Plant Cell **25,** 4110-4122.

Pedrazzini, E., Komarova, N.Y., Rentsch, D., and Vitale, A. (2013). Traffic routes and signals for the tonoplast. Traffic 14: 622–628.

Pichersky, E., and Lewinsohn, E. (2011). Convergent evolution in plant specialized metabolism. Ann. Rev. Plant Biol. **62,** 549-566.

Qiu, F., Yang, C., Yuan, L., Xiang, D., Lan, X., Chen, M., and Liao, Z. (2018). A phenylpyruvic acid reductase is required for biosynthesis of tropane alkaloids. Organic Letters **20,** 7807-7810.

Reina, M., Burgueno-Tapia, E., Bucio, M.A., and Joseph-Nathan, P. (2010). Absolute configuration of tropane alkaloids from *Schizanthus* species by vibrational circular dichroism. Phytochemistry **71,** 810-815.

Robins, R.J., Woolley, J.G., Ansarin, M., Eagles, J., and Goodfellow, B.J. (1994). Phenyllactic acid but not tropic acid is an intermediate in the biosynthesis of tropane alkaloids in *Datura* and *Brugansia* transformed root cultures. Planta **194,** 86-94.

Runguphan, W., Qu, X.D., and O'Connor, S.E. (2010). Integrating carbon-halogen bond formation into medicinal plant metabolism. Nature **468,** 461- 464.

Sainsbury, F., Thuenemann, E.C., and Lomonossoff, G.P. (2009). pEAQ: versatile expression vectors for easy and quick transient expression of heterologous proteins in plants. Plant Biotechnol. J. **7,** 682-693.

Schmidt, G.W., Jirschitzka, J., Porta, T., Reichelt, M., Luck, K., Torre, J.C.P., Dolke, F., Varesio, E., Hopfgartner, G., Gershenzon, J., and D'Auria, J.C. (2015). The last step in cocaine biosynthesis is catalyzed by a BAHD acyltransferase. Plant Physiol. **167,** 89-101.

Shirley, A.M., and Chapple, C. (2003). Biochemical characterization of sinapoylglucose:choline sinapoyltransferase, a serine carboxypeptidase-like protein that functions as an acyltransferase in plant secondary metabolism. J. Biol. Chem. **278,** 19870-19877.

Siddiqui, S., Sultana, N., Ahmed, S.S., and Haider, S.I. (1986). Isolation and structure of a new alkaloid datumetine from the leaves of *Datura metel*. J. Nat. Prod. **49,** 511-513.

Sinlapadech, T., Stout, J., Ruegger, M.O., Deak, M., and Chapple, C. (2007). The

hyper-fluorescent trichome phenotype of the *brt1* mutant of Arabidopsis is the result of a defect in a sinapic acid:UDPG glucosyltransferase. Plant J. **49,** 655-668.

Stehle, F., Brandt, W., Milkowski, C., and Strack, D. (2006). Structure determinants and substrate recognition of serine carboxypeptidase-like acyltransferases from plant secondary metabolism. FEBS Lett. **580,** 6366-6374.

Studier, F.W. (2005). Protein production by auto-induction in high-density shaking cultures. Protein Expres. Purif. **41,** 207-234.

Sundin, L., Vanholme, R., Geerinck, J., Goeminne, G., Hofer, R., Kim, H., Ralph, J., and Boerjan, W. (2014). Mutation of the inducible *ARABIDOPSIS THALIANA CYTOCHROME P450 REDUCTASE2* alters lignin composition and improves saccharification. Plant Physiol. **166,** 1956-1971.

Taha, A.M., and Rucker, G. (1978). C-13-NMR spectroscopy of tropane alkaloids. J. Pharm. Sci. **67,** 775-779.

Tamura, K., Peterson, D., Peterson, N., Stecher, G., Nei, M., and Kumar, S. (2011). MEGA5: Molecular evolutionary genetics analysis using maximum likelihood, evolutionary distance, and maximum parsimony methods. Mol. Biol. Evol. **28,** 2731-2739.

Tuominen, L.K., Johnson, V.E., and Tsai, C.J. (2011). Differential phylogenetic expansions in BAHD acyltransferases across five angiosperm taxa and evidence of divergent expression among *Populus* paralogues. Bmc Genomics **12**.

Weng, J.K., Philippe, R.N., and Noel, J.P. (2012). The rise of chemodiversity in plants. Science **336,** 1667-1670.

Winzer, T., Gazda, V., He, Z., Kaminski, F., Kern, M., Larson, T.R., Li, Y., Meade, F., Teodor, R., Vaistij, F.E., Walker, C., Bowser, T.A., and Graham, I.A. (2012). A *Papaver somniferum* 10-gene cluster for synthesis of the anticancer alkaloid noscapine. Science **336,** 1704-1708.

Xiao, M., Zhang, Y., Chen, X., Lee, E.J., Barber, C.J.S., Chakrabarty, R., Desgagne-Penix, I., Haslam, T.M., Kim, Y.B., Liu, E.W., MacNevin, G., Masada-Atsumi, S., Reed, D.W., Stout, J.M., Zerbe, P., Zhang, Y.S., Bohlmann, J., Covello, P.S., De Luca, V., Page, J.E., Ro, D.K., Martin, V.J.J., Facchini, P.J., and Sensen, C.W. (2013). Transcriptome analysis based on next-generation sequencing of non-model plants producing specialized metabolites of biotechnological interest. J. Biotechnol. **166,** 122-134.

Ziegler, J., and Facchini, P.J. (2008). Alkaloid biosynthesis: Metabolism and trafficking. Ann. Rev. Plant Biol. **59,** 735-769.

CHAPTER FIVE

Conclusions and Future Directions

In this thesis, I have identified and characterized five new enzymes in tropane alkaloid biosynthesis leading to scopolamine in *Atropa belladonna* using transcriptome and metabolome guided gene discovery. These enzymes fill three substantial gaps in the tropane alkaloid pathway, the formation of the tropinone core, the diversion of phenylalanine from primary to specialized metabolism, and the activation and joining of phenyllactic acid to tropine to form littorine (Bedewitz et al., 2014; Bedewitz et al., 2018). There remains a single potential missing enzyme to catalyze the reduction of hyoscyamine aldehyde to hyoscyamine before the pathway to scopolamine could be considered complete, but these discoveries enable the possibility of tropane engineering in heterologous systems as far as hyoscyamine aldehyde. Knowledge of the nearly-complete tropane pathway in *A. belladonna* may also lead to insight into tropane biosynthesis in other clades of the Solanaceae, from the commercial source of scopolamine, *Duboisia*, where tropanes and nicotine are produced together, to the food crops tomato, potato, and pepper where scopolamine is not produced. Further gains could be made in the Convolvulaceae, which through the identification of PMT and root-based tropane biosynthesis in *Calystegia sepium*, may share a common evolutionary tropane pathway origin with the Solanaceae (Scholl et al., 2001; Scholl et al., 2003; Teuber et al., 2007). In more distantly related plant families which make tropanes, such as Erythroxylaceae, Brassicaceae, and Proteaceae, filling in the tropane pathway of *A. belladonna* may not lead to immediate evolutionary insight, but it may provide the starting point for efforts to identify critical tropane reactions, such as chemical flexibility of polyketide synthases in formation of the tropane core, or the diversity of acylation mechanisms that can be recruited to decorate these alkaloids.

The reactions of PyKS and CYP82M3 may lead to insight into broader tropane, pyrrolidine, and piperidine biosynthesis and ecology

Sequential reactions by PYRROLIDINE POLYKETIDE SYNTHASE (PyKS) and CYP82M3 (TROPINONE SYNTHASE, TS) are required to extend *N*-methyl-Δ^1-pyrrolinium into 4-(1-methyl-pyrrolidine)-3-oxo-butanoic acid and then cyclize this intermediate into the first committed tropane alkaloid, tropinone (Bedewitz et al., 2018). The reactivity of *N*-methyl-Δ^1-pyrrolinium as an electrophile and 4-(1-methyl-pyrrolidine)-3-oxo-butanoic acid as a non-enzymatic, auto-decarboxylating nucleophile together lead to the co-production of two phylogenetically common pyrrolidine alkaloids, hygrine and cuscohygrine (Eich, 2008; Bedewitz et al., 2018). Between these reactions, much of the known alkaloid content of *Atropa belladonna* can be described.

Beyond the hypothesized mechanisms for biosynthesis of methylecgonone, *N*-methylpelletierine, anaferine, and granatanes, the identified reaction between an imine and a β-keto acid is enticing for the potential insight into piperidine alkaloids in diverse families (Bedewitz et al., 2018). Additional groups of such alkaloids include lobeline in *Lobelia inflata*, which is a member of the Campanulaceae used as a substitute for tobacco, and euphococcinine, a minor alkaloid occurring alongside pinidine and pinidinone in spruce (*Picea*) and pine (*Pinus*), which are gymnosperms in the Pinaceae (Figure 5.1) (Tawara et al., 1993; Felpin and Lebreton, 2004; Antonelli, 2007; Gerson et al., 2009). These compounds are substituted adjacent to their nitrogen on both sides of their piperidine ring, which suggests that there may be a TS-like enzyme activity in these species to produce a second imine after a presumptive first condensation reaction.

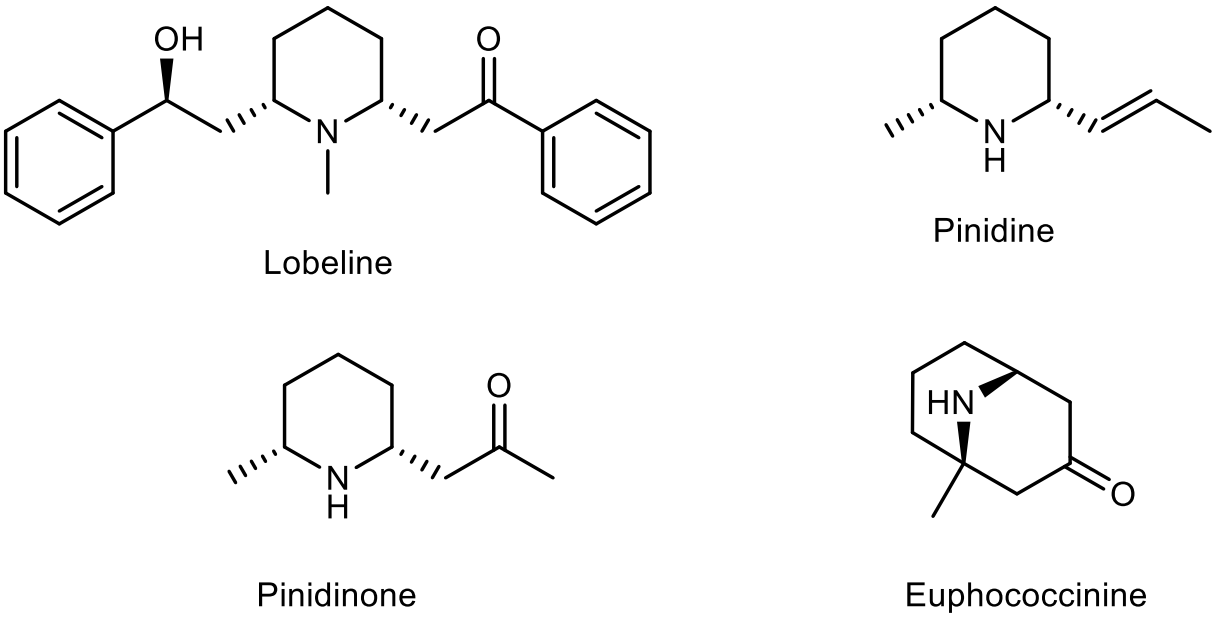

Figure 5.1 Select piperidine alkaloids from *Lobelia inflata*, *Picea* spp. and *Pinus* spp.

An aminotransferase bridges primary and specialized metabolism for tropanes

In *A. belladonna*, ArAT4, a lateral root specifically expressed L-PHENYLALANINE:4-HYDROXYPHENYLPYRUVATE AMINOTRANSFERASE, is critical to produce phenyllactic acid, such that its knockdown is sufficient to attenuate the levels of hyoscyamine and scopolamine to less than one third the level of control plants (Bedewitz et al., 2014). This aminotransferase is part of a family of six aromatic aminotransferases in *A. belladonna*, with several members expressed in the roots, though only ArAT4 contributes to biosynthesis of phenyllactic acid and aromatic tropane alkaloids. Phenylalanine and tyrosine were conventionally thought to be biosynthesized in plants through arogenic acid in plastids, not through cytosolic phenylpyruvic acid and 4-hydroxyphenylpyruvic acid, which is the more common pathway in bacteria and yeast (Whitaker et al., 1981; Braus, 1991; Fischer et al., 1993; Maeda and Dudareva, 2012). However, a cytosolic pathway from chorismic acid through phenylpyruvic acid has been identified in *Petunia hybrida* and *Arabidopsis thaliana* (Qian et al., 2019). Suppression of that pathway impaired the emission of *P. hybrida* floral volatiles derived from phenylalanine, as well as *A. thaliana* leaf emission of phenylacetaldehyde after wounding (Qian et al., 2019). This expands the role of cytosolic aromatic aminotransferases (ArATs) in plants, which at present appear to include aromatic amino acid biosynthesis, homeostasis, and specialized metabolism (Yoo et al., 2013; Bedewitz et al., 2014; Qian et al., 2019). The default fate of duplicated genes is loss through mutation unless a gene can gain a positive selection pressure through neofunctionalization, subfunctionalization, or gene dosage (Conant and Wolfe, 2008; Panchy et al., 2016). In higher plants, retention

of multiple duplicated copies of ancestral cytosolic ArATs implies that there are additional roles yet to be uncovered.

LITTORINE SYNTHASE and UGT84A27 fill in the pathway to littorine

In contrast to the tropane acylation reaction by the BAHD acyltransferase COCAINE SYNTHASE, littorine biosynthesis in *A. belladonna* requires the SCPL acyltransferase LITTORINE SYNTHASE (LS), with its requisite glucose ester substrate, glucosyl-1-*O*-D-phenyllactate derived through UGT84A27 (Schmidt et al., 2015). The rate of D-phenyllactic acid glucosylation is poor, such that it was not possible to purify the compound for enzyme kinetic studies of LS. An obvious next step is the directed evolution of UGT84A27 into a bona fide D-phenyllactic acid glucosyltransferase using the wealth of existing plant UGT structural data (Osmani et al., 2009; Wang, 2009; McArthur and Chen, 2016; Tiwari et al., 2016). This would permit testing the hypothesis that UGT84A27 is a rate limiting enzyme *in planta* for littorine, and subsequently hyoscyamine, biosynthesis, as well as provide the opportunity to purify the product glucose ester for kinetic analysis of LS. Toward the goal of kinetic analysis of LS, a method for purification of the enzyme would be required, as SCPLs possess undergo numerous post-translational modifications that complicate affinity tagging (Bontpart et al., 2015). UGT84A27 also straddles the boundary between primary and specialized metabolism, with its glucosylation reactions of the plant primary metabolites 4-coumaric acid, caffeic acid, and ferulic acid, all of which are phenolic acids, and the uncommon specialized metabolite D-phenyllactic acid. The metabolic fate of phenolic acid glucose esters is unclear in many of the plants which produce these compounds, but in *Arabidopsis* and *Brassica*, at least one, glucosyl-1-*O*-

sinapate, finds a role in specialized metabolism for production of sinapoyl malate and the anti-feedant sinapoyl choline (Lehfeldt et al., 2000; Milkowski et al., 2000; Milkowski et al., 2004; Sinlapadech et al., 2007). Through the existence of these sinapoylated specialized metabolites, it remains a possibility that there are additional unidentified phenolic compounds derived from phenolic glucose esters. For example, phenolic esters are known for a variety of metabolite types, including polyamines, flavonoids, sterols, and polyols (Mugford et al. 2009; Nishizaki et al., 2013; Munafo Jr. and Gianfagna, 2015; Wise 2017; Li et al., 2018b).

Exploration of tropane alkaloid biosynthesis in the Convolvulaceae

In addition to the Solanaceae, tropanes are also produced in the Convolvulaceae, Brassicaceae, Erythroxylaceae and other plant families. The near-complete status of the tropane alkaloid biosynthetic pathway in *A. belladonna* is potentially most useful toward identifying pathway components in the Convolvulaceae, which is more closely related to the Solanaceae, and which shares the first committed step, PMT (Teuber et al., 2007). It would be plausible to use the Solanaceous pathway to mine transcriptome databases of members of the Convolvulaceae in search of orthologous genes encoding enzymes for MPO, PyKS, TS, and TR. However, the search for acylation enzymes in the Convolvulaceae may be hindered by the general use of more orthodox phenolics as esters. The family accumulates tropine and pseudotropine esters of phenylpropanoids from cinnamic acid through trimethoxycinnamic acid, and of benzenoids from benzoic acid through gallic acid (Eich, 2008). Phenyllactic acid is diverted from the phenylpropanoid pathway before PHENYLALANINE AMMONIA LYASE (PAL) produces

cinnamic acid, and the commitment of cinnamic acid toward lignin precursors through the coenzyme A thioester of *p*-coumaric acid produced by 4-COUMARIC ACID LIGASE (4CL) (Fraser and Chapple, 2011). The early diversion of this compound may have necessitated the use of the glucose ester and SCPL based pathway rather than the more commonly found BAHD pathway, which uses coenzyme A thioesters. The ester groups found in the Convolvulaceae would be diverted after these steps, when the coenzyme A thioesters would be available, which would potentially support a role for BAHDs. A further line of support for BAHDs rather than SCPLs would be the presence of benzenoid esters analogous to the phenylpropanoid esters identified, and a lack of phenylacetate derivatives. These benzenoids could be generated through β-oxidation of the corresponding phenylpropanoid coenzyme A thioester, which is an attribute of the benzoic acid biosynthetic pathway, or via an as-yet unidentified non β-oxidative route (Qualley et al., 2012; Wildhalm and Dudareva, 2015).

Exploration of tropane alkaloid metabolism in another family may also be hindered by a lack of retention of coexpression. In the Solanaceae, tropane alkaloids are biosynthesized in the lateral roots, and labeling studies have shown incorporation of precursors in the roots for Convolvulaceae, but this does not necessarily mean that later tropane pathway reactions also occur exclusively in the roots. There are specialized metabolic pathways which span tissue types, such as the monoterpene indole alkaloid pathway of *Camptotheca acuminata*, where the tryptamine branch shows a broader tissue distribution than the iridoid branch, complicating transcriptome mining efforts (Sadre et al., 2016). There is a single point of evidence that this phenomenon may exist as well in

A. belladonna's tropane pathway. The gene encoding TRII is not solely expressed in roots, but is also expressed in stems, leaves, flowers, and green fruit (Bedewitz et al., 2014). TRII is the committed enzyme toward the calystegine branch of the tropane pathway through the production of pseudotropine, and this broadening of expression may hint at a separate localization for production of that set of compounds.

Toward completion and engineering of the tropane alkaloid biosynthetic pathway

Plant specialized metabolism research in the omics era has been characterized, in part, by an increasing pace of biosynthetic pathway gene discovery leading toward biochemically complete pathways and *de novo* specialized compound production in heterologous systems (Jirschitzka et al., 2013; Brown et al., 2015; Galanie et al., 2015; Li et al., 2018a). To date, efforts in tropane engineering have focused on overexpression of PMT, TRI, and H6H in native scopolamine producers due to the lack of enzymes to connect these three reactions. These genes have each been approached singly in *A. belladonna*, *Datura metel*, *Duboisia myoporoides×leichhardtii*, *Hyoscyamus muticus*, *Scopolia lurida*, almost exclusively in hairy root cultures, in attempts to push the whole pathway with PMT, or pull the scopolamine branch with TRI or H6H, with either little to no gained hyoscyamine and scopolamine, or insufficient gain to justify the added culturing expense for biomanufacturing (Yun et al., 1992; Jouhikainen et al., 1999; Moyano et al., 2002; Moyano et al., 2003; Palazón et al., 2003; Rothe et al., 2003; Richter et al., 2005; Zhao et al., 2017). Efforts using multiple enzymes, PMT and H6H, have found better success, both in hairy root cultures and whole transgenic plants, with the best individuals producing up to 411 mg L^{-1} in hairy root culture of *Hyoscyamus niger* and up to 5.13 mg

g dwt^{-1} in whole transgenic *A. belladonna* plants (Zhang et al., 2004; Wang et al., 2011; Yang et al., 2011; Xia et al., 2016).

The identification and characterization of PyKS, TS, ArAT4, and PPAR over the last several years marks substantial movement toward practical completion of the biosynthetic pathway from putrescine to scopolamine in the Solanaceae (Bedewitz et al., 2014; Bedewitz et al., 2018; Qiu et al., 2018). The characterization of UGT84A27 and LS extend these gains, and potentially leave the reduction of hyoscyamine aldehyde to hyoscyamine as the remaining missing enzyme of tropane alkaloid biosynthesis. In the course of identifying TS, a transient gene-stacking approach was used in *N. benthamiana* to divert putrescine to production of 4-(1-methyl-pyrrolidine)-3-oxo-butanoic acid and ultimately, tropinone (Bedewitz et al., 2018). The low production of tropinone suggests that TS is likely to be the rate-limiting enzyme for producing tropinone, while UGT84A27 is potentially a limiting step in the phenyllactic acid branch of the tropane pathway due to poor enzyme optimization for use of phenyllactic acid, indicating that, after PMT and H6H, these enzymes may be the next best candidates for tropane engineering. These issues could be addressed in multiple ways, first by directed evolution for faster, more efficient substrate clearance (Osmani et al., 2009; Wang, 2009; McArthur and Chen, 2016; Tiwari et al., 2016). Enhancing the level of active enzyme offers an alternative approach which could be pursued in tandem to catalytic optimization. This could take the form of simple strong-promoter driven overexpression, or protein engineering to enhance solubility and stability. Solubility engineering approaches have been used to enhance the activities of the rate limiting enzymes levoglucosan kinase, and simvastatin synthase, with promising

results compared to simply driving stronger expression. (Xie et al., 2009; Klesmith et al., 2015; Zhu et al., 2015).

Plant protection and defensive impact of individual tropanes and pyrrolidines

Knockdown of PyKS produces plants with very low levels of both tropanes and pyrrolidine alkaloids, while knockdown of TS leads to only an attenuation of tropane levels, and little effect on pyrrolidines (Bedewitz et al., 2018). The identification of these two key enzymes offers an opportunity to study the role of tropanes and pyrrolidines in their expected defensive role, as a hypothetical CRISPR knockout of TS would be expected to lack tropanes, but retain the phylogenetically conserved pyrrolidines, while a CRISPR knockout of PyKS would be expected to lack both tropane and pyrrolidines. These two individual knockouts would be useful in dissecting the protection granted by each broad alkaloid class in *A. belladonna* and species where tropanes and pyrrolidines are the major known alkaloids. The major derivatives of tropine in *A. belladonna* are hyoscyamine and scopolamine, alkaloids with anticholinergic activity, whereas the major derivatives of pseudotropine are the calystegines, compounds with *in vitro* glycosidase inhibitory activities (Asano et al., 1996; Goldman et al., 1996; Asano et al., 1997; Drager, 2004; Eich, 2008; Grynkiewicz and Gadzikowska, 2008). Similar studies could be undertaken with knockouts for either TRI, where tropine, littorine, and downstream aromatic alkaloids would be lost, or TRII, where pseudotropine and calystegines would be lost and the roles of each branch assessed. Phenyllactic acid has been investigated for possible use as an antifungal and antibacterial due to reported inhibition or toxicity against *Penicillium*, *Aspergillus*, *Listeria* and *Staphylococcus* when produced by lactic acid bacteria

(Lavermicocca et al., 2003; Ohhira et al., 2004; Svanström et al., 2013; Sorrentino et al., 2018). Knockouts of UGT84A27, which would be expected to overaccumulate phenyllactic acid, and ArAT4, which should lack that compound, could be used to probe whether this metabolite might have a similar role when it is produced in plants.

Individual compounds, particularly hyoscyamine and scopolamine, as well as crude *Datura stramonium* extracts have been assessed for their lethality and antifeedant activity in insect pests, indicating that the late-stage Solanaceous tropanes are potential *in planta* defense compounds (Detzel and Wink, 1993; Shields et al., 1998; González-Coloma et al., 2004). There is also some evidence using *Solanum* glycoalkaloids that mixes of compounds can be more effective than individual compounds (Mullin et al., 1997; Smith et al., 2001; Ventrella et al., 2014). The existence of calystegines in tomato and potato demonstrates that these species are genetically competent to produce tropane alkaloids, though they appear to be low in diversity and in the case of tomato, low in abundance as well (Asano et al., 1997). This opens a concept that these compounds could be restored or expanded though addition of the hyoscyamine branch of the tropane pathway under cell-specific promoters in tomato for the purpose of assessing the defensive impact of adding tropanes back into a background that is tropane poor, while also rich in glycoalkaloids, to study synergistic effects of these two groups of Solanaceous alkaloids.

REFERENCES

REFERENCES

Antonelli, A. (2008). Higher Level Phylogeny and Evolutionary Trends in Campanulaceae subfam. Lobelioideae: Molecular Signal Overshadows Morphology. Mol. Phylogenet. Evol. **46**: 1–18.

Asano, N., Kato, A., Kizu, H., Matsui, K., Watson, A.A., and Nash, R.J. (1996). Calystegine B4, a Novel Trehalase Inhibitor from *Scopolia japonica*. Carbohydr. Res. **293**: 195–204.

Asano, N., Kato, A., Matsui, K., Watson, A.A., Nash, R.J., Molyneux, R.J., Hackett, L., Topping, J., and Winchester, B. (1997). The Effects of Calystegines Isolated from Edible Fruits and Vegetables on Mammalian Liver Glycosidases. Glycobiology **7**: 1085–1088.

Bedewitz, M.A. et al. (2014). A Root-Expressed L-Phenylalanine:4-Hydroxyphenylpyruvate Aminotransferase Is Required for Tropane Alkaloid Biosynthesis in *Atropa belladonna*. Plant Cell **26**: 3745–3762.

Bedewitz, M.A., Jones, A.D., D'Auria, J.C., and Barry, C.S. (2018). Tropinone Synthesis via an Atypical Polyketide Synthase and P450-Mediated Cyclization. Nat. Commun. **9**: 5281.

Bontpart, T., Cheynier, V., Ageorges, A., and Terrier, N. (2015). BAHD or SCPL Acyltransferase? What a Dilemma for Acylation in the World of Plant Phenolic Compounds. New Phytol. **208**: 695–707.

Braus, G.H. (1991). Aromatic Amino Acid Biosynthesis in the Yeast *Saccharomyces cerevisiae*: a Model System for the Regulation of a Eukaryotic Biosynthetic Pathway. Microbiol. Rev. **55**: 349–370.

Brown, S., Clastre, M., Courdavault, V., and O'Connor, S.E. (2015). De novo Production of the Plant-Derived Alkaloid Strictosidine in Yeast. Proc. Natl. Acad. Sci. **112**: 3205–3210.

Conant, G.C. and Wolfe, K.H. (2008). Turning a Hobby into a Job: How Duplicated Genes Find New Functions. Nat. Rev. Genet. **9**: 938–950.

Detzel, A. and Wink, M. (1993). Attraction, Deterrence or Intoxication of Bees (*Apis mellifera*) by Plant Allelochemicals. Chemoecology **4**: 8–18.

Dräger, B. (2004). Chemistry and Biology of Calystegines. Nat. Prod. Rep. **21**: 211–223.

Eich, E. (2008). Solanaceae and Convolvulaceae: Secondary Metabolites - Biosynthesis, Chemotaxonomy, Biological and Economic Significance (Springer: Berlin).

Felpin, F.X. and Lebreton, J. (2004). History, Chemistry and Biology of Alkaloids from *Lobelia inflata*. Tetrahedron **60**: 10127–10153.

Fischer, R.S., Bonner, C.A., Boone, D.R., and Jensen, R.A. (1993). Clues from a Halophilic Methanogen about Aromatic Amino Acid Biosynthesis in Archaebacteria. Arch. Microbiol. **160**: 440–446.

Fraser, C.M. and Chapple, C. (2011). The Phenylpropanoid Pathway in Arabidopsis. Arab. B. **9**: e0152.

Galanie, S., Thodey, K., Trenchard, I.J., Interrante, M.F., and Smolke, C.D. (2015). Complete Biosynthesis of Opioids in Yeast. Science (80-.). **349**: 1095–1100.

Gerson, E.A., Kelsey, R.G., and St Clair, J.B. (2009). Genetic Variation of Piperidine Alkaloids in *Pinus ponderosa*: A Common Garden Study. Ann. Bot. **103**: 447–457.

Goldmann, A., Message, B., Tepfer, D., Molyneux, R.J., Duclos, O., Boyer, F.D., Pan, Y.T., and Elbein, A.D. (1996). Biological Activities of the Nortropane Alkaloid, Calystegine B2, and Analogs: Structure-Function Relationships. J. Nat. Prod. **59**: 1137–1142.

González-Coloma, A., Reina, M., Medinaveitia, A., Guadaño, A., Santana, O., Martínez-Díaz, R., Ruiz-Mesía, L., Alva, A., Grandez, M., Díaz, R., Gavín, J.A., and De La Fuente, G. (2004). Structural Diversity and Defensive Properties of Norditerpenoid Alkaloids. J. Chem. Ecol. **30**: 1393–1408.

Grynkiewicz, G. and Gadzikowska, M. (2008). Tropane Alkaloids as Medicinally Useful Natural Products and their Synthetic Derivatives as New Drugs. Pharmacol. Reports **60**: 439–463.

Jirschitzka, J., Dolke, F., and Auria, J.C.D. (2013). Increasing the Pace of New Discoveries in Tropane Alkaloid Biosynthesis. In Advances in Botanical Research (Elsevier Inc.), pp. 39–72.

Jouhikainen, K., Lindgren, L., Jokelainen, T., Hiltunen, R., Teeri, T.H., and Oksman-Caldentey, K.M. (1999). Enhancement of Scopolamine Production in *Hyoscyamus muticus* L. Hairy Root Cultures by Genetic Engineering. Planta **208**: 545–551.

Klesmith, J.R., Bacik, J.P., Michalczyk, R., and Whitehead, T.A. (2015). Comprehensive Sequence-Flux Mapping of a Levoglucosan Utilization Pathway in *E. coli*. ACS Synth. Biol. **4**: 1235–1243.

Lavermicocca, P., Valerio, F., and Visconti, A. (2003). Antifungal Activity of Phenyllactic Acid Against Molds Isolated from Bakery Products. Appl. Environ. Microbiol. **69**: 634–640.

Lehfeldt, C., Shirley, A.M., Meyer, K., Ruegger, M.O., Cusumano, J.C., Viitanen, P. V., Strack, D., and Chapple, C. (2000). Cloning of the SNG1 Gene of *Arabidopsis* Reveals a Role for a Serine Carboxypeptidase-Like Protein as an Acyltransferase in Secondary Metabolism. Plant Cell **12**: 1295–1307.

Li, Y., Li, S., Thodey, K., Trenchard, I., Cravens, A., and Smolke, C.D. (2018). Complete Biosynthesis of Noscapine and Halogenated Alkaloids in Yeast. Proc. Natl. Acad. Sci. **115**: E3922–E3931.

Li, Z., Zhao, C., Zhao, X., Xia, Y., Sun, X., Xie, W., Ye, Y., Lu, X., and Xu, G. (2018). Deep Annotation of Hydroxycinnamic Acid Amides in Plants Based on Ultra-High-Performance Liquid Chromatography-High-Resolution Mass Spectrometry and Its in Silico Database. Anal. Chem. **90**: 14321–14330.

Maeda, H. and Dudareva, N. (2012). The Shikimate Pathway and Aromatic Amino Acid Biosynthesis in Plants. Annu. Rev. Plant Biol. **63**: 73–105.

McArthur, J.B. and Chen, X. (2016). Glycosyltransferase Engineering for Carbohydrate Synthesis. Biochem. Soc. Trans. **44**: 129–142.

Milkowski, C., Baumert, A., Schmidt, D., Nehlin, L., and Strack, D. (2004). Molecular Regulation of Sinapate Ester Metabolism in *Brassica napus*: Expression of Genes, Properties of the Encoded Proteins and Correlation of Enzyme Activities with Metabolite Accumulation. Plant J. **38**: 80–92.

Milkowski, C., Baumert, A., and Strack, D. (2000). Identification of Four *Arabidopsis* Genes Encoding Hydroxycinnamate Glucosyltransferases. FEBS Lett. **486**: 183–184.

Moyano, E., Jouhikainen, K., Tammela, P., Palazón, J., Cusidó, R.M., Piñol, M.T., Teeri, T.H., and Oksman-Caldentey, K.M. (2003). Effect of pmt Gene Overexpression on Tropane Alkaloid Production in Transformed Root Cultures of *Datura metel* and *Hyoscyamus muticus*. J. Exp. Bot. **54**: 203–211.

Moyano, E., Fornalé, S., Palazón, J., Cusidó, R.M., Bagni, N., and Piñol, M.T. (2002). Alkaloid Production in *Duboisia* Hybrid Hairy Root Cultures Overexpressing the pmt Gene. Phytochemistry **59**: 697–702.

Mugford, S.T. et al. (2009). A Serine Carboxypeptidase-Like Acyltransferase Is Required for Synthesis of Antimicrobial Compounds and Disease Resistance in Oats. Plant Cell **21**: 2473–2484.

Mullin, C.A., González-Coloma, A., Gutiérrez, C., Reina, M., Eichenseer, H., Hollister, B., and Chyb, S. (1997). Antifeedant Effects of Some Novel Terpenoids on Chrysomelidae Beetles: Comparisons with Alkaloids on an Alkaloid-Adapted and nonadapted Species. J. Chem. Ecol. **23**: 1851–1866.

Munafo, J.P. and Gianfagna, T.J. (2015). Quantitative Analysis of Phenylpropanoid Glycerol Glucosides in Different Organs of Easter Lily (*Lilium longiflorum* Thunb.). J. Agric. Food Chem. **63**: 4836–4842.

Nishizaki, Y., Yasunaga, M., Okamoto, E., Okamoto, M., Hirose, Y., Yamaguchi, M., Ozeki, Y., and Sasaki, N. (2013). *p*-Hydroxybenzoyl-Glucose is a Zwitter Donor for the Biosynthesis of 7-Polyacylated Anthocyanin in *Delphinium*.

Ohhira, I., Kuwaki, S., Morita, H., Suzuki, T., Tomita, S., Hisamatsu, S., Sonoki, S., and Shinoda, S. (2004). Identification of 3-Phenyllactic Acid As a Possible Antibacterial Substance Produced by *Enterococcus faecalis* TH 10. Biocontrol Sci. **9**: 77–81.

Osmani, S.A., Bak, S., and Møller, B.L. (2009). Substrate Specificity of Plant UDP-Dependent Glycosyltransferases Predicted from Crystal Structures and Homology Modeling. Phytochemistry **70**: 325–347.

Palazón, J., Moyano, E., Cusidó, R.M., Bonfill, M., Oksman-Caldentey, K.M., and Piñol, M.T. (2003). Alkaloid Production in *Duboisia* Hybrid Hairy Roots and Plants Overexpressing the h6h Gene. Plant Sci. **165**: 1289–1295.

Panchy, N., Lehti-Shiu, M.D., and Shiu, S.-H. (2016). Evolution of Gene Duplication in Plants. Plant Physiol. **171**: 2294–2316.

Qian, Y., Lynch, J.H., Guo, L., Rhodes, D., Morgan, J.A., and Dudareva, N. (2019). Completion of the Cytosolic Post-Chorismate Phenylalanine Biosynthetic Pathway in Plants. Nat. Commun. **10**: 15.

Qiu, F., Yang, C., Yuan, L., Xiang, D., Lan, X., Chen, M., and Liao, Z. (2018). A Phenylpyruvic Acid Reductase Is Required for Biosynthesis of Tropane Alkaloids. ACS Org. Lett. **20**: 7807–7810.

Qualley, A. V., Widhalm, J.R., Adebesin, F., Kish, C.M., and Dudareva, N. (2012). Completion of the core β-oxidative pathway of benzoic acid biosynthesis in plants. Proc. Natl. Acad. Sci. **109**: 16383–16388.

Richter, U., Rothe, G., Fabian, A.K., Rahfeld, B., and Dräger, B. (2005). Overexpression of Tropinone Reductases Alters Alkaloid Composition in *Atropa belladonna* Root Cultures. J. Exp. Bot. **56**: 645–652.

Rothe, G., Hachiya, A., Yamada, Y., Hashimoto, T., and Dräger, B. (2003). Alkaloids in Plants and Root Cultures of *Atropa belladonna* Overexpressing Putrescine *N*-Methyltransferase. J. Exp. Bot. **54**: 2065–2070.

Sadre, R., Magallanes-Lundback, M., Pradhan, S., Salim, V., Mesberg, A., Jones, A.D., and DellaPenna, D. (2016). Metabolite Diversity in Alkaloid Biosynthesis: A Multilane (Diastereomer) Highway for Camptothecin Synthesis in *Camptotheca acuminata*. Plant Cell **28**: 1926–1944.

Schmidt, G.W., Jirschitzka, J., Porta, T., Reichelt, M., Luck, K., Torre, J.C.P., Dolke, F., Varesio, E., Hopfgartner, G., Gershenzon, J., and D'Auria, J.C. (2015). The Last Step in Cocaine Biosynthesis Is Catalyzed by a BAHD Acyltransferase. Plant Physiol. **167**: 89–101.

Scholl, Y., Höke, D., and Dräger, B. (2001). Calystegines in *Calystegia sepium* Derive from the Tropane Alkaloid Pathway. Phytochemistry **58**: 883–889.

Scholl, Y., Schneider, B., and Dräger, B. (2003). Biosynthesis of Calystegines: 15N NMR and Kinetics of Formation in Root Cultures of *Calystegia sepium*. Phytochemistry **62**: 325–332.

Shields, V.D.C., Smith, K.P., Arnold, N.S., Gordon, I.M., Shaw, T.E., and Waranch, D. (2008). The Effect of Varying Alkaloid Concentrations on the Feeding Behavior of Gypsy Moth Larvae, *Lymantria dispar* (L.) (Lepidoptera: Lymantriidae). Arthropod. Plant. Interact. **2**: 101–107.

Sinlapadech, T., Stout, J., Ruegger, M.O., Deak, M., and Chapple, C. (2007). The Hyper-Fluorescent Trichome Phenotype of the *brt1* Mutant of *Arabidopsis* is the Result of a Defect in a Sinapic Acid:UDPG Glucosyltransferase. Plant J. **49**: 655–668.

Smith, D.B., Roddick, J.G., and Jones, J.L. (2001). Synergism Between the Potato Glycoalkaloids α-Chaconine and α-Solanine in Inhibition of Snail Feeding. Phytochemistry **57**: 229–234.

Sorrentino, E., Tremonte, P., Succi, M., Iorizzo, M., Pannella, G., Lombardi, S.J., Sturchio, M., and Coppola, R. (2018). Detection of Antilisterial Activity of 3-Phenyllactic Acid using *Listeria innocua* as a Model. Front. Microbiol. **9**: 1373.

Svanström, Å., Boveri, S., Boström, E., and Melin, P. (2013). The Lactic Acid Bacteria Metabolite Phenyllactic Acid Inhibits both Radial Growth and Sporulation of Filamentous Fungi. BMC Res. Notes **6**: 464.

Tawara, J.N., Blokhin, A., Foderaro, T.A., Stermitz, F.R., and Hope, H. (1993). Toxic Piperidine Alkaloids from Pine (*Pinus*) and Spruce (*Picea*) Trees. New Structures and a Biosynthetic Hypothesis. J. Org. Chem. **58**: 4813–4818.

Teuber, M., Azemi, M.E., Namjoyan, F., Meier, A.C., Wodak, A., Brandt, W., and Dräger, B. (2007). Putrescine *N*-Methyltransferases - A Structure-Function Analysis. Plant Mol. Biol. **63**: 787–801.

Tiwari, P., Sangwan, R.S., and Sangwan, N.S. (2016). Plant Secondary Metabolism Linked Glycosyltransferases: An Update on Expanding Knowledge and Scopes. Biotechnol. Adv. **34**: 714–739.

Ventrella, E., Marciniak, P., Adamski, Z., Rosiński, G., Chowański, S., Falabella, P., Scrano, L., and Bufo, S.A. (2015). Cardioactive Properties of Solanaceae Plant Extracts and Pure Glycoalkaloids on *Zophobas atratus*. Insect Sci. **22**: 251–262.

Wang, X. (2009). Structure, Mechanism and Engineering of Plant Natural Product Glycosyltransferases. FEBS Lett. **583**: 3303–3309.

Wang, X., Chen, M., Yang, C., Liu, X., Zhang, L., Lan, X., Tang, K., and Liao, Z. (2011). Enhancing the Scopolamine Production in Transgenic Plants of *Atropa belladonna* by Overexpressing pmt and h6h Genes. Physiol. Plant. **143**: 309–315.

Whitaker, R.J., Byng, G.S., Gherna, R.L., and Jensen, R.A. (1981). Diverse Enzymological Patterns of Phenylalanine Biosynthesis in Pseudomonads are Conserved in Parallel with Deoxyribonucleic Acid Homology Groupings. J. Bacteriol. **147**: 526–534.

Widhalm, J.R. and Dudareva, N. (2015). A familiar ring to it: Biosynthesis of plant benzoic acids. Mol. Plant **8**: 83–97.

Wise, M.L. (2018). Tissue distribution of avenanthramides and gene expression of hydroxycinnamoyl-CoA : hydroxyanthranilate N-hydroxycinnamoyl transferase (HHT) in benzothiadiazole-treated oat (*Avena sativa*). Can. J. Plant Sci. **98**: 444–456.

Xia, K., Liu, X., Zhang, Q., Qiang, W., Guo, J., Lan, X., Chen, M., and Liao, Z. (2016). Promoting Scopolamine Biosynthesis in Transgenic *Atropa belladonna* Plants with pmt and h6h Overexpression Under Field Conditions. Plant Physiol. Biochem. **106**: 46–53.

Xie, X., Pashkov, I., Gao, X., Guerrero, J.L., Yeates, T.O., and Tang, Y. (2009). Rational Improvement of Simvastatin Synthase Solubility in *Escherichia coli* Leads to Higher Whole-Cell Biocatalytic Activity. Biotechnol. Bioeng. **102**: 20–28.

Yang, C., Chen, M., Zeng, L., Zhang, L., Liu, X., Lan, X., Tang, K., and Liao, Z. (2011). Improvement of Tropane Alkaloids Production in Hairy Root Cultures of *Atropa belladonna* by Overexpressing pmt and h6h Genes. Plant Omics **4**: 29–33.

Yoo, H., Widhalm, J.R., Qian, Y., Maeda, H., Cooper, B.R., Jannasch, A.S., Gonda, I., Lewinsohn, E., Rhodes, D., and Dudareva, N. (2013). An Alternative Pathway Contributes to Phenylalanine Biosynthesis in Plants via a Cytosolic Tyrosine:Phenylpyruvate Aminotransferase. Nat. Commun. **4**: 2833.

Yun, D.J., Hashimoto, T., and Yamada, Y. (1992). Metabolic Engineering of Medicinal Plants: Transgenic Atropa belladonna with an Improved Alkaloid Composition. Proc. Natl. Acad. Sci. **89**: 11799–11803.

Zhang, L. et al. (2004). Engineering Tropane Biosynthetic Pathway in *Hyoscyamus niger* Hairy Root Cultures. Proc. Natl. Acad. Sci. **101**: 6786–6791.

Zhao, K., Zeng, J., Zhao, T., Zhang, H., Qiu, F., Yang, C., Zeng, L., Liu, X., Chen, M., Lan, X., and Liao, Z. (2017). Enhancing Tropane Alkaloid Production Based on the Functional Identification of Tropine-Forming Reductase in *Scopolia lurida*, a Tibetan Medicinal Plant. Front. Plant Sci. **8**: 1745.

Zhu, J., Lin, J.L., Palomec, L., and Wheeldon, I. (2015). Microbial Host Selection Affects Intracellular Localization and Activity of Alcohol-O-Acetyltransferase. Microb. Cell Fact. **14**: 35.